Université catholique de Louvain

Secteur des sciences et technologies

Institut de recherche en mathématique et physique

Centre for Cosmology, Particle Physics and Phenomenology

Minimal Flavour Violation in a custodial Two Higgs Doublet Model

Doctoral dissertation presented by

Elvira Cerveró García

in fulfilment of the requirements for the degree of Doctor in Sciences

Jury

Prof. Vincent Lemaître (*chairman*)	UCL, Belgium
Prof. Jean-Marc Gérard (*advisor*)	UCL, Belgium
Prof. Fabio Maltoni	UCL, Belgium
Prof. Christophe Delaere	UCL, Belgium
Prof. Michel Tytgat	ULB, Belgium
Prof. Christopher Smith	Université Grenoble Alpes, France

July 2017

"Everything comes gradually and at its appointed hour"
Ovid

I would like to thank my advisor, Professor Jean-Marc Gérard, for giving me the opportunity of carrying out and achieving this work. His passion and enthusiasm have encouraged me to deepen in the understanding of nature through scientific research.

I also want to thank all the members of my jury, Professors Vincent Lemaître, Fabio Maltoni, Christophe Delaere, Michel Tytgat and Christopher Smith. I am honoured that they have taken the time to assess this work and contribute to its improvement with their relevant questions and remarks.

My gratitude extends to the numerous professors, fellow PhD students and students that have in one way or another influenced my learning since I arrived to this univerity already twelve years ago. I am unable to name each and everyone of them, but I can only say thank you for helping me to become a physicist and making me always feel at home.

I cannot finish without thanking all the people around me that have brought this project to completion. They have been discretely supporting me with their patience, their affection and especially with their ears and advice when I most needed it. I think of course of my family: my parents that encouraged me from afar while making their presence felt, and my siblings Pepe, Ana, Jorge and Pilar. There are so many friends that have helped me in numerous ways during these years that I am unable to list them all here. From Belgium to Spain and now Italy I hope all of you can discover in this work your small or big grain of sand that has made achieving this work possible.

Abstract

Refined measurements of the new scalar discovered during the first run of the LHC through more accumulated data have shown an impressive consistency with the Standard Model (SM) Higgs boson and its spontaneous symmetry breaking mechanism. However, there are numerous theoretical and experimental motivations to study alternative scenarios such as the Two Higgs Doublet Model (2HDM).

The approach taken in this work falls in the context of the current success of the SM. While studying physics beyond the SM, one needs to ponder about the properties of the latter that make it so succesful and to think about the advantages or solutions the New Physics model might offer.

On the one hand, while concentrating in the implications of a 2HDM in the flavour sector and in order to provide predictions that could be experimentally observed in the near future, we assume a Minimal Flavour Violation (MFV) hypothesis for the new flavour structures beyond the SM. In this way, additional fine-tuning, mass hierarchies or CP violating phases absent in the SM are avoided. On the other hand, the custodial symmetry that rises accidentally in the SM is hardly maintained in New Physics models with a broader scalar sector. Its experimental test is given by the ρ parameter that can be determined through electroweak precision tests. In this work, we consider a particular case in the 2HDM class where the custodial symmetry is preserved. The study of the phenomenology concerning flavour quantities coming from the neutral strange B mesons system, such as the mass diference or the two muons rare decay, or from CP violation in the neutral kaon system, provides then interesting constraints in the framework of this custodial invariant 2HDM with MFV.

Contents

Introduction

The last few years have been a very exciting period for the field of particle physics. After decades of imposing itself, both mathematically and experimentally, as the most consistent model in order to describe the behaviour of elementary particles and fundamental interactions, the success of the Standard Model (SM) has certainly reached a peak with the discovery of the new scalar at the LHC.

During the previous decades, although being used as the most reliable way to describe particle physics phenomena, the SM was hardly considered as the definite theory to describe high energy physics and this for several reasons. One of the main reasons was due to the fact that the mechanism able to account for gauge bosons and fermion masses, known as the Brout-Englert-Higgs (BEH) mechanism, predicted the existence of a scalar particle that had not been detected for almost fourty years. Moreover, despite this mechanism being able to provide masses to the elementary particles of the SM in a consistent way, it introduced additional questions concerning naturalness. First, the BEH mechanism seems unable to account for the fermion masses striking hierarchy that is especially manifest when considering the small neutrino masses and the very heavy top quark. Second, the BEH mechanism does not introduce a principle that accounts for the fact that the Higgs boson mass is so light compared to the Planck scale. This fine-tuning problem, known as the hierarchy problem, as well as other sectors of the SM that were considered *problematic* either theoretically or experimentally have motivated an abundant research in

phenomenology during the past few decades by studying alternative theoretical models. Countless attempts Beyond the Standard Model (BSM) have been proposed with the aim of both solving the previously mentioned unconsistencies and providing new predictions to be tested by the high energy experiments, while waiting for the potential observation of the Higgs boson.

The new boson discovered during the first run of the LHC [1, 2] seems to have confirmed the SM as the correct theory at the electroweak scale with a scalar particle associated to the spontaneous symmetry breaking of the gauge theory. The refinement of the measurements of the new scalar properties through more accumulated data shows an impressive consistency with the SM and its spontaneous symmetry breaking mechanism. Such a discovery is not only historical in how it accurately confirms a theory developped four decades beforehand but also because of the technology, the experimental precision and the human effort needed to provide it.

Besides the search for the Higgs boson, other important results have been brought to us in the past few years. The observation of the very rare decays $B_s \to \mu^+\mu^-$ by the LHCb and CMS experiments at the LHC [3] has opened the way for the indirect observation (or constraint) of new physics through loop effects. The impressive improvement in the determination of flavour physics observables, both in the theoretical field and in the experimental one, have provided us with the unitarity triangle fit [4] that also confirms the SM and its Cabibbo-Kobayashi-Maskawa (CKM) quark mixing matrix as the best theoretical framework in order to explain flavour and CP violation. Progress in the lepton sector mixing has also been made and many improvements in the precision of the parameters involved are expected in the following years.

Together with the success of the SM, it is undeniable that BSM models suffer from serious constraints that go from almost ruling out the model as a whole to allowing for a surviving parameter space that is no longer appropriate to account for the physics problems these models were supposed to solve in the beginning. In that sense, these past few years have been very exciting from the experimental point of view, but have become tougher in the phenomenological field. It is worth to mention that data from the second run of the LHC in 2015 showed an excess of events in the Higgs analysis of the diphoton decay channel at around 750 GeV [5, 6] and brought back some excitement in the theoretical

community with the possibility of a not SM-like scalar. However, later results from data taken during 2016 by CMS combined with the previous data show no significant excess [7]. Therefore, there are no significant hints on new scalar (or other) bosons for now.

In the flavour sector, some unexpected experimental results have also drawn the attention of many during the past few years. The protagonist has been the inconsistency between the LHCb measurement of one of the angular observables (P_5') of the $B \to K^* \mu^+ \mu^-$ decay and its SM prediction. A first local discrepancy of 3.7σ was observed in [8] and it has been supported by the more recently observed 3.4σ deviation with respect to the SM [9]. This result has already encouraged numerous studies on possible NP contributions to P_5' [10–12]. It is in such a context that our work falls. Its very first aim is to study models with an additional scalar doublet compared to the SM, known as Two Higgs Doublet Models (2HDM). This kind of models have been widely studied in the literature and have even motivated direct searches analyses at colliders. Some popular BSM models like Supersymmetry (SUSY) contain a restricted two Higgs doublet scalar sector. The amount of parameters introduced by this class of models can be reduced through several hypotheses. The approach we have taken for this work falls in the context of the current success of the SM. While studying BSM models one needs to ponder about what are the properties of the SM that make it so succesful and think about the advantages or solutions the NP model might offer. While concentrating in the implications of a 2HDM in the flavour sector in order to provide predictions that could be experimentally observed in the near future, we have tried to keep what makes the SM flavour description so successful, i.e. the CKM mixing matrix. This paradigm accurately accounts for the observations concerning both flavour and CP violation by introducting a mixing matrix with a single complex phase in the case of three flavour generations. When studying a model with two scalar doublets, new flavour structures beyond the SM ones are allowed. We have therefore constrained our model in such a way that the new flavour structures do not introduce additional fine-tuning, mass hierarchies or CPV phases with respect to the SM. In order to do so, we have considered the Minimal Flavour Violation (MFV) hypothesis.

Another property of the SM that is hardly maintained in BSM models with a

broader scalar sector is the experimental test of its custodial symmetry given by the ρ parameter that can be determined through EW precision tests. When introducing additional scalars, corrections to this parameter are in principle sizable and the current precision in this sector is very high. This constitutes the main reason why, in this work, we have considered a particular case in the 2HDM class where the custodial symmetry, that in the SM rises accidentally, is preserved.

This work is divided in three main chapters. The first one introduces the SM while focalizing on the properties we have mentioned before and that are going to be exploited in the next chapters. The second chapter focuses on the 2HDM and the possible cases one can study following the different SM properties one desires to keep. In the third chapter, we study a particular 2HDM that conserves custodial symmetry and whose flavour structure follows the MFV prescription. We study the phenomenology of this model mainly concerning three flavour quantities ϵ_K, ΔM_{B_s} and $\mathcal{B}(B_s \to \mu^+\mu^-)$ to finally draw the main conclusions about the status of the model.

Chapter 1

The Standard Model

Relativistic processes and collision phenomena involving the elementary particles take place at too high energies and momenta to be described by ordinary Quantum Mechanics. In this regime, the most suitable framework to account for these processes is Quantum Field Theory, where the dynamical variables that describe a given physical system are fields, i.e. variables labelled by the space-time coordinates, and independent of each other. The Standard Model is the Quantum Field Theory describing the electroweak and strong interactions between the elementary particles of nature. Based on Gauge invariance, that means, symmetries where the parameters can depend on space-time. These local symmetries will give rise to conservation laws that can be verified by experiments.

In this chapter, we will describe the SM with a particular emphasis on electroweak interactions. We do not intend to give an exhaustive description of the model, but rather to state the formalism and main features that will be of interest in the following chapters.

1.1 The Standard Model basics

1.1.1 Fermions, Bosons and electroweak interactions

To begin with, let us take a look at the interaction Lagrangian that describes weak interactions at low energies, the so-called Fermi Lagrangian[1]. The terms responsible for neutron beta decay and muon decay are given by the following terms of the Lagrangian

$$\mathcal{L} = -\frac{G^\beta}{\sqrt{2}}\bar{p}\gamma^\alpha(1-a\gamma_5)n\bar{e}\gamma_\alpha(1-a\gamma_5)\nu_e - \frac{G^\mu}{\sqrt{2}}\bar{\nu_\mu}\gamma^\alpha(1-\gamma_5)\mu\bar{e}\gamma_\alpha(1-\gamma_5)\nu_e. \quad (1.1)$$

The value $a = 1.239 \pm 0.09$ can be extracted from hyperon decays while the experimental values of the neutron and muon lifetimes [14]:

$$\tau_n = 880.3 \pm 1.1s \qquad \tau_\mu = (2.1969811 \pm 0.0000022) \times 10^{-6}s, \quad (1.2)$$

allow us to determine the constants G^β and G^μ

$$G^\beta = G^\mu = G_F = (1.16637 \pm 0.00001) \times 10^{-5}\text{GeV}^{-2}. \quad (1.3)$$

Such a result suggests the universality of weak interactions. This theory is manifestly non-renormalizable since the Lagrangian in (1.1) generates operators of dimension 6. Therefore, it breaks the unitarity of the S matrix since the cross-sections of the related processes grow endlessly with energy. However, the Fermi theory already contains the physical information to build a well defined theory of weak interactions. The gauge theory that we want to build has to reduce to the form (1.1) in the low-energy limit such that the Fermi four-fermion interaction can be interpreted as the effective interaction vertex that arises from the exchange of a very massive vector compared to its momentum. Such an approach solves the problem of renormalizability, since gauge theories are renormalizable. It also partially solves the unitarity problem, since the charged vector boson mass acts as a cut-off to avoid the growth of cross-sections with energy. However, the massive vector theory is not unitary without an underlying Higgs mechanism. A famous example is given by the $WW \to WW$ scattering that needs the Higgs contribution to show its unitary

[1] This section is based on notes of an introductury course to the Standard Model of Electroweak Interactions by Giovanni Ridolfi [13].

behavior, but we will introduce said mechanism later on.
The succesful gauge theory of weak interactions proposed by Glashow, Weinberg and Salam [15–17] is based on the local symmetry group $SU(2)_L \times U(1)_Y$. To each generator of the symmetry we can associate a vectorial field that will mediate the corresponding interaction. The B_μ field will be associated to the Y generator of the $U(1)_Y$ symmetry while the $W_\mu^{1,2,3}$ fields will be associated to the $SU(2)_L$ generators $T_{1,2,3}$ that are defined by the relation

$$[T^a, T^b] = i\epsilon^{abc}T^c. \tag{1.4}$$

A coupling constant will be associated to each gauge group, g for $SU(2)_L$ and g' for $U(1)_Y$. The strength tensors of these fields are respectively:

$$W^a_{\mu\nu} = \partial_\mu W^a_\nu - \partial_\nu W^a_\mu + g\epsilon^{abc}W^b_\mu W^c_\nu \tag{1.5}$$

$$B_{\mu\nu} = \partial_\mu B_\nu - \partial_\nu B_\mu, \tag{1.6}$$

giving rise to the following gauge interaction Lagrangian

$$\mathcal{L}_G = -\frac{1}{4}W^a_{\mu\nu}W_a^{\mu\nu} - \frac{1}{4}B_{\mu\nu}B^{\mu\nu}. \tag{1.7}$$

Let us now move on to the matter fields. The theory contains three generations of left and right-handed chiral quarks and leptons. The left-handed fermions transform as $SU(2)_L$ doublets

$$Q_L = \begin{pmatrix} u_L \\ d_L \end{pmatrix} \qquad L_L = \begin{pmatrix} \nu^\ell_L \\ \ell_L \end{pmatrix}, \tag{1.8}$$

and the right-handed fermions u_R, d_R, and ℓ_R transform as $SU(2)_L$ singlets while right-handed neutrinos ν^ℓ_R do not enter the theory. Building the covariant derivative

$$D_\mu = \partial_\mu - igT_aW^a_\mu - ig'\frac{Y}{2}B_\mu, \tag{1.9}$$

the $SU(2)_L \times U(1)_Y$ invariant matter Lagrangian is therefore given by

$$\begin{aligned} \mathcal{L} &= i\bar{Q}_L D_\mu\gamma^\mu Q_L + i\bar{u}_R D_\mu\gamma^\mu u_R + i\bar{d}_R D_\mu\gamma^\mu d_R \\ &\quad + i\bar{L}_L D_\mu\gamma^\mu L_L + i\bar{\ell}_R D_\mu\gamma^\mu \ell_R \qquad (1.10) \\ &= \mathcal{L}_k + \mathcal{L}_c + \mathcal{L}_n. \qquad (1.11) \end{aligned}$$

The complete kinetic component of the Lagrangian reads:

$$\mathcal{L}_k = i\bar{Q}_L \not{D} Q_L + i\bar{u}_R \not{D} u_R + i\bar{d}_R \not{D} d_R + i\bar{L}_L \not{D} L_L + i\bar{\ell}_R \not{D} \ell_R. \tag{1.12}$$

Therefore, making use of the definitions

$$W_\mu^\pm \equiv \frac{1}{\sqrt{2}}(W_\mu^1 \mp iW_\mu^2) \qquad T^\pm \equiv \frac{1}{2}(T^1 \pm iT^2), \tag{1.13}$$

the charged sector of the Lagrangian becomes

$$\begin{aligned}\mathcal{L}_c &= \frac{g}{\sqrt{2}}\bar{Q}_L\gamma^\mu T^+ Q_L W_\mu^+ + \frac{g}{\sqrt{2}}\bar{Q}_L\gamma^\mu T^- Q_L W_\mu^- \\ &\quad + \frac{g}{\sqrt{2}}\bar{L}_L\gamma^\mu T^+ L_L W_\mu^+ + \frac{g}{\sqrt{2}}\bar{L}_L\gamma^\mu T^- L_L W_\mu^-.\end{aligned} \tag{1.14}$$

Since the matrix T_3 is diagonal, the W_μ^3 field is neutral and so is the B_μ field. We can actually perform a θ_W ($\tan\theta_W = g'/g$) rotation in the neutral fields space

$$\begin{pmatrix} B_\mu \\ W_\mu^3 \end{pmatrix} = \begin{pmatrix} \cos\theta_W & -\sin\theta_W \\ \sin\theta_W & \cos\theta_W \end{pmatrix} \begin{pmatrix} A_\mu \\ Z_\mu \end{pmatrix}. \tag{1.15}$$

This way, the neutral sector of the Lagrangian is given in terms of the electromagnetic field currents, associated to A_μ, and the weak neutral currents, associated to Z_μ:

$$\begin{aligned}\mathcal{L}_n &= \bar{\Psi}\gamma_\mu \left(g\sin\theta_W T^3 + \frac{Y}{2}g'\cos\theta_W \right) \Psi A^\mu \\ &\quad + \bar{\Psi}\gamma_\mu \left(g\cos\theta_W T^3 - \frac{Y}{2}g'\sin\theta_W \right) \Psi Z^\mu\end{aligned} \tag{1.16}$$

with Ψ representing all the matter fields of the theory. The electromagnetic charge is therefore given by:

$$eQ = g\sin\theta_W T^3 + \frac{Y}{2}g'\cos\theta_W. \tag{1.17}$$

Since the hypercharge Y always appears combined with the coupling constant g', we have the freedom of rescaling the hypercharge by a factor and hide it in g'. Therefore, the lepton hypercharge is conventionally fixed to $Y(L) = -1$. From this convention and from (1.17), we then obtain the relations:

$$g\sin\theta_W = g'\cos\theta_W = e \qquad \rightarrow \qquad T^3 + \frac{Y}{2} = Q. \tag{1.18}$$

This gauge theory has proved itself succesful not only to provide a renormalizable Lagrangian for the weak interactions, but also to account for the electromagnetic interactions. However, an issue concerning the bosons masses

remains. The photon, mediator associated to the A_μ field, is most probably massless since the current experimental bound [14] reads

$$m_\gamma < 1 \times 10^{-18}\text{eV}. \tag{1.19}$$

However, in order for the weak interactions gauge theory to match the Fermi Lagrangian in (1.1) both the Fermi effective theory

$$-\frac{G_F}{\sqrt{2}}\bar{u}\gamma^\mu(1-\gamma_5)d\bar{e}\gamma_\mu(1-\gamma_5)\nu_e, \tag{1.20}$$

and the gauge theory where the process is induced by the exchange of a virtual W boson of momentum q

$$\left(\frac{g}{\sqrt{2}}\bar{u}_L\gamma^\mu d_L\right)\frac{1}{q^2-m_W^2}\left(\frac{g}{\sqrt{2}}\bar{e}_L\gamma_\mu\nu_L^e\right). \tag{1.21}$$

In the low-energy limit, $q^2 \to 0$, the Fermi theory is recovered only if the W has a mass that verifies

$$\frac{G_F}{\sqrt{2}} = \left(\frac{g}{2\sqrt{2}}\right)^2\frac{1}{m_W^2}. \tag{1.22}$$

Using (1.18), we obtain a lower bound for m_W:

$$m_W \geq 37.3 \text{ GeV}. \tag{1.23}$$

The weak interaction mediators are therefore quite heavy. However, introducing a gauge boson mass term in the $SU(2)_L \times U(1)_Y$ Lagrangian would explicitely break the gauge symmetry and spoil the renormalizability and unitarity of the theory once again. A mechanism must be provided in order to introduce mass terms for the gauge bosons without losing these properties.

1.1.2 The Spontaneous Symmetry Breaking mechanism

The Spontaneous Symmetry Breaking (SSB) mechanism will allow us to solve the problem we encountered at the end of the last section. The main idea of this mechanism, known as the Brout-Englert-Higgs (BEH) mechanism [18–20], consists in keeping the Lagrangian invariant under gauge symmetry transformations while allowing the vacuum to break the symmetry.

The abelian case

In order to illustrate the principle let us begin with a simple abelian case, mainly a $U(1)$ gauge theory (like quantum electrodynamics), coupled with a single complex scalar field ϕ. The Lagrangian concerning the scalar field reads:

$$\mathcal{L}_\phi = (D_\mu\phi)^\dagger(D^\mu\phi) - V(\phi) \quad \text{with} \quad D_\mu = \partial_\mu - ieA_\mu. \tag{1.24}$$

$V(\phi)$ is the scalar field potential which, after imposing gauge invariance and renormalizability, takes the form

$$V(\phi) = -\mu^2\phi^2 + \lambda\phi^4, \tag{1.25}$$

with μ and λ being real positive parameters. The condition on λ ensures that the potential is grounded from below in order to have a ground state. Let us now explain the condition on μ. As we have mentioned previously the principle of spontaneously broken symmetries consists in keeping the Lagrangian invariant under gauge symmetry transformations while allowing the vacuum to break the symmetry. This can be achieved if the potential has a degenerate set of states with minimal energy, which transform under the gauge symmetry as the members of a given multiplet. If one of those states is arbitrarily selected as the ground state of the system, the symmetry is said to be spontaneously broken. This condition is achieved with the choice of μ being real positive since it ensures that the minimum of the potential V is not given by a single minimum $\phi = 0$ but it is given by an infinite number of degenerate minima with a non-zero value verifying the relation:

$$|\phi|^2 = \frac{\mu^2}{2\lambda} \equiv \frac{1}{2}v. \tag{1.26}$$

All these vacua are connected by gauge transformations that change the phase of the field ϕ but conserve the modulus. The system will choose one of these degenerated vacuum configurations spontaneously breaking the symmetry. After acquiring a vacuum expectation value (vev), that we chose to be real, we can expand the scalar field in terms of two real fields such as:

$$\phi(x) = \frac{1}{\sqrt{2}}[v + H(x) + iG(x)]. \tag{1.27}$$

After making use of the relation (1.26), the potential (1.25) becomes:

$$V(\phi) = \lambda v^2 H^2 + \lambda v H(H^2 + G^2) + \frac{\lambda}{4}(H^2 + G^2)^2. \tag{1.28}$$

The H field has therefore acquired a mass $m_H^2 = 2\lambda v^2$ while the G field is kept massless. Actually, the G field could have been removed from the beginning with an appropriate choice of gauge transformation, meaning that this field is actually unphysical in the unitary gauge. Regarding the scalar kinetic part of the Lagrangian, after SSB, it contains a mass term for the gauge boson of the form:

$$\frac{1}{2}e^2 v^2 A_\mu A^\mu. \tag{1.29}$$

This shows how the SSB mechanism is actually able to provide mass terms to the gauge bosons of the theory, at scales below v, without explicitly breaking the gauge invariance of the theory. For each massive gauge boson, a Goldstone scalar disappears (in this case the G field) from the physical spectrum in order to conserve the number of degrees of freedom. As a consequence of the BEH mechanism, only one physical scalar H state appears, the so-called Higgs boson.

The $SU(2)_L \times U(1)_Y$ SSB mechanism

The first requirement to be imposed to the scalar field responsible for the spontaneous breaking of the SM symmetry is that it transforms non-trivially under the gauge group. Furthermore, it must leave the $U(1)$ part of the symmetry unbroken since the photon needs to stay massless. The simplest way to do so is to assign the scalar field to a doublet representation of $SU(2)$

$$\phi = \begin{pmatrix} \phi_1 \\ \phi_2 \end{pmatrix}. \tag{1.30}$$

In analogy with the previous case, the most general scalar potential is given by:

$$V(\phi) = -\mu^2|\phi|^2 + \lambda|\phi|^4. \tag{1.31}$$

It has a minimum at

$$|\phi|^2 = \frac{\mu^2}{2\lambda} \equiv \frac{1}{2}v. \tag{1.32}$$

Since we want the vacuum configuration

$$\langle\phi\rangle = \frac{1}{\sqrt{2}}\begin{pmatrix} v_1 \\ v_2 \end{pmatrix} \qquad \text{with} \qquad |v_1|^2 + |v_2|^2 = v \tag{1.33}$$

to preserve the electric charge, we can already fix the value of the hypercharge. Indeed, the invariance of the vacuum under $U(1)_{em}$ transformations requires

$$\begin{pmatrix} Q_1 & 0 \\ 0 & Q_2 \end{pmatrix} \begin{pmatrix} v_1 \\ v_2 \end{pmatrix} = \begin{pmatrix} \frac{1}{2} + \frac{Y}{2} & 0 \\ 0 & -\frac{1}{2} + \frac{Y}{2} \end{pmatrix} \begin{pmatrix} v_1 \\ v_2 \end{pmatrix} = \begin{pmatrix} 0 \\ 0 \end{pmatrix}, \quad (1.34)$$

where we used the result in (1.18). We have therefore two possible configurations:

$$1)\ v_1 = 0;\ |v_2| = v;\ Y = 1 \qquad 2)\ v_2 = 0;\ |v_1| = v;\ Y = -1. \quad (1.35)$$

We chose the first configuration and, similar to the abelian case, we expand the scalar doublet around its vacuum through the parametrization

$$\phi(x) = \frac{1}{\sqrt{2}} \begin{pmatrix} 0 \\ v + H(x) \end{pmatrix}. \quad (1.36)$$

Unlike our discussion in the abelian case, here, we have made a gauge choice in order to eliminate the unphysical Goldstone Boson from the beginning. The scalar potential becomes:

$$V(\phi) = \frac{1}{2}(2\lambda v^2)H^2 + \lambda v H^3 + \frac{\lambda}{4}H^4. \quad (1.37)$$

Replacing (1.36) in the $(D_\mu\phi)^\dagger(D^\mu\phi)$ term, we obtain:

$$(D_\mu\phi)^\dagger(D^\mu\phi) = \frac{1}{2}\partial^\mu H \partial_\mu H + \left[\frac{1}{4}gW^{+\mu}W^-_\mu + \frac{1}{8}(g^2 + g'^2)Z^\mu Z_\mu\right](H + v). \quad (1.38)$$

As a result, there are no mass terms for the photon, while the W and Z bosons have both acquired a mass:

$$m_W^2 = \frac{g^2 v^2}{4} \quad (1.39)$$

$$m_Z^2 = \frac{v^2}{4}(g^2 + g'^2). \quad (1.40)$$

From these two last equations, we can derive the quite interesting tree-level mass relation:

$$m_Z^2 = \frac{m_W^2}{\cos^2\theta_W} \quad (1.41)$$

which will be discussed later on. Finally, the value of the vacuum v can be obtained from the experimental value of G_F and the relation (1.22)

$$v^2 = \frac{1}{G_F\sqrt{2}} \simeq (246.22\ \text{GeV})^2. \quad (1.42)$$

1.1.3 Fermion masses and flavour mixing

So far, we have been able to construct a gauge invariant theory of electroweak interactions with a scalar field whose vacuum spontaneously breaks the symmetry allowing the generation of masses for the W and Z gauge bosons. However, there are still two issues that need to be solved. On the one hand fermion mass terms are also forbidden by the gauge symmetry of the theory. On the other hand, we should still specify how does the scalar field ϕ couple to the fermions. In this section we will show how these two problems can be solved together. The most general, renormalizable, gauge invariant Lagrangian which couples the scalar field to the fermions of the theory is a Yukawa sector that reads:

$$\mathcal{L}_Y = -\bar{Q'}_L \phi Y'_D d'_R - \bar{Q'}_L \tilde{\phi} Y'_U u'_R - \bar{L'}_L \phi Y'_\ell \ell'_R + h.c. \quad \text{with} \quad \tilde{\phi} = i\tau_2 \phi^*. \tag{1.43}$$

Note that, since the theory does not account for right-handed neutrinos, the lepton Yukawa sector contains only one term and its hermitian conjugate. Taking the parametrization for the Higgs field in (1.36) it is easy to notice that the left handed neutrinos do not couple to the scalar field either. The primes assigned to the fermions and their couplings are due to the fact that the $Y'_{D,U,\ell}$ couplings are arbitrary 3×3 matrices mixing the quark and lepton of different families. These matrices can actually be diagonalized by bi-unitary transformations defined by:

$$\left.\begin{array}{l} d'_{L,R} = V^d_{L,R} d_{L,R} \\ u'_{L,R} = V^u_{L,R} u_{L,R} \\ \ell'_{L,R} = V^\ell_{L,R} \ell_{L,R} \end{array}\right\} \quad \Rightarrow \quad \left\{\begin{array}{l} Y_D = V_L^{d\dagger} Y'_D V_R^d \\ Y_U = V_L^{u\dagger} Y'_U V_R^u \\ Y_\ell = V_L^{\ell\dagger} Y'_\ell V_R^\ell \end{array}\right. . \tag{1.44}$$

After diagonalisation and using the gauge choice in (1.36), the Yukawa Lagrangian becomes:

$$\mathcal{L}_Y = -\frac{1}{\sqrt{2}}(v+H) \sum_{f=1}^{3} \left(\bar{d}^f (Y_D)_{ff} d^f + \bar{u}^f (Y_U)_{ff} u^f + \bar{\ell}^f (Y_\ell)_{ff} \ell^f \right), \tag{1.45}$$

where we sum over the fermion flavours f. We can identify the fermion mass terms as being those related to the scalar vev v

$$M_D = \frac{v}{\sqrt{2}} Y_D; \qquad M_U = \frac{v}{\sqrt{2}} Y_U; \qquad M_\ell = \frac{v}{\sqrt{2}} Y_\ell. \tag{1.46}$$

The transformations in (1.44) leave invariant the neutral current Lagrangian (1.16) due to the unitary nature of the $V_{L,R}^{u,d,\ell}$ matrices. We will emphasize this feature in a later section. Let us, for now, analyse what are the consequences of such transformations on the charged current Lagrangian (1.14). Since the up and down quarks couple to the scalar through different Yukawa terms in (1.43), the general transformations in (1.44) is not the same for both up and down quarks. As a consequence, the quark charged current Lagrangian becomes:

$$\mathcal{L}_c^q = \frac{g}{\sqrt{2}}\bar{u}_L^i\gamma^\mu(V_L^{u\dagger}V_L^d)_{ij}d_L^j W_\mu^+ + \frac{g}{\sqrt{2}}\bar{d}_L^i\gamma^\mu(V_L^{d\dagger}V_L^u)_{ij}u_L^j W_\mu^-. \tag{1.47}$$

The matrix

$$V_{CKM} \equiv V_L^{u\dagger}V_L^d, \tag{1.48}$$

is known as the Cabibbo-Kobayashi-Maskawa mixing matrix. It is the unitary matrix responsible for the mixing between the different quark families. Yet, the values of its entries need to be determined by experiments. It is also responsible for CP violation in the flavour sector, but we will come back to this feature later on.

However, in the lepton case, since the neutrinos do not couple to the scalar field, we have yet to specify a transformation law for the left-handed neutrinos. We actually have the freedom to choose the same transformation as the charged leptons. We therefore obtain:

$$\mathcal{L}_c^\ell = \frac{g}{\sqrt{2}}\bar{\ell}_L^i\gamma^\mu(V_L^{\ell\dagger}V_L^\ell)_{ij}\nu_L^j W_\mu^+ + \frac{g}{\sqrt{2}}\bar{\nu}_L^i\gamma^\mu(V_L^{\ell\dagger}V_L^\ell)_{ij}\ell_L^j W_\mu^-. \tag{1.49}$$

Since the V_L^ℓ matrix is unitary ($V_L^{\ell\dagger}V_L^\ell = \mathbf{1}$), we conclude that, in the original formulation of the SM, there is flavour conservation in the lepton charged currents. However, experiments have long suggested that neutrinos do actually mix because they have non-zero masses [14]. This constitutes a very important discovery that has led to the 2015 Nobel Prize, awarded to Takaaki Kajita and Arthur B. McDonald "*for the discovery of neutrino oscillations, which shows that neutrinos have mass*"[2]. Although we will not discuss the topic in this work, let us recall that a succesful theoretical explanation of this phenomenon is given by the so-called "see-saw mechanism" [21] that manages to introduce very small mass terms for the neutrinos in the context of the $SU(2)_L \times U(1)_Y$

[2]The Nobel Prize in Physics 2015 press release.

symmetry. Mixing between different neutrino flavours is also successfully accounted for in this mechanism.

1.1.4 Quantum Chromodynamics

Before finishing the section about the SM, we briefly introduce Quantum Chromodynamics (QCD). QCD is the gauge theory that describes the strong interactions between the quarks and the gluons, which are the QCD mediators. Given the purpose of this work, we will not give an exhaustive description of the strong sector of the SM, but rather a short summary of its main features. Strong interactions are characterized by three basic properties: asymptotic freedom, confinement and dynamical chiral symmetry breaking. The confinement hypothesis, requires that there are only colour-singlet configurations corresponding to meson ($q\bar{q}$) and baryon (qqq) states. This is among others one of the main reasons to base the theory of colour interactions on the group $SU(3)$. The QCD Lagrangian is invariant under $SU(3)_C$ colour transformations, with coulour being the charge associated to the QCD Gauge theory. The quarks behave as the 3-dimensional fundamental representation of $SU(3)_C$ with therefore three colour charges, while the gluons transform under the 8-dimensional adjoint representation generated by the Gell-Mann matrices, that satisfy the commutation relations

$$\left[\lambda^a, \lambda^b\right] = 2if^{abc}\lambda_c \qquad a = 1, 2, ..., 8, \tag{1.50}$$

where f^{abc} are real and totally antisymmetric constants. In order to build an invariant Lagrangian under $SU(3)$ local transformations $\theta_a(x)$, we need to change the quark derivatives of the free quark Lagrangian into covariant derivatives, introducing this way the gluon gauge bosons $G^\mu_a(x)$

$$D^\mu q_f \equiv \left(\partial^\mu - ig_s\frac{\lambda^a}{2}G^\mu_a(x)\right) q_f \equiv \left(\partial^\mu - ig_s G^\mu(x)\right) q_f \tag{1.51}$$

In order for the Lagrangian to be invariant, the quark and gluon fields transform as

$$q^\alpha_f \quad \rightarrow \quad (q^\alpha_f)' = q^\alpha_f - ig_s\left(\frac{\lambda^a}{2}\right)_{\alpha\beta}\delta\theta_a q^\beta_f \tag{1.52}$$

$$G^\mu_a \quad \rightarrow \quad (G^\mu_a)' = G^\mu_a - \partial^\mu(\delta\theta_a) + g_s f^{abc}\delta\theta_b G^\mu_c. \tag{1.53}$$

Introducing the gluon field strengths

$$G_a^{\mu\nu} = \partial^\mu G_a^\nu - \partial^\nu G_a^\mu + g_s f^{abc} G_b^\mu G_c^\nu, \tag{1.54}$$

we finally obtain the $SU(3)_C$ invariant QCD Lagrangian

$$\mathcal{L}_{QCD} \equiv -\frac{1}{4} G_a^{\mu\nu} G^a_{\mu\nu} + \sum_f \bar{q}_f (i\gamma_\mu D^\mu - m_f) q_f. \tag{1.55}$$

The Lagrangian given above looks very simple because of its symmetry properties, but it contains very rich physics in it. We can actually decompose the different terms of the Lagrangian to derive some praticular properties of the strong interactions.

$$\mathcal{L}_{QCD} = -\frac{1}{4} \left(\partial^\mu G_a^\nu - \partial^\nu G_a^\mu\right) \left(\partial_\mu G^a_\nu - \partial_\nu G^a_\mu\right) + \sum_f \bar{q}_f^\alpha (i\gamma_\mu \partial^\mu - m_f) q_f^\alpha \tag{1.56}$$

$$+ g_s G_a^\mu \sum_f \bar{q}_f^\alpha \gamma_\mu \left(\frac{\lambda^a}{2}\right)_{\alpha\beta} q_f^\beta - \frac{g_s}{2} f^{abc} \left(\partial^\mu G_a^\nu - \partial_\nu G_a^\mu\right) G_{b\mu} G_{c\nu} \tag{1.57}$$

$$- g_s^2 f^{abc} f_{ade} G_b^\mu G_c^\nu G_\mu^d G_\nu^e \tag{1.58}$$

The first two terms contain the gluon and quark kinetic terms, which give rise to the corresponding propagators. The third term contains the interaction between quarks and gluons. Finally, due to the non-abelian character of $SU(3)_C$, the last two terms are generated, containing the cubic and quartic gluon self-interactions with the same coupling g_s as the fermionic piece of the Lagrangian. Because of the gluonic self-interactions, the QCD coupling becomes smaller at short distances, leading to an asymptotically-free quantum field theory. Perturbation theory can then be applied at large momentum transfers. The resulting predictions have achieved a remarkable success, explaining a wide range of phenomena in terms of a single coupling. The growing of the running coupling at low-energies is consistent with the confinement of quarks and gluons into colour-singlet hadronic states. However there is still no rigorous proof of this property and the dynamical details of hadronization remain unknown.

We have previously mentioned the dynamical symmetry breaking of the chiral symmetry as one of the three basic properties of strong interactions. Indeed, the QCD Lagrangian is invariant under $SU(n_F)_L \times SU(n_F)_R$ in the absence of quark masses, with n_F the number of flavours. However, this chiral symmetry, which should be approximately good in the light quark sector (u,d,s), is not seen in the hadronic spectrum. Although hadrons can be classified in

$SU(3)_V$ representations, degenerate multiplets with opposite parity do not exist. Besides, the octet of pseudoscalar mesons happens to be much lighter than all the other hadronic states. To be consistent with this experimental fact, $SU(3)_L \times SU(3)_R$ spontaneously breaks into $SU(3)_{L+R}$ and an octet of pseudoscalar massless bosons appears in the theory. These Goldston Bosons can be identified with the eight lightest hadronic states (π^+, π^-, π^0, η, K^+, K^-, K^0 and $\bar{K}^0$) whose small masses are generated by the quark-mass matrix, which explicitly breaks the global chiral symmetry of the QCD Lagrangian. The Goldstone nature of the pseudoscalar mesons implies strong constraints on their interactions, which can be most easily analyzed on the basis of an effective Lagrangian. This has motivated the developpement of the chiral effective theory.
As a final remark, we underline the fact that just like how electroweak interactions do not couple to colour, strong interactions do not couple to flavour either, giving rise to the final SM symmetry group

$$SU(2)_L \times U(1)_Y \times SU(3)_C. \tag{1.59}$$

1.2 Accidents and accidental symmetries of the Standard Model

The SM of electroweak interactions together with its strong interaction extension has shown an astonishing success in its aim to describe physical phenomena in particle physics. However, a non-negligible part of this success is due to some features of the model that do not result from main theoretical foundations. In fact, the SM presents additional features and global symmetries that show up accidentally in some sectors. They provide interesting tests of the model which can be verified experimentally with an impressive accuracy. At the same time, the SM presents its own problems, pointing to the idea that the SM may not be the final story concerning the description of elementary particles and fundamental interactions.

1.2.1 Flavour Changing Neutral Currents

We have mentioned before that flavour is conserved in the SM neutral current Lagrangian (1.16) due to the unitarity of the diagonalization matrices in (1.44). Let us take a deeper look at this feature as well as at its important experimental consequences. The conservation of flavour by the neutral current Lagrangian ensures the absence of this kind of currents at tree-level. However, with the help of the flavour changing charged currents, one can construct one-loop and higher order diagrams which mediate FCNC processes. Let us illustrate this feature in the Feynman diagram formalism.

Box diagrams

These diagrams involve the exchange of virtual $W^{\pm}$ bosons between different flavoured quarks or leptons. Examples of box diagram contributions to $K^0 - \bar{K}^0$ transitions are given in fig.1.1.

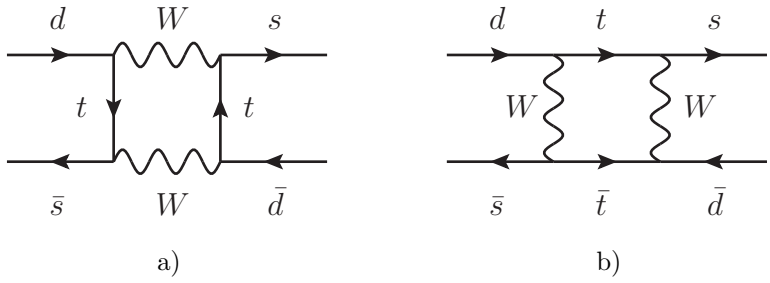

Figure 1.1: *Box diagrams of the top-quark contribution to the $K^0 - \bar{K}^0$ mixing*

Similar diagrams to Fig.1.1a), where the outcoming fermions are leptons, contribute to $K \to \pi\bar{\nu}\nu$ rare decays.

Penguin diagrams

The so-called Penguin diagrams concern loops between different flavoured quarks involving mainly t quarks as well as $W^{\pm}$ bosons. A penguin diagram contributing to $K \to \pi\nu\bar{\nu}$ decays is shown in fig.1.2.

The fact that these decays take place only as loop effects makes them particularly useful for testing possible loop contributions involving new particles Beyond the Standard Model (BSM). Decays like $K \to \pi\nu\bar{\nu}$ are very rare since they only take place through box and penguin loop diagrams and are therefore very suppressed. The current measurement of the branching ratio of $K^+ \to \pi^+\bar{\nu}\nu$ is based on a combination of seven events observed by the BNL-E787 and BNL-E949 collaborations [22]

$$\mathcal{B}(K^+ \to \pi^+\nu\bar{\nu}) = (1.73^{+1.15}_{-1.05}) \times 10^{-10}. \tag{1.60}$$

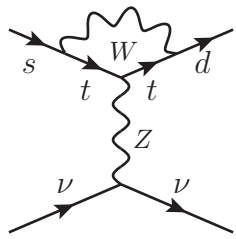

Figure 1.2: *Penguin diagram of the top-quark contribution to the $K \to \pi\nu\bar{\nu}$ decay*

The NA62 experiment at CERN expects to provide $\mathcal{O}(100)$ signal candidates on this decay by the end of 2017. The KOTO experiment at KEK will try to achieve SM sensibility in the $K^0 \to \pi^0\bar{\nu}\nu$ observation with a 3σ branching ratio and a $\pm 10\%$ accuracy in a second stage. These kind of rare decays constitute very important probes of the FCNC suppression mechanism of the SM and privileged channels in order to obtain evidence of NP.

Higgs mediated FCNC

We have previously argued that the neutral current gauge lagrangian is left invariant by the transformations in (1.44) which ensure that there are no gauge mediated FCNC at tree level. Once the mass matrices are diagonalised by those same transformations, there are no Higgs mediated FCNC either in the SM. Besides, the fact that the Higgs boson couplings to fermions are given by the fermion masses, makes its contribution to higher order effects, like penguin diagrams, almost negligible. In models with more involved scalar sectors, like

we will see in the next chapter with a 2HDM, one can generally expect Higgs mediated FCNC at tree-level. The very low rate of FCNC observations constitutes one of the main constraints to models with a broader scalar sector as well as a place to look for possible BSM effects.

1.2.2 The Custodial Symmetry

The mass relation between the weak interaction gauge bosons in (1.41) can be parametrized in the following way:

$$\rho \equiv \frac{m_W^2}{m_Z^2 \cos^2 \theta_W} = 1. \tag{1.61}$$

This relation holds at tree-level in the SM but could receive sizeable quantum contributions. However, we will show in this section that the Higgs Lagrangian conserves a symmetry that prevents the ρ parameter of receiving large corrections. Even if the Higgs Lagrangian is obviously $SU(2)_L \times U(1)_Y$ invariant by construction, the Higgs potential displays a wider $SU(2)_L \times SU(2)_R$ symmetry. In order to clearly see this, it is useful to define the following matrix:

$$\Phi = (\phi, \tilde{\phi}) = \begin{pmatrix} \phi^+ & \phi^{0*} \\ \phi^0 & -\phi^- \end{pmatrix}. \tag{1.62}$$

Making use of this formalism, the scalar potential can be writen in terms of the Φ matrix as:

$$V(\Phi) = -\frac{\mu^2}{2}\mathrm{Tr}(\Phi^\dagger \Phi) + \frac{\lambda}{2}\mathrm{Tr}(\Phi^\dagger \Phi)^2. \tag{1.63}$$

Both the fields ϕ and $\tilde{\phi}$, defined in (1.43), transform as doublets of $SU(2)$. Therefore, the Φ field transforms under a $SU(2)_L \times SU(2)_R$ symmetry

$$\Phi \to L \Phi R^\dagger, \tag{1.64}$$

leaving the potential (1.63) invariant. We can also try to write the Higgs kinetic term in a $SU(2)_L \times SU(2)_R$ invariant way. The covariant derivative can be writen is terms of Φ as:

$$D_\mu \Phi = \partial_\mu \Phi + i\frac{g}{2} T^i \cdot W_\mu^i \Phi - i\frac{g'}{2} B_\mu \Phi T_3. \tag{1.65}$$

Under generic $SU(2)_L$ and $U(1)_Y$, Φ transforms as follows:

$$SU(2)_L \quad : \quad \Phi \to L\Phi \tag{1.66}$$

$$U(1)_Y \quad : \quad \Phi \to \Phi e^{-\frac{i}{2}T_3\theta}. \tag{1.67}$$

The $SU(2)_L$ transformations leave the kinetic term $1/2\mathrm{Tr}(D_\mu\Phi^\dagger D^\mu\Phi)$ invariant. However, we can already guess that this will not be the case for $SU(2)_R$ transformations due to the g' term in (1.65). The global symmetry becomes therefore manifest in the Higgs kinetic terms only in the $g' \to 0$ limit if Φ transforms as:

$$SU(2)_L \times SU(2)_R : \qquad \Phi \to L\Phi R^\dagger, \tag{1.68}$$

$$\frac{1}{2}\mathrm{Tr}(D_\mu\Phi^\dagger)D^\mu\Phi = \mathrm{Tr}R(D_\mu\Phi^\dagger)L^\dagger L D^\mu\Phi R^\dagger. \tag{1.69}$$

As a consequence, in the $g' \to 0$ limit, the scalar Lagrangian shows a global $SU(2)_L \times SU(2)_R$ symmetry. Once SSB takes place, the $SU(2)_L \times SU(2)_R$ symmetry breaks into $SU(2)_{L+R}$ corresponding to the case where $L = R$. This vectorial symmetry is the so-called custodial symmetry. In the custodial limit, the W^+, W^- and W^3 bosons form a triplet of the global $SU(2)_{L+R}$, since there is no mixing between the neutral gauge bosons, while the photon remains massless. In the more general case where g' does not cancel and the custodial symmetry is not exact, the neutral gauge bosons mix and the $(W^1_\mu, W^2_\mu, W^3_\mu, B_\mu)$ mass matrix takes the form:

$$\begin{pmatrix} a & 0 & 0 & 0 \\ 0 & a & 0 & 0 \\ 0 & 0 & a & b \\ 0 & 0 & b & c \end{pmatrix} = \begin{pmatrix} \frac{g^2v^2}{4} & 0 & 0 & 0 \\ 0 & \frac{g^2v^2}{4} & 0 & 0 \\ 0 & 0 & \frac{g^2v^2}{4} & \frac{gg'v^2}{4} \\ 0 & 0 & \frac{gg'v^2}{4} & \frac{g'^2v^2}{4} \end{pmatrix} \tag{1.70}$$

After diagonalisation the masses of the physical neutral states Z and γ are

$$m_Z^2 \quad = \quad a + c = \frac{v^2}{4}(g^2 + g'^2) \tag{1.71}$$

$$m_\gamma^2 \quad = \quad ac - b^2 = 0. \tag{1.72}$$

This ensures the mass relation in (1.41) and therefore the identity $\rho = 1$ at tree-level. However, because the custodial symmetry is not actually conserved through the Higgs kinetic couplings, gauge and Higgs boson loop corrections to the mass terms are expected to be proportional to g'^2 and induce radiative

corrections to the ρ parameter. These $\Delta\rho$ corrections are related to the oblique parameter T [23] defined by:

$$\Delta\rho = \rho - 1 = \alpha T = \frac{g^2}{\sin^2\theta_W^2}[\Pi_{WW}(0) - \Pi_{ZZ}(0)], \tag{1.73}$$

where $\alpha = \frac{e^2}{4\pi}$ and the functions $\Pi_{WW,ZZ}(q^2)$ are the coefficients of the Minkowski metric in the gauge bosons propagators. This relation is only valid in the limit where q^2 terms can be neglected in the isospin violating pieces of the Π coefficients and q^4 terms elsewhere. Actually, gauge and scalar bosons loops will not be the only ones contributing to $\Delta\rho$. In fact the Yukawa Lagrangian (1.43) breaks the custodial symmetry as well. However, the only corrections expected to be of actual importance are those due to heavier fermions, mainly t and b quarks. The Higgs boson and fermion loop corrections to ρ are given by [24–26]

$$\Delta\rho_H = \frac{11 G_F m_Z^2 \sin^2\theta_W}{24\sqrt{2}\pi^2} \ln\frac{m_H^2}{m_Z^2}, \tag{1.74}$$

$$\Delta\rho_f = \frac{3G_F}{8\sqrt{2}\pi^2}\left(m_t^2 + m_b^2 - 2\frac{m_t^2 m_b^2}{m_t^2 - m_b^2}\ln\frac{m_t^2}{m_b^2}\right). \tag{1.75}$$

The first correction is caused by the custodial symmetry breaking in the gauge sector and vanishes in the limit $\theta_W = 0$ ($g' \to 0$). The second correction is due to the custodial symmetry breaking in the Yukawa sector. By taking the limit $x \equiv \frac{m_t}{m_b} \to 1$, one can easily verify that the correction vanishes. This is due to the fact that it is the splitting between the up and down masses that breaks the custodial symmetry in the fermion sector. Since the top and bottom masses splitting is the biggest one, their contribution dominates the corrections. When trying to translate the quark Yukawa couplings in (1.43) into the formalism introduced in (1.62) one can easily verify that the only custodial invariant Yukawa Lagrangian that one can build is

$$\mathcal{L}_Y = -\bar{Q}_L \Phi Y' Q_R, \tag{1.76}$$

implying $Y' = Y'_D = Y'_U$ and ultimately the top and bottom mass degeneracy $m_t = m_b$.

Furthermore, the scalar correction behaves logarithmically with the Higgs mass while the fermion correction and the gauge boson corrections show a quadratic dependence on the masses but with opposite sign. All these features put together contribute to the smallness of the $\Delta\rho$ corrections.

Up until now, the relation between the ρ parameter corrections and the oblique parameter T has been used as a mean to constrain the Higgs mass from electroweak precision fits. In the past, the same method had led to the prediction of the top quark mass before its descovery. However, since the discovery of the new scalar particle at the LHC, believed to be the SM Higgs boson, the last missing electroweak piece, i.e. m_H, has been found and new fits have been carried out in order to assess the validity of the SM at the electroweak scale. The oblique parameters (S, T, U) contain information on vacuum polarisation corrections and are therefore very sensitive to new physics. The results in Fig.1.3 show the impressive compatibility of the latest electroweak precision fit with SM prediction.

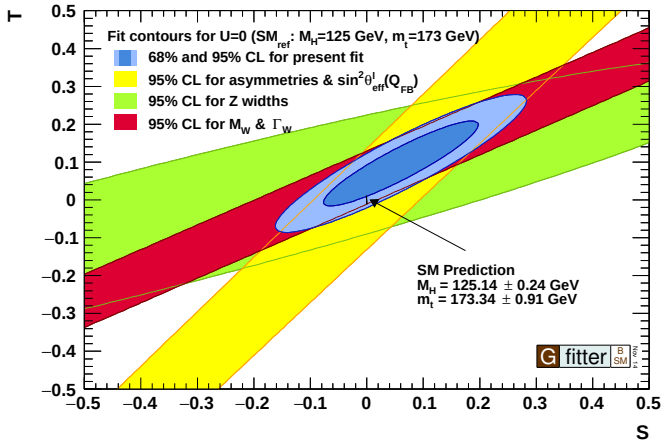

Figure 1.3: *Contours of 68% and 95% confidence level in the TS-plane, where U was constrained to 0 in the fit (blue ellipses). Individual constraints are shown at 95% confidence level, from the asymmetry measurements (yellow), partial decay widths of the Z-boson (green), and the mass and total width of the W boson, m_W an Γ_W (red)* [27]

1.2.3 The Flavour Symmetry

The matter lagrangian of the SM contains the fermion kinetic and gauge interaction terms:

$$\mathcal{L} = i\bar{Q}^i_L \not{D} Q^i_L + i\bar{u}^i_R \not{D} d^i_R + i\bar{d}^i_R \not{D} d^i_R + i\bar{L}^i_L \not{D} L^i_L + i\bar{\ell}^i_R \not{D} \ell^i_R. \tag{1.77}$$

In the absence of fermion masses, this Lagrangian presents a group of accidental global symmetries. Indeed, the matter lagrangian is invariant under a class of global transformations where each fermion $SU(2) \times U(1)$ representation is allowed to be multiplied by an arbitrary constant phase. In the SM, where there are three generations of quarks and leptons, each global transformation leaves invariant a different $U(3)$ symmetry:

$$\begin{array}{ll} U(3)_{Q_L}: & Q_L^i \to U_{Q_L}^{ij} Q_L^j, \\ U(3)_{u_R}: & u_R^i \to U_{u_R}^{ij} u_R^j, \\ U(3)_{d_R}: & d_R^i \to U_{d_R}^{ij} d_R^j, \\ U(3)_{L_L}: & L_L^i \to U_{L_L}^{ij} L_L^j, \\ U(3)_{\ell_R}: & \ell_R^i \to U_{\ell_R}^{ij} \ell_R^j. \end{array} \tag{1.78}$$

The product symmetry group can actually be redefined as follows:

$$G_f = SU(3)_Q^3 \times SU(3)_L^2 \times U(1)_B \times U(1)_L \times U(1)_Y \times U(1)_{PQ} \times U(1)_{\ell_R}, \tag{1.79}$$

where

$$SU(3)_Q^3 = SU(3)_{Q_L} \times SU(3)_{u_R} \times SU(3)_{d_R} \tag{1.80}$$

$$SU(3)_L^2 = SU(3)_{L_L} \times SU(3)_{\ell_R}. \tag{1.81}$$

This way, we can easily identify some well known symmetries. In the SM, the $U(1)_B$ and $U(1)_L$ can be identified with the symmetries associated to baryon and lepton number conservation respectively. While due to anomalies, B and L are not conserved, B-L remains a true symmetry of the SM. $U(1)_Y$ is the global version of the local gauge symmetry that is spontaneously broken and the two remaining $U(1)$ groups can be identified with the Peccei-Quinn symmetry and with a global rotation of a single $SU(2)_L$ singlet. The $SU(3)_Q^3$ and $SU(3)_L^2$ symmetries are actually explicitely broken by the Yukawa Lagrangian (1.43) and will be of interest in the formulation of Minimal Flavour Violation developed in the next chapter.

1.2.4 CP-violation

Since only left-handed fermions and right-handed antifermions couple to the $W^\pm$ bosons, there is a maximal breaking of parity P (left-right symmetry) and

charge conjugation C (particle-antiparticle symmetry) in the gauge sector of the SM. However, the combined transformation CP still seems to be a good symmetry of the SM Lagrangian in (1.11) despite what the observed matter-antimatter asymmetry of the universe suggests. The CPT theorem guarantees that the product of the three discrete transformations is an exact symmetry of any local and Lorentz-invariant quantum field theory preserving unitarity and micro-causality. Therefore, a violation of CP requires a corresponding violation of time reversal. Since T is an antiunitary transformation, this requires the presence of relative complex phases between different interfering amplitudes. Experimentally, some phenomena observed in the neutral kaon system and in B meson decays display a violation of the CP symmetry. These phenomena can in fact be accounted for in the SM framework thanks to the Cabibbo-Kobayashi-Maskawa mixing matrix in (1.48).

The Cabibbo-Kobayashi-Maskawa mixing matrix

In 1973, while only three light quarks (u, d, s) had been discovered, M. Kobayashi and T. Maskawa [28] used a simple parameter counting to prove that if the number of quark generations was equal to or greater than three, then all the complex phases in V_{CKM} matrix could not be absorbed by a field redefinition. If this is true, a possible source of CP violation could be introduced in the SM. Indeed, the CKM matrix defined in (1.48) is an arbitrary $n_g \times n_g$ unitary matrix, where n_g is the number of quark generations, determined by n_g^2 parameters. However, field redefinitions of the type $\Psi \to e^{i\alpha}\Psi$ applied to the quark fields, allow us to remove $2n_g - 1$ parameters. A unitary matrix can be understood as a complex extension of an orthogonal matrix. Since the number of paramenters of an orthogonal matrix is $\frac{1}{2}n_g(n_g - 1)$, we can identify those parameters as the Euler angles of a unitary matrix, while the remaining parameters are the complex phases. If we carry out the parameter counting we obtain the number of complex phases of the $n_g \times n_g$ CKM matrix as:

$$\begin{aligned} \#_{phases} = \#_{param} - \#_{angles} &= n_g^2 - (2n_g - 1) - \left(\frac{1}{2}n_g(n_g - 1)\right) \\ &= \frac{1}{2}(n_g - 1)(n_g - 2). \end{aligned} \tag{1.82}$$

Therefore, in the case of two generations, there are no complex phases and only a rotation between the quark fields as described by the Cabibbo angle [29]. Kobayashi and Maskawa predicted that if there was an additional generation of quarks, then the mixing matrix would contain a complex phase which would account for the observed CP violating phenomena. The b and t quarks were discovered in 1977 and 1995 respectively, confirming the relevance of Kobayashi and Maskawa's claim.

With three generations of quarks, the CKM matrix can therefore be described by three angles and one phase. The standard CKM parametrization [14] reads:

$$V_{CKM} = \begin{pmatrix} c_{12}c_{13} & s_{12}c_{13} & s_{13}e^{-i\delta_{13}} \\ -s_{12}c_{23} - c_{12}s_{23}s_{13}e^{i\delta_{13}} & c_{12}c_{23} - s_{12}s_{23}s_{13}e^{i\delta_{13}} & s_{23}c_{13} \\ s_{12}s_{23} - c_{12}c_{23}s_{13}e^{i\delta_{13}} & -c_{12}s_{23} - s_{12}c_{23}s_{13}e^{i\delta_{13}} & c_{23}c_{13} \end{pmatrix}, \tag{1.83}$$

where $c_{ij} = \cos\theta_{ij}$ and $s_{ij} = \sin\theta_{ij}$. The angles θ_{ij} can all be forced to lie in the first quadrant by an appropriate redefinition of quark field phases so that $c_{ij} \geq 0$, $s_{ij} \geq 0$ and $0 \geq \delta_{13} \leq 2\pi$. δ_{13} is the only complex phase in the SM and therefore the only possible source of CP violation. In order to experimentally determine the values of the V_{CKM} entries, one takes advantage of the hadronic decays wich are associated to flavour changing quark transitions through charged currents. However, since the quarks are confined to hadrons, an important difficulty in the theoretical estimation arises. Indeed, the following amplitude of a semileptonic decay

$$A[H \to H'\ell^-\nu_\ell] \approx \frac{G_F}{\sqrt{2}} V_{ij} \langle H|\bar{u}_i\gamma_\mu(1-\gamma_5)d_j|H\rangle \bar{\ell}\gamma^\mu(1-\gamma_5)\nu_\ell, \tag{1.84}$$

involves a hadronic matrix element whose evaluation introduces important uncertainties due to its non-perturbative nature. These matrix elements are parametrized by form factors that are computed theoretically making use of kinematical properties and symmetry principles. Therefore, the experimental precision in the estimation of the CKM matrix elements is limited by the accuracy of the theoretical estimation of the form factors. However, important improvements have been achieved in this field and our knowledge of the CKM matrix elements has progressed. Moreover, the measured entries reveal a rather hierarchical pattern with the diagonal elements being close to one and $|V_{us}| = 0.2253 \pm 0.0008$. The Wolfenstein parametrisation [14] takes advantage of this hierarchy and estimates every CKM matrix element as a development

in terms of $\lambda \approx |V_{us}|$:

$$V_{CKM} = \begin{pmatrix} 1-\lambda^2/2 & \lambda & A\lambda^3(\rho - i\eta) \\ -\lambda & 1-\lambda^2/2 & A\lambda^2 \\ A\lambda^3(1-\rho-i\eta) & -A\lambda^2 & 1 \end{pmatrix} + \mathcal{O}(\lambda^4). \quad (1.85)$$

The new parameters are related to the standard parametrisation (1.83) through the following relations:

$$\lambda \cong s_{12}; \quad A\lambda^2 \cong s_{23}; \quad A\lambda^3(\rho - i\eta) = s_{13}e^{-i\delta}. \quad (1.86)$$

We have pointed out the V_{CKM} complex phase as the only possible source of CP violation in the SM. However, in order for CP violation to be actually observed in one particular process, several additional conditions must be verified. In the kaon sector, for example, CP violation appears at the loop level with same charge quark loops. If these loops involve quarks degenerated in mass, the loop function becomes a constant, and the CKM matrix contribution cancels out due its unitarity. These necessary conditions can all be summarized in the formalism we will develop here. Let us start with the main reason for the appearance of the CKM matrix, i.e., the impossibility of simultaneously diagonalizing both the up and down quark mass matrices. This implies:

$$\left[Y'_U Y'^{\dagger}_U, Y'_D Y'^{\dagger}_D\right] = V^u_L \left[Y_U Y^{\dagger}_U, V_{CKM} Y_D Y^{\dagger}_D V^{\dagger}_{CKM}\right] V^{u\dagger}_L \neq 0. \quad (1.87)$$

Note that any power of the trace of this commutator defines an invariant since the trace:

$$Tr\left[Y'_U Y'^{\dagger}_U, Y'_D Y'^{\dagger}_D\right]^n = \mathrm{Tr}\left[Y_U Y^{\dagger}_U, V_{CKM} Y_D Y^{\dagger}_D V^{\dagger}_{CKM}\right]^n \quad (1.88)$$

only depends on physical parameters, i.e., the quark masses and V_{CKM} parameters. Under a T (CP) transformation, the CKM matrix transforms:

$$V_{CKM} \xrightarrow{T} V^*_{CKM} \quad (1.89)$$

and the invariant in (1.88):

$$\mathrm{Tr}\left[Y'_U Y'^{\dagger}_U, Y'_D Y'^{\dagger}_D\right]^n \xrightarrow{T} (-1)^n \mathrm{Tr}\left[Y'_U Y'^{\dagger}_U, Y'_D Y'^{\dagger}_D\right]^n. \quad (1.90)$$

The condition for CP violation therefore becomes:

$$Tr\left[Y'_U Y'^{\dagger}_U, Y'_D Y'^{\dagger}_D\right]^{2n+1} \neq 0 \quad n \geq 1. \quad (1.91)$$

We can actually relate the trace of any power of the commutator to its determinant through the Cayley-Hamilton theorem (see (2.95)). Therefore, using the relations in (1.46), we obtain that the condition for CP violation in the SM with three generations is in fact:

$$\begin{aligned} \det\left[M_U M_U^\dagger, M_D M_D^\dagger\right] &= 2i(m_t^2-m_u^2)(m_t^2-m_c^2)(m_c^2-m_u^2) \\ &\quad (m_b^2-m_d^2)(m_b^2-m_s^2)(m_s^2-m_d^2)\mathcal{J} \\ &\neq 0, \end{aligned} \tag{1.92}$$

with

$$\mathcal{J} = \pm \mathrm{Im}\left[(V_{CKM})_{ij}(V_{CKM}^\dagger)_{jk}(V_{CKM})_{kl}(V_{CKM}^\dagger)_{li}\right] \tag{1.93}$$

for any i,j,k,l. $\mathcal{J}$ is known as the Jarlskog invariant [30]. Two major remarks can be made about this result.

- If two same charge quarks are degenerated in mass, the invariant vanishes and no CP violation effect can be observed.
- Since every CP violating observable in the SM is related to the Jarlskog invariant and $|\mathcal{J}| \simeq A^2\lambda^6\eta < 10^{-4}$, CP violation effects are expected to be very small. One of the main CP violation observables in hadronic decays are the so-called CP asymmetries. In the case of a $M \to f$ decay and its CP conjugate $\bar{M} \to \bar{f}$, these quantities are defined by

$$a_{CP} \equiv \frac{\Gamma(M \to f) - \Gamma(\bar{M} \to \bar{f})}{\Gamma(M \to f) + \Gamma(\bar{M} \to \bar{f})} \tag{1.94}$$

  where Γ are the decay widths. Therefore, in order to observe a sizeable CP asymmetry in the hadronic sector, one should look at very suppressed decays.

The unitarity condition of the V_{CKM} matrix can be used as an interesting tool in order to test the validity of the CKM mechanism to describe CP violation in the SM. Let us take the following non-diagonal unitarity conditions

$$V_{ud}^* V_{us} + V_{cd}^* V_{cs} + V_{td}^* V_{ts} = 0, \tag{1.95}$$

$$V_{us}^* V_{ub} + V_{cs}^* V_{cb} + V_{ts}^* V_{tb} = 0, \tag{1.96}$$

$$V_{ub}^* V_{ud} + V_{cb}^* V_{cd} + V_{tb}^* V_{td} = 0. \tag{1.97}$$

These unitarity relations describe triangles in the complex space with areas of size $|\mathcal{J}|/2$. If there is no CP violation, the triangles would become segments along the real axis. Given the known values of the CKM elements, the most interesting triangle is defined by (1.97) since all its sides are of the same order of magnitude, i.e. $\mathcal{O}(\lambda^3)$. Moreover, one of its sides lies on the real axis. The sides of the triangle are acknowledgeably small, meaning that the relevant phenomena are rare. However, the amount of CP violating phenomena is of the same order of magnitude which means that, once enough decay data are collected, the observed CP asymmetries are sizeable. This triangle involves a lot of B mesons physics and all the experimental constraints on its parameters have been put together in Fig.1.4. The $(\bar{\rho}, \bar{\eta})$ coordinates correspond to the Wolfenstein parametrization taken beyond $\mathcal{O}(\lambda^4)$ and are related to the (ρ, η) parameters in (1.86) by a factor $(1-\lambda^2/2)$. The overall agreement between the different observables in the Standard Model global fit is impressive and shows the success of the CKM mechanism in the description of flavour mixing and CP violation.

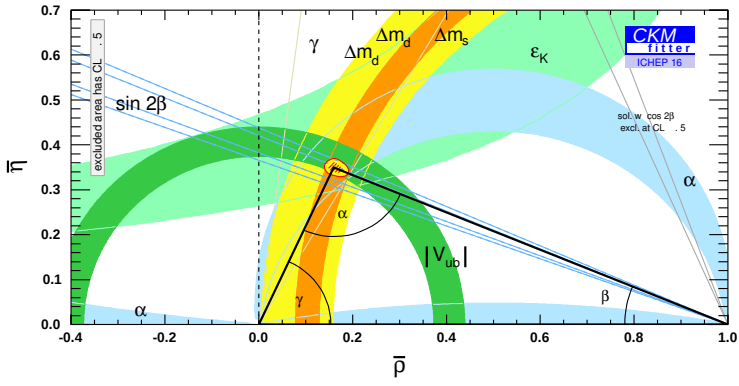

Figure 1.4: *Constraints on the CKM $(\bar{\rho}, \bar{\eta})$ coordinates from the global SM CKM fit.* [4]

The strong CP problem

The strong CP problem can be understood as a consequence of the solution proposed by 't Hooft to solve the $U(1)_A$ problem in QCD through the inclusion of topological effects called instantons.

In the limit of massless quarks, the QCD Lagrangian introduced in (1.55) is invariant under $U(n_F)_L \times U(n_F)_R$. Considering only the lightest quarks, i.e. $m_q \ll \Lambda_{QCD}$, one would expect the product symmetry $U(2)_L \times U(2)_R$ to be a good symmetry of the observations. Experimentally, $U(2)_V = SU(2)_I \times U(1)_B$ being the product of the isospin and the baryon number vectorial symmetries, are compatible with the observations. The axial ones, on the other hand, are broken spontaneously by the quark condensates $\langle u\bar{u}\rangle = \langle d\bar{d}\rangle \neq 0$. The so-called $U(1)_A$ problem rises through the realisation, that even though pions have very light masses, there are no other light states in the hadronic spectrum that could act as the pseudo-Goldstone bosons associated with the $U(1)_A$ breaking.
The solution proposed by 't Hooft [31] consists of taking into account the complex structure of the QCD vacuum implying that $U(1)_A$ is not a true symmetry of the QCD Lagrangian even in the limit of very small quark masses. In this limit, a $U(1)_A$ transformation of the quark fields

$$q_f \to e^{i\alpha\gamma_5/2} q_f \tag{1.98}$$

leaves the QCD Lagrangian (1.55) invariant. However, once the QCD vacuum structure is taken into account, the action is modified and a new term must be added to the QCD Lagrangian

$$\theta_{QCD} \frac{g_s^2}{32\pi^2} G_a^{\mu\nu} \tilde{G}^a_{\mu\nu}, \tag{1.99}$$

where $\theta_{QCD} = \alpha$ is a free parameter. This term is actually CP violating and cannot be set to zero by imposing CP invariance in the strong sector. This is due to the fact that, since CP is not a symmetry of the whole SM Lagrangian, divergent contributions would appear from the electroweak sector at the quantum level. In fact, when the total theory is included, one realises that in order to diagonalise the complex quark mass matrix to move to the physical basis, one must perform a chiral transformation on all the quark flavours:

$$q_f \to e^{i\alpha\gamma_5/2n_f} q_f \tag{1.100}$$

implying

$$\theta_{QFD} = arg \det (Y'_U Y'_D) . \tag{1.101}$$

As a consequence, the physical $\bar{\theta}$ reads:

$$\bar{\theta} = \theta_{QCD} + \theta_{QFD}. \tag{1.102}$$

The two contributions are *a priori* independent, θ_{QFD} is the argument of the determinant of the quark mass matrix while θ_{QCD} is an arbitrary coefficient. The physical $\bar{\theta}$ can be constrained through experimental data on the neutron dipole moment setting the upper limit:

$$\bar{\theta} \lesssim 10^{-10}. \tag{1.103}$$

Since CP is already broken due to CKM, the SM does not acquire any additional symmetry when $\bar{\theta} \to 0$. The substantial amount of fine-tuning necessary to satisfy the bound in (1.103) is often called the strong CP problem. To this day it remains one of the most puzzling issues of the SM. Several kinds of solutions have been considered up to now. The simplest one requires the vanishing of one of the quark masses. If that is the case, (1.101) receives no contributions and $\bar{\theta}$ can be set to zero. Another solution implies a model with two scalar doublets and will be discussed in the following chapter.

1.3 Evidence and constraints on the SM scalar

In 2012, the CMS [1] and ATLAS [2] collaborations claimed the observation of a new boson at around 125 GeV. The main decay channels where measurements have been taken are W^+W^-, ZZ, $b\bar{b}$, $\tau^+\tau^-$ and $\gamma\gamma$. The $b\bar{b}$ channel has been enforced by the data provided by the Tevatron experiments D0 and CDF. Each channel provides a different sensitivity due to the presence of backgrounds and different mass resolutions. Moreover, they target different production and decay mechanisms, providing both a complementary study of the new boson couplings and properties as well as some insight into the compatibility of the new particle with the SM Higgs boson. In order to state that the discovered boson is indeed the one predicted by the SM, one must confirm that the spin-parity-charge conjugation $J^{PC} = 0^{++}$ and the couplings are as predicted by the theory.

The $\gamma\gamma$ and ZZ decays provide the most precise value of the boson mass because of their excellent mass resolution of the reconstructed diphoton and four-lepton final states. The $W^+W^- \to \ell^+\nu\ell^-\bar{\nu}$ has very high sensitivity but poor mass resolution because of the neutrinos in the final state. The $b\bar{b}$ and $\tau^+\tau^-$ decays, on the other hand, are polluted by large backgrounds and have lower sensitivity

and mass resolution. The latest measurement of the boson mass by the CMS [32] and ATLAS [33] are respectively

$$m_H(\text{CMS}) = 125.02^{+0.26}_{-0.27}(\text{stat})^{+0.14}_{-0.15}(\text{syst}) \text{ GeV}, \quad (1.104)$$

$$m_H(\text{ATLAS}) = 125.36 \pm 0.37(\text{stat}) \pm 0.18(\text{syst}) \text{ GeV}. \quad (1.105)$$

In 2015 a combination of mass measurements between both LHC experiments using the Run 1 data sets was provided [34]. Only $\gamma\gamma$ and ZZ decays were used, leading to the final result:

$$m_H(\text{LHC}) = 125.09 \pm 0.21(\text{stat}) \pm 0.11(\text{syst}) \text{ GeV}. \quad (1.106)$$

The first 13 TeV results in the four-lepton final state, are already available too [35], and are compatible with the Run 1 data. Taking the signal strength to be the ratio between the measured cross section and the one predicted by the SM, it provides a good estimation of the compatibility between the data and the theory. Fig.1.5 shows the 68% confidence level regions for the individual channel measurement of each experiment, as well as for the combined result.

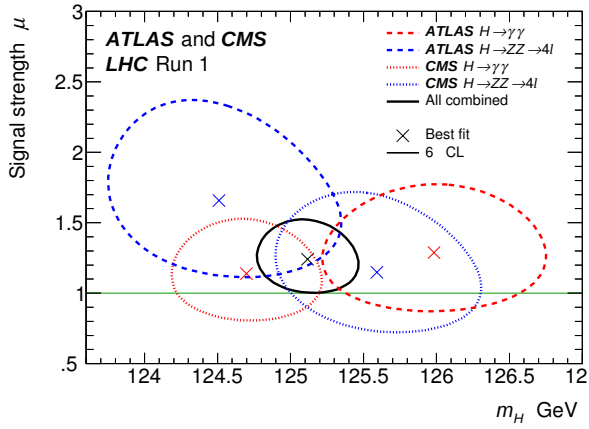

Figure 1.5: *Summary of likelihood scans in the 2D plane of signal strength $\mu = \hat{\sigma}/\hat{\sigma}_{SM}$ versus Higgs boson mass m_H for the ATLAS and CMS experiments. The 68% CL confidence regions of the individual measurements are shown by the dashed curves and that of the overall combination by the solid curve. The markers indicate the respective best-fit values* [34]

More detailed analysis of the compatibility between the individual channels and the SM expectations has been provided by both ATLAS [36] and CMS [32].

Both experiments mainly focus on diboson final state decays and include signal strengths of production-tagged events. This allows for the study of the production mechanisms and gives further insight into the nature of the discovered boson. In the LHC, the main production mechanism is gluon gluon fusion (ggH). However, vector boson fusion (VBF), VH and ttH production have non-negligible contributions to some of the analyzed decays. Since the signature of the observed event is somewhat different depending on the production mechanism, it is possible to tag the events corresponding to those signatures and study their compatibility with the SM expectations. Fig.1.6 shows the signal strengths of the production tagged categories corresponding to different final states for both ATLAS and CMS. The SM Higgs boson mass is 125.5 GeV in the case of the ATLAS experiment and 125 GeV for CMS. No significant deviations from the SM are observed, reinforcing the SM nature of the observed boson.

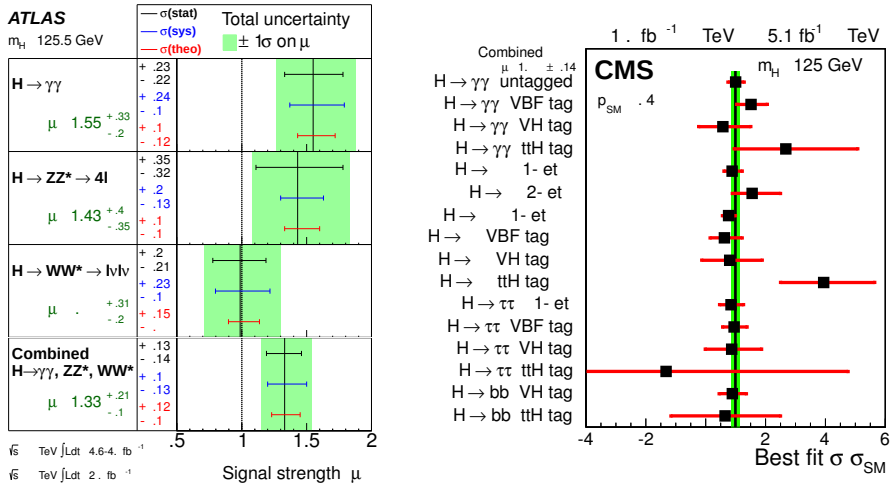

Figure 1.6: *Values of the signal strengths $\mu = \hat{\sigma}/\hat{\sigma}_{SM}$ grouped by predominant decay mode and production mode tag in both ATLAS (left) [36] and CMS (right) [32] experiments.*

The previous analyses assume the scalar nature of the observed boson. However, as already mentioned, the spin-parity-charge conjugation must be confirmed by the experiment as well. Analyses of these properties have been carried out by both experiments. The ATLAS experiment analysis [37] uses diboson decays and rules out some specific models with quantum numbers

$J^P = 0^-, 1^+, 1^-, 2^+$ to a 97.8% confidence level. The CMS experiment analysis [38] uses the same decays and rules out spin-one and spin-two scenarios, and also shows that positive parity is strongly preferred.

Besides Higgs direct searches, the LHC has a large number of ongoing analyses expected to further enlighten the Higgs sector and the SM as a whole. We wish to underline the role of the rare decays $B_{s,d} \to \mu^+\mu^-$. The B_s decay has been observed for the first time by the CMS and LHCb experiments with a six standard deviations significance for the combined measurement [3]. The B_d decay combined significance is three standard deviations and an upper limit has been set on the decay rate. These FCNC decays are considered rare because their branching ratios are extremely small. On the one hand, they are only generated at the loop level and are therefore highly suppressed and, on the other hand, there is a helicity suppression factor m_μ/m_b. They are very interesting for testing New Physics scenarios because, being so highly suppressed, they are very sensitive to the mechanism of quark flavour mixing (similar to $K \to \bar{\nu}\nu$ decays). Although in the SM framework they do not provide any additional information about the Higgs boson, they do constrain models with richer electroweak SSB mechanisms and will play an important role in this work. The theoretical prediction of this rare decay is very clean because the only particles involved in the final state are leptons and the uncertainty is mainly due to the B mesons decay constants. With the improvement of lattice calculations, the theoretical predictions within the SM are [39]:

$$\mathcal{B}(B_s \to \mu^+\mu^-)_{SM} = (3.65 \pm 0.23) \times 10^{-9}, \tag{1.107}$$

$$\mathcal{B}(B_d \to \mu^+\mu^-)_{SM} = (1.06 \pm 0.09) \times 10^{-10}. \tag{1.108}$$

The latest measurements provided by LHCb and CMS combined results [3] are:

$$\mathcal{B}(B_s \to \mu^+\mu^-)_{LHC} = (2.8^{+0.7}_{-0.6}) \times 10^{-9} \quad \text{with } 6.2\sigma \text{ significance}, \tag{1.109}$$

$$\mathcal{B}(B_d \to \mu^+\mu^-)_{LHC} = (3.9^{+1.4}_{-2.6}) \times 10^{-10} \quad \text{with } 3.2\sigma \text{ significance} \tag{1.110}$$

showing a very strong compatibility with the SM prediction. At this level, it is worth mentioning the more recent results released by the LHCb collaboration [40]

$$\mathcal{B}(B_s \to \mu^+\mu^-)_{LHC} = (3.0 \pm 0.6^{+0.3}_{-0.2}) \times 10^{-9} \quad \text{with } 7.8\sigma \text{ significance}, \tag{1.111}$$

$$\mathcal{B}(B_d \to \mu^+\mu^-)_{LHC} = (1.5^{+1.2+0.2}_{-1.0-0.1}) \times 10^{-10} \quad \text{with } 1.6\sigma \text{ significance} \tag{1.112}$$

This last result seems to relax a possible tension that had been pointed out between the $B_d \to \mu^+\mu^-$ decay rate predicted by the SM (1.108) and the combined experimental result in (1.110).

1.4 Status of the SM after the Higgs Boson discovery

After the LHC discovery of the Higgs Boson, the SM has confirmed itself as the most convincing theory at the electroweak scale, pushing New Physics above 1 TeV. It explains with an astonishing accuracy a large amount of experimental data and has all its ingredients experimentally verified. Given the newly discovered scalar, the first question to arise is whether the new boson corresponds to the unique scalar predicted by the SM or if it could be a door into a richer electroweak SSB scenario. Besides, if it is indeed a fundamental scalar, some mechanism must be found in order to stabilize its mass. Since there is some new physics at a higher scale Λ_{NP}, quantum corrections to the scalar mass are expected to grow with the new physics scale such as [41]

$$\delta m_h^2 \sim \frac{g^2}{(4\pi)^2}\Lambda_{NP}^2 \log\left(\frac{\Lambda_{NP}^2}{m_h^2}\right). \tag{1.113}$$

The SM provides mechanisms to avoid these kinds of problems in the case of the other elementary particles. The fermion masses are protected by chiral symmetry, while the gauge boson masses are protected by gauge symmetry. Every attempt to provide a mechanism to protect the scalar mass contains predictions which are yet to be observed or which have already been very constrained by the LHC results. Some examples are Supersymmetry, scale symmetry or a dynamical electroweak symmetry breaking. This question is one of the most striking ones of the SM and still remains unanswered.
With the scalar discovery, the last unknown piece of the SM Lagrangian has been provided, i.e. the quartic scalar coupling:

$$\lambda = \frac{m_h^2}{2v^2} = 0.13. \tag{1.114}$$

At the electroweak scale, the scalar mass quantum corrections are dominated by the top loops. It has been shown [42] that the current values of m_h and

m_t ensure an almost stable scalar potential up to the Planck scale M_{Pl}. The metastability of the vacuum implies that the SM could be valid up to M_{Pl} and that the possibility of not observing any new physics phenomena in the following years is not unlikely.

The confirmation of the new scalar couplings being very close to the SM Higgs ones excludes many New Physics contributions. For example, additional fermion contributions to the Higgs production and decay rates are excluded; the $H \to \gamma\gamma$ decay rate heavily constrains models with charged scalars contributing to the loops, etc. The astonishing success of the SM flavour predictions already mentioned in a previous section highly constrains New Physics as well. Only models with SM-like suppression mechanisms, such as Minimal Flavour Violation, are still possible at the 1 TeV scale.

Although the success of the SM is undeniable, New Physics still seems necessary to provide answers to many pending questions. The very diverse mass scales between the different elementary particles are still not understood. The hierarchy existing between the different fermion masses and mixing parameters, as well as the dynamics of flavour and CP violation, need to be properly explained. Questions about Dark Matter and Dark Energy are still numerous. The only observed evidence of BSM physics is neutrino mixing. However, the neutrino oscillation data imply a pattern of leptonic mixing very different from the one in the quark sector, raising additional questions. Although the most trending New Physics scenarios have suffered from the LHC's very constraining results, not all questions have been answered and future experiments, like HL-LHC or FCC, are still expected to provide some insight.

Chapter 2

Custodial Symmetry and Minimal Flavour Violation in a 2HDM

The Higgs doublet of the Standard Model is the minimal way to account for the $SU(2)_L \times U(1)_Y \to U(1)_{em}$ SSB mechanism as it has been described in the first chapter. However, more complex models with an extended scalar sector might be able to preserve the experimentally favoured SM features previously underlined and provide a wider phenomenology. The motivations behind models with enlarged scalar sectors are many. In supersymmetric models, for example, the scalar particles belong to a chiral representation of the supersymmetry, while their complex conjugates belong to multiplets with opposite chirality. Since the Lagrangian needs to be supersymmetric, multiplets with different chiralities cannot appear together in any term of the Lagrangian. Therefore, with only one Higgs doublet it would not be possible to provide masses to both up and down quarks. Besides, since every chiral multiplet contains chiral spin $-1/2$ particles as well, the need for an additional scalar doublet becomes evident when trying to cancel the anomalies. Models with two Higgs doublets have also become interesting in order to provide Dark Matter (DM) candidates. A widely studied case is the so-called Inert Doublet Model [43–45]. In this model

one of the doublets does not couple to fermions and does not acquire a vev; therefore, the lightest Higgs particle of the inert doublet is stable and can be considered in DM searches. The Peccei-Quinn models, which will be discussed in more detail further on, also introduce a second scalar doublet in order to spontaneously break the symmetry able to solve the strong CP problem. Models with horizontal symmetries, which try to account for the structure of the quark mass matrices, motivate models with an extended scalar sector as well. It can be proved that in these models, an additional scalar doublet is needed in order to spontaneously break the horizontal symmetry in a way compatible with the observed fermion masses and flavour mixing parameters. Finally, another motivation to study 2HDMs is the fact that the SM is unable to account for the observed baryon asymmetry of the Universe. Models with two Higgs doublets are able to introduce additional sources of CP violation. In this study, however, we adopt yet another perspective and analyze a particular Two Higgs Doublet Model (2HDM) [46] that minimizes the loss of the SM accidental symmetries. Later, we will study the consequences at the LHC, especially those concerning flavour physics.

2.1 The general 2HDM

Since the flavour sector will play an important role in this work, we start our introduction of the 2HDM with the Yukawa interactions. In a generic $\{\Phi_1, \Phi_2\}$ basis, the 2HDM Yukawa sector takes the following form:

$$\mathcal{L}_{\rm Y} = -\bar{Q}'_L \left(\Delta'_D \Phi_1 + \Gamma'_D \Phi_2\right) d'_R - \bar{Q}'_L \left(\Delta'_U \tilde{\Phi}_1 + \Gamma'_U \tilde{\Phi}_2\right) u'_R + \text{h.c.} \qquad (2.1)$$

where $\tilde{\Phi}_i = i\tau_2 \Phi_i^*$. Both Higgs fields carry non vanishing vacuum expectation values (vevs) which take the form:

$$\langle \Phi_1 \rangle = \begin{pmatrix} 0 \\ v_1/\sqrt{2} \end{pmatrix} \quad \text{and} \quad \langle \Phi_2 \rangle = \begin{pmatrix} 0 \\ v_2 e^{i\delta}/\sqrt{2} \end{pmatrix}, \qquad (2.2)$$

in order to break $SU(2)_L \times U(1)_Y$ into $U(1)_{em}$. Complex Higgs vevs are assumed and without loss of generality a relative complex phase δ can be assigned to v_2.

2.1.1 The scalar potential

The most general 2HDM scalar potential expressed in the general $\{\Phi_1, \Phi_2\}$ basis is explicitly given by

$$\begin{aligned} V(\Phi_1,\Phi_2) =& m_{11}^2\Phi_1^\dagger\Phi_1 + m_{22}^2\Phi_2^\dagger\Phi_2 + \frac{1}{2}\Lambda_1\left(\Phi_1^\dagger\Phi_1\right)^2 + \frac{1}{2}\Lambda_2\left(\Phi_2^\dagger\Phi_2\right)^2 + \\ &+ \Lambda_3\left(\Phi_1^\dagger\Phi_1\right)\left(\Phi_2^\dagger\Phi_2\right) + \Lambda_4\left(\Phi_1^\dagger\Phi_2\right)\left(\Phi_2^\dagger\Phi_1\right) + \\ &+ \left[-m_{12}^2\Phi_1^\dagger\Phi_2 + \left(\frac{1}{2}\Lambda_5\Phi_1^\dagger\Phi_2 + \Lambda_6\Phi_1^\dagger\Phi_1 + \Lambda_7\Phi_2^\dagger\Phi_2\right)\left(\Phi_1^\dagger\Phi_2\right)\right. \\ &\left.+\text{h.c.}\right] \end{aligned} \tag{2.3}$$

The m_{ij} parameters have mass squared dimensions whereas the Λ_i are dimensionless. Since hermiticity does not force m_{12} and $\Lambda_{5,6,7}$ to be real, the counting of free parameters of the scalar potential gives $6 + 8 = 14$. However, there are some restrictions to be imposed on the potential for it to fulfill the SSB mechanism requirements or to preserve additional symmetries.

The scalar potential is bounded from below. The stability of the potential requires that there is no direction in field space along which the potential tends to $-\infty$. Given the richness of the field space of the 2HDM, it is not straightforward to work out in a comprehensive way all the conditions under which the scalar potential is bounded from below. Besides, depending on how we define the way the potential is bounded this condition means:

- The quartic potential (V_4) has to be strictly greater than zero in every field direction.
- The quartic potential (V_4) has to be greater than zero in every field direction. However, in this case, we should make sure that when $V_4 = 0$ the quadratic part of the potential (V_2) is bounded from below, i.e. $V_2 \geq 0$ in every direction.

However, some necessary conditions are easy to establish. As an example, in the direction $|\Phi_{1(2)}| = 0$ and $|\Phi_{2(1)}| \to +\infty$, $V_4 > 0$ provided that $\Lambda_{2(1)} > 0$.

The scalar potential conserves CP. As a first step, in order to simplify the analysis, we consider a scalar potential that does not generate CP violation. Given the success of the CKM mechanism in explaining the CP violation phenomena observed, we do not wish to add any additional CP violation sources. For now, we will not try to obtain all the necessary conditions to avoid explicit CP violation since the topic will be studied later on. Just for illustration, assuming that all the scalar potential parameters are real is a sufficient condition.

The scalar potential does not generate spontaneous CP violation. As in the previous case, it is sufficient (but not necessary) to consider the $\Phi_{1,2}$ vev as being real :

$$\langle\Phi_1\rangle = \begin{pmatrix} 0 \\ v_1/\sqrt{2} \end{pmatrix} \quad \text{and} \quad \langle\Phi_2\rangle = \begin{pmatrix} 0 \\ v_2/\sqrt{2} \end{pmatrix}, \quad \text{with} \quad v_{1,2} \in \mathbb{R} \tag{2.4}$$

In the next section 2.2.3 we will give more details on the necessary conditions for CP to be spontaneously broken as well as some important consequences of models with spontaneous CP violation.

Vacuum stability. Let us assume that the scalar potential is bounded from below and that it can neither generate explicit nor spontaneous CP violation. In the following Higgs fields parametrization:

$$\Phi_1 = \begin{pmatrix} \varphi_1^+ \\ (v_1 + \mathrm{Re}\varphi_1^0 + i\mathrm{Im}\varphi_1^0)/\sqrt{2} \end{pmatrix} \text{ and } \Phi_2 = \begin{pmatrix} \varphi_2^+ \\ (v_2 + \mathrm{Re}\varphi_2^0 + i\mathrm{Im}\varphi_2^0)/\sqrt{2} \end{pmatrix} \tag{2.5}$$

it appears that the scalar potential carries linear terms in the neutral $\mathrm{Re}\varphi_i^0$ fields. In order to ensure that there is no vev for the physical fields, i.e. $\langle\mathrm{Re}\varphi_i^0\rangle = 0$, the scalar potential should satisfy:

$$\frac{\partial V_{\text{linear}}}{\partial \mathrm{Re}\varphi_i^0} = 0. \tag{2.6}$$

This condition implies:

$$m_{11}^2 = m_{12}\frac{v_2}{v_1} - \frac{1}{2}v^2\left[\Lambda_1\frac{v_1^2}{v^2} + \Lambda_{345}\frac{v_2^2}{v^2} + 3\Lambda_6\frac{v_1}{v}\frac{v_2}{v} + \Lambda_7\frac{v_2^2}{v^2}\frac{v_2}{v_1}\right], \tag{2.7}$$

$$m_{22}^2 = m_{12}\frac{v_1}{v_2} - \frac{1}{2}v^2\left[\Lambda_2\frac{v_2^2}{v^2} + \Lambda_{345}\frac{v_1^2}{v^2} + \Lambda_6\frac{v_1^2}{v^2}\frac{v_1}{v_2} + 3\Lambda_7\frac{v_1}{v}\frac{v_2}{v}\right], \tag{2.8}$$

where

$$\Lambda_{ij\cdots k} \equiv \Lambda_i + \Lambda_j + \cdots + \Lambda_k \;\text{ and }\; v^2 \equiv v_1^2 + v_2^2 = \frac{4m_W^2}{g^2} = (246\text{ GeV})^2. \quad (2.9)$$

Note that $m_{ii}^2 \to -m_{ii}^2$ would also satisfy the condition. Equations (2.7) and (2.8) can be re-written as:

$$m_{11}^2 = m_{12}^2 t_\beta - \frac{1}{2}v^2\left[\Lambda_1 c_\beta^2 + \Lambda_{345} s_\beta^2 + 3\Lambda_6 s_\beta c_\beta + \Lambda_7 s_\beta^2 t_\beta\right], \quad (2.10)$$

$$m_{22}^2 = m_{12}^2 t_\beta^{-1} - \frac{1}{2}v^2\left[\Lambda_2 s_\beta^2 + \Lambda_{345} c_\beta^2 + \Lambda_6 c_\beta^2 t_\beta^{-1} + 3\Lambda_7 s_\beta c_\beta\right]. \quad (2.11)$$

if we define

$$t_\beta = \tan\beta \equiv \frac{v_2}{v_1}, \;\; c_\beta = \cos\beta \equiv v_1/v \;\text{ and }\; s_\beta = \sin\beta \equiv v_2/v, \quad (2.12)$$

where we can assume $0 \le \beta \le \pi/2$ given that the Higgs fields can always be transformed such that both v_1 and v_2 are positive.

Mass spectrum. We can now figure out the Higgs mass spectrum. First, let us analyze the charged degrees of freedom. The corresponding mass matrix is given by

$$\frac{\partial^2 V_{\text{quadratic}}}{\partial\varphi_i^+\partial\varphi_j^-} = \begin{pmatrix} m_{11}^2 + \frac{1}{2}v^2(\Lambda_1 c_\beta^2 + \Lambda_3 s_\beta^2 + 2\Lambda_6 s_\beta c_\beta) & -2m_{12}^2 + \frac{1}{2}v^2(\Lambda_6 c_\beta^2 + \Lambda_{45} s_\beta c_\beta + \Lambda_7 s_\beta^2) \\ -2m_{12}^2 + \frac{1}{2}v^2(\Lambda_6 c_\beta^2 + \Lambda_{45} s_\beta c_\beta + \Lambda_7 s_\beta^2) & m_{22}^2 + \frac{1}{2}v^2(\Lambda_2 s_\beta^2 + \Lambda_3 c_\beta^2 + 2\Lambda_7 s_\beta c_\beta) \end{pmatrix}. \quad (2.13)$$

Once diagonalized, the (normalized) eigenvectors $G^\pm$ and $H^\pm$, given by

$$\begin{pmatrix} G^\pm \\ H^\pm \end{pmatrix} = \begin{pmatrix} c_\beta & s_\beta \\ -s_\beta & c_\beta \end{pmatrix}\begin{pmatrix} \varphi_1^\pm \\ \varphi_2^\pm \end{pmatrix}, \quad (2.14)$$

exhibit the following mass spectrum:

$$m_{G^\pm}^2 = 0, \quad (2.15)$$

$$m_{H^\pm}^2 = \frac{m_{12}^2}{s_\beta c_\beta} - \frac{1}{2}v^2\left(\Lambda_{45} + \Lambda_6 t_\beta^{-1} + \Lambda_7 t_\beta\right). \quad (2.16)$$

The massless fields $G^\pm$ are the would-be Goldstone bosons that provide the $W^\pm$ gauge bosons with their longitudinal polarization. The charged $H^\pm$ on the

other hand are dynamical fields, absent in the Standard Model. Concerning the pseudoscalar fields, we obtain:

$$\frac{\partial^2 V_{\rm quadratic}}{\partial {\rm Im}\varphi_i^0 \partial {\rm Im}\varphi_j^0} = \begin{pmatrix} m_{12}^2 t_\beta - \frac{1}{2}v^2 t_\beta(\Lambda_6 c_\beta^2 + \Lambda_7 s_\beta^2 + 2\Lambda_5 s_\beta c_\beta) & -m_{12}^2 + \frac{1}{2}v^2(\Lambda_6 c_\beta^2 + \Lambda_5 s_\beta c_\beta + \Lambda_7 s_\beta^2) \\ -m_{12}^2 + \frac{1}{2}v^2(\Lambda_6 c_\beta^2 + \Lambda_5 s_\beta c_\beta + \Lambda_7 s_\beta^2) & \frac{m_{12}^2}{t_\beta} - \frac{v^2}{2t_\beta}(\Lambda_6 c_\beta^2 + \Lambda_7 s_\beta^2 + 2\Lambda_5 s_\beta c_\beta) \end{pmatrix}. \tag{2.17}$$

The (normalized) eigenvector spectrum is given by

$$\begin{pmatrix} G^0 \\ A^0 \end{pmatrix} = \begin{pmatrix} c_\beta & s_\beta \\ -s_\beta & c_\beta \end{pmatrix} \begin{pmatrix} {\rm Im}\varphi_1^0 \\ {\rm Im}\varphi_2^0 \end{pmatrix}, \tag{2.18}$$

and contains both a massless and a massive field:

$$m_{G^0}^2 = 0 \tag{2.19}$$

$$m_{A^0}^2 = \frac{m_{12}^2}{s_\beta c_\beta} - \frac{1}{2}v^2\left(2\Lambda_5 + \Lambda_6 t_\beta^{-1} + \Lambda_7 t_\beta\right). \tag{2.20}$$

The massless would-be Goldstone boson G^0 is responsible for the Z^0 gauge boson mass whereas A^0 remains a dynamical field. Since we have assumed that the scalar potential is CP conserving, this later field does not mix with the remaining neutral Higgs fields which we will analyze afterwards. In this case indeed, A^0 has a definite parity quantum number O^{-+}; it is a pseudoscalar neutral field absent in the Standard Model. Note that we obtain the mass relation

$$m_{H^\pm}^2 = m_{A^0}^2 + \frac{1}{2}v^2(\Lambda_5 - \Lambda_4). \tag{2.21}$$

Eventually, the scalar neutral Higgs fields mix according to the following mass matrix:

$$\frac{\partial^2 V_{\rm quadratic}}{\partial {\rm Re}\varphi_i^0 \partial {\rm Re}\varphi_j^0} = \begin{pmatrix} M_{11}^2 & M_{12}^2 \\ M_{12}^2 & M_{22}^2 \end{pmatrix} \tag{2.22}$$

with

$$M_{11}^2 = m_{12}^2 t_\beta + \frac{1}{2}v^2(2\Lambda_1 c_\beta^2 - \Lambda_7 t_\beta s_\beta^2 + 3\Lambda_6 s_\beta c_\beta), \tag{2.23a}$$

$$M_{12}^2 = -m_{12}^2 + \frac{1}{2}v^2(2\Lambda_{345} s_\beta c_\beta + 3\Lambda_6 c_\beta^2 + 3\Lambda_7 s_\beta^2), \tag{2.23b}$$

$$M_{12}^2 = -m_{12}^2 + \frac{1}{2}v^2(2\Lambda_{345} s_\beta c_\beta + 3\Lambda_6 c_\beta^2 + 3\Lambda_7 s_\beta^2), \tag{2.23c}$$

$$M_{22}^2 = m_{12}^2 t_\beta^{-1} + \frac{1}{2}v^2 t_\beta^{-1}(2\Lambda_2 s_\beta^2 - \Lambda_6 t_\beta^{-1} c_\beta^2 + 3\Lambda_7 s_\beta c_\beta). \tag{2.23d}$$

In this case, there is no massless eigenvector and both mass spectrum and eigenvector decomposition are intricate. The eigenfields are given by

$$\begin{pmatrix} H \\ h \end{pmatrix} = \begin{pmatrix} c_\alpha & s_\alpha \\ -s_\alpha & c_\alpha \end{pmatrix} \begin{pmatrix} \mathrm{Re}\varphi_1^0 \\ \mathrm{Re}\varphi_2^0 \end{pmatrix}. \tag{2.24}$$

In this commonly used convention, the diagonalization of the mass matrix

$$\begin{pmatrix} m_H^2 & 0 \\ 0 & m_h^2 \end{pmatrix} = \begin{pmatrix} M_{11}^2 \cos^2\alpha + M_{22}^2 \sin^2\alpha + M_{12}^2 \sin 2\alpha & \frac{1}{2}(2M_{12}^2 \cos 2\alpha + (M_{22}^2 - M_{11}^2)\sin 2\alpha) \\ \frac{1}{2}(2M_{12}^2 \cos 2\alpha + (M_{22}^2 - M_{11}^2)\sin 2\alpha) & M_{11}^2 \sin^2\alpha + M_{22}^2 \cos^2\alpha - M_{12}^2 \sin 2\alpha \end{pmatrix} \tag{2.25}$$

is ensured provided that

$$\tan 2\alpha = \frac{2M_{12}^2}{M_{11}^2 - M_{22}^2}, \tag{2.26}$$

or equivalently

$$\sin 2\alpha = \frac{2M_{12}^2}{\sqrt{(M_{11}^2 - M_{22}^2)^2 + 4(M_{12}^2)^2}}, \tag{2.27}$$

$$\cos 2\alpha = \frac{M_{11}^2 - M_{22}^2}{\sqrt{(M_{11}^2 - M_{22}^2)^2 + 4(M_{12}^2)^2}}, \tag{2.28}$$

with $-\pi/2 \leq \alpha \leq \pi/2$. The eigenvalues can be easily extracted from the eigenvalue equation:

$$\det \begin{pmatrix} M_{11}^2 - \lambda & M_{12}^2 \\ M_{12}^2 & M_{22}^2 - \lambda \end{pmatrix} = 0, \tag{2.29}$$

and they explicitly read

$$m_{H,h} = \frac{1}{2}\left[M_{11}^2 + M_{22}^2 \pm \sqrt{(M_{11}^2 - M_{22}^2)^2 + 4(M_{12}^2)^2}\right] \tag{2.30}$$

assuming $m_H \geq m_h$. Therefore, unlike the SM, the 2HDM contains two dynamical neutral scalar Higgses. Finally, let us note the following transformation rules between the $\{\Phi_1, \Phi_2\}$ and the physical fields:

$$\varphi_1^\pm = c_\beta G^\pm - s_\beta H^\pm, \tag{2.31}$$

$$\varphi_2^\pm = s_\beta G^\pm + c_\beta H^\pm, \tag{2.32}$$

$$\varphi_1^0 = \frac{1}{\sqrt{2}}\left[c_\alpha H - s_\alpha h + i\left(c_\beta G^0 - s_\beta A^0\right)\right], \tag{2.33}$$

$$\varphi_2^0 = \frac{1}{\sqrt{2}}\left[s_\alpha H + c_\alpha h + i\left(s_\beta G^0 + c_\beta A^0\right)\right]. \tag{2.34}$$

2.1.2 The Higgs basis

The 2HDM Lagrangian is invariant under unitary transformations between the two Higgs fields [47]. This specific feature allows us to define the so-called Higgs basis $\{H_1, H_2\}$ as follows:

$$\langle H_1 \rangle = \begin{pmatrix} 0 \\ v/\sqrt{2} \end{pmatrix} \quad \text{and} \quad \langle H_2 \rangle = \begin{pmatrix} 0 \\ 0 \end{pmatrix}, \tag{2.35}$$

via the following unitary transformation:

$$\begin{pmatrix} H_1 \\ H_2 \end{pmatrix} = \begin{pmatrix} \cos\beta & \sin\beta e^{-i\delta} \\ -\sin\beta e^{i\xi} & \cos\beta e^{-i(\delta-\xi)} \end{pmatrix} \begin{pmatrix} \Phi_1 \\ \Phi_2 \end{pmatrix}. \tag{2.36}$$

The free parameter ξ can be chosen to fix the phase of the H_2 field. As a consequence, there exist an infinite number of equivalent Higgs bases parametrized by the H_2 phase. For future purposes, let us consider the case $\xi = \delta$. In this basis, the Yukawa sector Lagrangian in (2.1) takes the following form:

$$\mathcal{L}_Y = -\bar{Q}'_L \left(Y'_D H_1 + Z'_D H_2\right) d'_R - \bar{Q}'_L \left(Y'_U \tilde{H}_1 + Z'_U \tilde{H}_2\right) u'_R + \text{h.c.} \tag{2.37}$$

where

$$Y'_D = \cos\beta \Delta'_D + \sin\beta \Gamma'_D e^{i\delta}, \tag{2.38a}$$

$$Y'_U = \cos\beta \Delta'_U + \sin\beta \Gamma'_U e^{-i\delta}, \tag{2.38b}$$

$$Z'_D = -\sin\beta \Delta'_D e^{-i\delta} + \cos\beta \Gamma'_D, \tag{2.38c}$$

$$Z'_U = -\sin\beta \Delta'_U e^{i\delta} + \cos\beta \Gamma'_U. \tag{2.38d}$$

We can now use the following fields definition:

$$H_1 = \begin{pmatrix} H_1^+ \\ H_1^0 \end{pmatrix} = \begin{pmatrix} G^+ \\ (v + H + iG^0)/\sqrt{2} \end{pmatrix}, \tag{2.39}$$

$$H_2 = \begin{pmatrix} H_2^+ \\ H_2^0 \end{pmatrix} = \begin{pmatrix} H^+ \\ (R + iI)/\sqrt{2} \end{pmatrix}. \tag{2.40}$$

Note that in the case where the potential does not violate CP, as in the discussion of the previous section, the I field can be identified with the pseudoscalar A^0. This basis, where there is only one vev, will show itself to be very useful in order to identify the quark and boson masses.

2.1.3 Quarks and Higgses mass eigenstates

In the Higgs basis the quark masses are generated by the H_1 vev after SSB:

$$\begin{array}{ccc} SU(2)_L \otimes U(1)_Y & \xrightarrow{\text{SSB}} & U(1)_{\text{em}} \\ \mathcal{L}_{\text{Y}} & \xrightarrow{\text{SSB}} & -\frac{v}{\sqrt{2}}\left(\bar{d}'_L Y'_D d'_R + \bar{u}'_L Y'_U u'_R\right) + \dots \end{array} \tag{2.41}$$

Without any further assumptions, the complex matrices $Y'_{U,D}$ are arbitrary. However, we can always place ourselves in a basis where the quark fields are mass eigenstates. This can be achieved by using the bi-unitary transformations

$$u'_{L,R} = V^u_{L,R} u_{L,R} \quad \text{and} \quad d'_{L,R} = V^d_{L,R} d_{L,R}. \tag{2.42}$$

The full Yukawa sector can then be decomposed as

$$\mathcal{L}_{\text{Y}} = \mathcal{L}_{\text{mass}} + \mathcal{L}_{\text{neutral}} + \mathcal{L}_{\text{charged}}, \tag{2.43}$$

where

$$\mathcal{L}_{\text{mass}} = -\bar{d}_L M_D d_R - \bar{u}_L M_U u_R + \text{h.c.} \tag{2.44}$$

$$\mathcal{L}_{\text{neutral}} = -\frac{\sqrt{2}}{v}\left[\bar{d}_L\left(M_D H_1^0 + Z_D H_2^0\right) d_R + \bar{u}_R\left(M_U H_1^0 + Z_U^\dagger H_2^0\right) u_L\right] + \text{h.c.} \tag{2.45}$$

$$\begin{aligned} \mathcal{L}_{\text{charged}} = -\frac{\sqrt{2}}{v}\big[&\bar{u}_L V_{CKM}\left(M_D H_1^+ + Z_D H_2^+\right) d_R \\ &-\bar{u}_R\left(M_U H_1^+ + Z_U^\dagger H_2^+\right) V_{CKM} d_L\big] + \text{h.c.}, \end{aligned} \tag{2.46}$$

with

$$Z_{U,D} = \frac{v}{\sqrt{2}} V_L^{d,u\dagger} Z'_{d,u} V_R^{d,u}, \tag{2.47}$$

and

$$M_U = \frac{v}{\sqrt{2}} V_L^{u\dagger} Y'_U V_R^u = \begin{pmatrix} m_u & 0 & 0 \\ 0 & m_c & 0 \\ 0 & 0 & m_t \end{pmatrix}, \tag{2.48}$$

$$M_D = \frac{v}{\sqrt{2}} V_L^d Y'_D V_R^{d\dagger} = \begin{pmatrix} m_d & 0 & 0 \\ 0 & m_s & 0 \\ 0 & 0 & m_b \end{pmatrix}. \tag{2.49}$$

In the above expressions, we used the CKM matrix defined in (1.48).
In the previous section we have thouroughly studied the formalism of a CP-conserving 2HDM in the generic basis. Such an approach can be motivated

by the success of the CKM mechanism in order to account for CP violation in hadron physics. However, as we have mentioned in the beginning of the chapter, the CP violation mechanism present in the SM is unable to account for the observed baryon asymmetry of the Universe. If the symmetry is not imposed by hand, a 2HDM is able to provide additional sources of CP violation that can be interesting to study. Therefore, let us now consider a more general case where CP is not necessarily a symmetry of the potential, and derive the Higgs bosons masses departing from the Higgs basis. For now we will still hide all the details concerning mixing effects in the potential by introducing a generic mixing matrix in the neutral Higgs space:

$$\begin{pmatrix} H \\ R \\ I \end{pmatrix} = \mathcal{O} \begin{pmatrix} S_1 \\ S_2 \\ S_3 \end{pmatrix}. \tag{2.50}$$

Since the $\{H, R, I\}$ mass matrix must be symmetric by hermicity of the Lagrangian, the $\mathcal{O}$ matrix can be taken as orthogonal ($\mathcal{O} = \mathcal{O}^T$) independently of any $V(H_1, H_2)$ potential. However, if the Higgs potential is not invariant under CP, the mixing between the H and R fields with the pseudoscalar I indicates that the final mass eigenstates will not be CP eigenstates.

Let us illustrate these aspects in a more explicit way. Similar to (2.3), the most general renormalizable $SU(2)_L \otimes U(1)_Y$ gauge invariant potential in the Higgs basis reads:

$$\begin{aligned} V(H_1, H_2) =& \mu_1 H_1^\dagger H_1 + \mu_2 H_2^\dagger H_2 + \lambda_1 \left(H_1^\dagger H_1\right)^2 + \lambda_2 \left(H_2^\dagger H_2\right)^2 + \\ &+ \lambda_3 \left(H_1^\dagger H_1\right)\left(H_2^\dagger H_2\right) + \lambda_4 \left(H_1^\dagger H_2\right)\left(H_2^\dagger H_1\right) + \\ &+ \Big[\mu_{12} H_1^\dagger H_2 + \left(\lambda_5 H_1^\dagger H_2 + \lambda_6 H_1^\dagger H_1 + \lambda_7 H_2^\dagger H_2\right)\left(H_1^\dagger H_2\right) \\ &+ \text{h.c.}\Big]. \end{aligned} \tag{2.51}$$

The parameters μ_i and λ_i are not all independent. As we already explained in the previous section, additional requirements, such as the vacuum configuration, imply that linear terms are not allowed in either H, R or I. Therefore, since

$$V(H_1, H_2)|_{\text{linear}} = 2v\left[\, H(2\lambda_1 v^2 + \mu_1) + R(\text{Re}\lambda_6 v^2 + \text{Re}\mu_{12}) - I(\text{Im}\lambda_6 v^2 + \text{Im}\mu_{12})\right], \tag{2.52}$$

we conclude that the existence of a stable minimum requires

$$\mu_1 = -2\lambda_1 v^2, \tag{2.53}$$

$$\mu_{12} = -\lambda_6 v^2. \tag{2.54}$$

Under these conditions, the scalar potential becomes

$$V(H_1, H_2) = -\lambda_1 v^4 + m^2_{H^\pm} H^+ H^- + \frac{1}{2}\begin{pmatrix} H & R & I \end{pmatrix} M_N \begin{pmatrix} H \\ R \\ I \end{pmatrix} + ... \tag{2.55}$$

with

$$m^2_{H^\pm} = \mu_2 + v^2\lambda_3, \tag{2.56}$$

$$M_N = \begin{pmatrix} 4v^2\lambda_1 & 2v^2 \mathrm{Re}\lambda_6 & -2v^2 \mathrm{Im}\lambda_6 \\ 2v^2 \mathrm{Re}\lambda_6 & m^2_{H^\pm} + (\lambda_4 + 2\mathrm{Re}\lambda_5)v^2 & -2v^2 \mathrm{Im}\lambda_5 \\ -2v^2 \mathrm{Im}\lambda_6 & -2v^2 \mathrm{Im}\lambda_5 & m^2_{H^\pm} + (\lambda_4 - 2\mathrm{Re}\lambda_5)v^2 \end{pmatrix}. \tag{2.57}$$

The neutral Higgs mixing matrix is indeed symmetric and the would-be Goldstone bosons $G^{\pm,0}$ are found massless. This is a particularity of this choice of base where no additional mass diagonalization is needed in order to remove the Goldstone bosons. In the particular case where all the μ_i and λ_i parameters are real, the potential is invariant under CP and, as expected, we obtain:

$$M_N = \begin{pmatrix} 4v^2\lambda_1 & 2v^2\lambda_6 & 0 \\ 2v^2\lambda_6 & m^2_{H^\pm} + (\lambda_4 + 2\lambda_5)v^2 & 0 \\ 0 & 0 & m^2_{H^\pm} + (\lambda_4 - 2\lambda_5)v^2 \end{pmatrix}. \tag{2.58}$$

This choice of base will be widely used in the rest of this work, especially concerning the Yukawa sector.

2.2 Accidental Symmetries in the 2HDM

In the previous chapter, we have emphasized the accidental symmetries of the SM and their respective impact on phenomenology. Once a second $SU(2)_L$ scalar doublet is introduced, most of these SM features are no longer preserved

and one needs to introduce a mechanism that allows the model to account for the experimental data. In this section we will review, one by one, the different accidental symmetries of the SM and introduce the necessary constraints on the 2HDM which are favoured by the experimental results.

2.2.1 FCNC and Natural Flavour Conservation in the 2HDM

Flavour changing neutral currents (FCNC) are absent at tree-level in the SM. Once a second scalar doublet is introduced, FCNC easily arise. Firstly, let us have a look at the 2HDM neutral Yukawa Lagrangian:

$$\mathcal{L}_{\text{neutral}} = -\frac{\sqrt{2}}{v}\left[\bar{d}_L\left(M_D H_1^0 + Z_D H_2^0\right) d_R + \bar{u}_R\left(M_U H_1^0 + Z_U^\dagger H_2^0\right) u_L\right] + \text{h.c.} \tag{2.59}$$

In the SM, diagonalizing the mass matrices M_U and M_D automatically diagonalizes the Yukawa interactions. In the 2HDM, $M_{D,U}$ and $Z_{D,U}$ are not simultaneously diagonalizable in general and therefore, the Yukawa couplings are not always flavour diagonal. The neutral Higgs scalars in H_2^0 will mediate FCNC such as dsH.

These FCNC can cause difficulties regarding phenomenology, since the dsH interactions would for example contribute to $K^0 - \bar{K}^0$ mixing at tree-level. Since the Higgs couplings to fermions are related to their masses, tree-level FCNC involving top quarks would imply neutral Higgs masses of the order of 1 TeV in order to account for the experimental data. There are, therefore, two main possibilities to confront FCNC in the 2HDM: either a mechanism is found in order to justify why the couplings of tree-level FCNC are very small, or an additional condition is imposed to the model in order to get rid of tree-level FCNC. The latter possibility will be explained in this section while models with small tree-level FCNC will be dicussed later on.

Glashow and Weinberg [48] and Paschos [49] proved that the necessary and sufficient condition to avoid FCNC at tree-level in 2HDM is given by three conditions for all the fermions of a given charge and helicity:

- they transform under the same irreducible representation of $SU(2)$;
- they correspond to the same eigenvalue of T_3;

- there is a basis in which they all receive their contributions in the mass matrix from a single source.

In the SM, where all the fermions transform as left-handed doublets and right-handed singlets, the previous conditions are obviously satisfied by the fact that since all right-handed fermions of a given charge couple to the single Higgs multiplet. However, in the 2HDM, the conditions are fulfilled for two particular models. These models can be enforced through the introduction of additional symmetries. The resulting models of this type are commonly known as 2HDM with Natural Flavour Conservation (NFC).
In the type-I 2HDM, all quarks couple to just one of the Higgs doublets, while in the type-II 2HDM, the $Q = 2/3$ right-handed quarks couple to one Higgs doublet and the $Q = -1/3$ right-handed quarks couple to the other doublet. These two types can be achieved by imposing $\mathbb{Z}_2$ discrete symmetries with the following transformations of the Higgs doublets implemented in the generic basis (2.2):[1]

$$\textbf{Type-I:} \qquad \Phi_1 \to -\Phi_1 \Rightarrow \Delta'_D = \Delta'_U = 0, \tag{2.60}$$

$$\textbf{Type-II:} \qquad \Phi_1 \to -\Phi_1, d'_R \to -d'_R \Rightarrow \Gamma'_D = \Delta'_U = 0. \tag{2.61}$$

One might wonder why the $\mathbb{Z}_2$ symmetry has not been imposed directly in the Higgs basis (2.35). Actually, if that had been the case, since in the Higgs basis only one doublet (H_1) receives a non-zero vev, we would have obtained vanishing mass terms for all fermions in a type-II scenario and the sole remaining option would have been a type-I scenario where all fermions couple to H_1. In that case, all the new physical fields would belong to H_2. While this might be an interesting model that provides a natural candidate for dark matter, still it remains a very particular case that strongly restrains the phenomenological possibilities. If, on the other hand, the $\mathbb{Z}_2$ is chosen to be manifest in a generic basis and also promoted to be a symmetry of the Higgs potential, or at least broken only softly, then it will also be manifest in the Higgs basis while keeping the NFC models general enough. Regarding the couplings of the leptons to the Higgs doublets, it is conventionally assumed that the right-handed leptons

[1] Note that the original Peccei-Quinn models along with the supersymmetric models give the same Yukawa couplings as in the type-II 2HDM, but they get them through continuous symmetries.

satisfy the same discrete symmetry as the d'_R and couple to the same Higgs boson as the $Q = -1/3$ quarks. However, such a requirement is not imposed by the Paschos-Glashow-Weinberg theorem, and there are two additional NFC models. The first one is commonly known as lepton-specific or X model and requires that all the right-handed quarks couple to Φ_2 while all the right-handed leptons couple to Φ_1. The flipped or Y model requires that the $Q = 2/3$ right-handed quarks couple to Φ_2, and the $Q = -1/3$ right-handed quarks couple to Φ_1 while all right-handed leptons couple to Φ_2.

Another model that somehow satisfies the NFC conditions, without imposing a particular symmetry, is the aligned 2HDM introduced in [50]. This model assumes that the Yukawa coupling matrices for each doublet are actually proportionally related. In this case, the diagonalization of the mass matrices automatically implies the diagonalization of the other coupling matrices and FCNC are avoided at tree-level. The proportionality constants between the Yukawa matrices are free parameters of this model and are allowed to be complex.

A general formalism can be introduced where all these NFC models are contained. Considering the Lagrangian in (2.1), the definition in (2.5) and the relations (2.14), (2.18) and (2.24), the general NFC Yukawa interaction Lagrangian can be written as follows:

$$\mathcal{L}_{neutral} = -\sum_{f=u,d,\ell} \frac{m_f}{v}\left(\xi_h^f \bar{f} f h + \xi_H^f \bar{f} f H + i\xi_A^f \bar{f}\gamma_5 f A\right) \quad , \tag{2.62}$$

$$\mathcal{L}_{charged} = -\left\{\frac{\sqrt{2}V_{ud}}{v}\bar{u}\left(m_u \xi_A^u \frac{1-\gamma_5}{2} + m_d \xi_A^d \frac{1+\gamma_5}{2}\right) d H^+ + \frac{\sqrt{2}m_\ell \xi_A^\ell}{v}\bar{\nu}_L \ell_R H^+ + h.c.\right\}. \tag{2.63}$$

The phenomenology of these models has been widely studied and a rather complete review can be found in [51]. The latest results at LHC have also provided important constraints on these models parameters [52–60].

Up to now, we have only considered the Yukawa sector in order to avoid tree-level FCNC. However, if discrete symmetries are imposed, they should also hold in all the other sectors of the model to ensure the renormalizability of the theory. The $\mathbb{Z}_2$ symmetries actually reduce the scalar potential parameters, since they enforce the following conditions in (2.3):

$$m_{12} = \Lambda_6 = \Lambda_7 = 0. \tag{2.64}$$

	Type-I	Type-II	Lepton-specific	Flipped
ξ_h^u	$\frac{\cos\alpha}{\sin\beta}$	$\frac{\cos\alpha}{\sin\beta}$	$\frac{\cos\alpha}{\sin\beta}$	$\frac{\cos\alpha}{\sin\beta}$
ξ_h^d	$\frac{\cos\alpha}{\sin\beta}$	$-\frac{\sin\alpha}{\cos\beta}$	$\frac{\cos\alpha}{\sin\beta}$	$-\frac{\sin\alpha}{\cos\beta}$
ξ_h^ℓ	$\frac{\cos\alpha}{\sin\beta}$	$-\frac{\sin\alpha}{\cos\beta}$	$-\frac{\sin\alpha}{\cos\beta}$	$\frac{\cos\alpha}{\sin\beta}$
ξ_H^u	$\frac{\sin\alpha}{\sin\beta}$	$\frac{\sin\alpha}{\sin\beta}$	$\frac{\sin\alpha}{\sin\beta}$	$\frac{\sin\alpha}{\sin\beta}$
ξ_H^d	$\frac{\sin\alpha}{\sin\beta}$	$\frac{\cos\alpha}{\cos\beta}$	$\frac{\sin\alpha}{\sin\beta}$	$\frac{\cos\alpha}{\cos\beta}$
ξ_H^ℓ	$\frac{\sin\alpha}{\sin\beta}$	$\frac{\cos\alpha}{\cos\beta}$	$\frac{\cos\alpha}{\cos\beta}$	$\frac{\sin\alpha}{\sin\beta}$
ξ_A^u	$-\cot\beta$	$-\cot\beta$	$-\cot\beta$	$-\cot\beta$
ξ_A^d	$\cot\beta$	$-\tan\beta$	$\cot\beta$	$-\tan\beta$
ξ_A^ℓ	$\cot\beta$	$-\tan\beta$	$-\tan\beta$	$\cot\beta$

Table 2.1: Yukawa couplings of the fermions to the neutral Higgs bosons in the different NFC models.

However, the m_{12} term is usually kept since it only breaks the symmetry softly through a dimension-two term, avoiding divergent corrections.

2.2.2 Custodial invariant 2HDM

Unlike the SM, the most general scalar potential of the 2HDM is not invariant under custodial symmetry. This means that quantum corrections to the ρ parameter introduced in (1.61) could be very important. These corrections are measured by the parameter T defined in (1.73) and have been calculated in 2HDM theories. The deviations from the SM radiative corrections in a general 2HDM are given by [61]:

$$\begin{aligned}\alpha T &= -\frac{3g'^2}{64\pi^2}\sum_{i=1}^{3}\frac{\mathcal{O}_{i1}^2}{M_W^2-M_Z^2}L(m_{H_i}^2,m_{H_{ref}}^2)\\ &\quad+\frac{g^2}{64\pi^2 m_W^2}\left[\sum_{i=1}^{3}(1-\mathcal{O}_{i1}^2)F(m_{H_i}^2,m_{H^+}^2)-\frac{1}{2}\sum_{\substack{i,j,k=1\\ i\neq j\neq k}}^{3}\mathcal{O}_{i1}^2F(m_{H_j}^2,m_{H_k}^2)\right],\end{aligned} \tag{2.65}$$

with $\mathcal{O}_{ij}$ being the entries of the matrix defined in (2.50) and the L and F loop-funtions given by

$$L(x,y)=F(x,m_Z^2)-F(x,m_W^2)+F(y,m_W^2)-F(y,m_Z^2), \tag{2.66}$$

$$F(x,y)=\frac{x+y}{2}-\frac{xy}{x-y}\log\frac{x}{y}\ \ (\lim_{y\to x}F(x,y)=0). \tag{2.67}$$

The H_{ref} corresponds to the SM boson that is taken as a reference to study the deviations from this point. The first term in (2.65) contains radiative corrections due to gauge boson loops. This term is similar to the SM custodial breaking term, but contains contributions from the additional neutral bosons. It grows logarithmically with the bosons masses and will not cancel even if $SU(2)_L \times SU(2)_R$ is imposed to the 2HDM potential. However, the second term receives contributions caused by the breaking of custodial symmetry in the scalar potential and grows quadratically with the scalar masses. Yet, one can see that the correction cancels if there exists one neutral boson H_i such that

$$m_{H_i} = m_{H^+} \quad \text{and} \quad \mathcal{O}_{i1} = 0. \tag{2.68}$$

From this correction alone we already understand that imposing the custodial symmetry will imply such mass relations between the scalars.
Let us now construct a custodial invariant 2HDM potential. Similar to what we did in the SM case, we can introduce the following representations for the Higgs doublets Φ_i [61]:

$$M_i = (i\tau_2\Phi_i^*, \Phi_i) \equiv \begin{pmatrix} \phi_i^{0*} & \phi_i^+ \\ -\phi_i^- & \phi_i^0 \end{pmatrix} \qquad i = 1, 2. \tag{2.69}$$

They transform under the $SU(2)_L \times SU(2)_R$ symmetry as follows:

$$M_i \to L M_i R^\dagger. \tag{2.70}$$

We can now write the scalar potential that is left invariant under these transformations:

$$\begin{aligned} V(M_1, M_2) \;=\; & \frac{1}{2}m_{11}^2 \mathrm{tr}[M_1^\dagger M_1] + m_{22}^2 \mathrm{tr}[M_2^\dagger M_2] + \frac{1}{8}\Lambda_1 \left(\mathrm{tr}[M_1^\dagger M_1]\right)^2 \\ & + \frac{1}{8}\Lambda_2 \left(\mathrm{tr}[M_2^\dagger M_2]\right)^2 + \frac{1}{4}\Lambda_3 \mathrm{tr}[M_1^\dagger M_1]\mathrm{tr}[M_2^\dagger M_2] \\ & + \frac{1}{2}\Lambda_4 \left(\mathrm{tr}[M_1^\dagger M_2]\right)^2 - m_{12}^2 \mathrm{tr}[M_1^\dagger M_2] \\ & + \frac{1}{2}\left(\Lambda_6 \mathrm{tr}[M_1^\dagger M_1] + \Lambda_7 \mathrm{tr}[M_2^\dagger M_2]\right) \mathrm{tr}[M_1^\dagger M_2], \end{aligned} \tag{2.71}$$

with $\mathrm{tr}[M_i^\dagger M_j] = \Phi_i^\dagger \Phi_j + \Phi_j^\dagger \Phi_i$. Comparing it to the conditions on the general potential introduced in (2.3), we realize that here all the parameters m_{ij} and Λ_i need to be real and the additional relation $\Lambda_4 = \Lambda_5$ needs to be imposed to

get, from equation (2.21), the following mass degeneracy:

$$m^2_{H^\pm} = m^2_{A^0}. \tag{2.72}$$

There is, however, another way of defining the $SU(2)_L \times SU(2)_R$ symmetry matrix invariants that regroups both doublets in a single representation:

$$M_{21} = (i\tau_2\Phi_2^*, \Phi_1) \equiv \begin{pmatrix} \phi_2^{0*} & \phi_1^+ \\ -\phi_2^- & \phi_1^0 \end{pmatrix}. \tag{2.73}$$

In this case the matrix transforms as follows under $SU(2)_L \times SU(2)_R$ like:

$$M_{21} \to L M_{21} R^\dagger. \tag{2.74}$$

Here, the potential can be written as

$$\begin{aligned} V(M_{12}) \quad = \quad & m^2_{11}\mathrm{tr}[M^\dagger_{21}M_{21}] - m^2_{12}\left(\det[M_1^\dagger M_2] + h.c.\right) \\ & + \frac{1}{2}\Lambda_1\left(\mathrm{tr}[M^\dagger_{21}M_{21}]\right)^2 + \Lambda_4 \det[M^\dagger_{21}M_{21}] + \\ & \frac{1}{2}\left(\Lambda_5 \det(M_{21})^2 + h.c\right) + \left(\Lambda_6 \det(M_{21})\mathrm{tr}[M^\dagger_{21}M_{21}] + h.c\right)^2. \end{aligned} \tag{2.75}$$

The conditions on the potential parameters are $m_{11} = m_{22}$; $\Lambda_1 = \Lambda_2 = \Lambda_3$; $\Lambda_6 = \Lambda_7$; and m_{12}, Λ_5 and Λ_6 are complex. Although it is less clear than in the previous case, it can actually be proved that the previous conditions on the potential parameters lead to similar mass degeneracy as in (2.72) but with the H^0 scalar [61].

Even though the two resulting potentials are different, the two previous models are actually two different formalisms of the same case. In [62], it has been shown that the two models are related through a basis change and contain the same physics.

Yet another possibility has been suggested by the authors in [63]. They state that since the actual gauge symmetry is $SU(2)_L \times U(1)_Y$, the $SU(2)_R$ transformation of the second doublet is not totally fixed by the transformation of the first doublet, and find a more general transformation rule:

$$M_1 \quad \to \quad L M_1 R^\dagger, \tag{2.76}$$

$$M_2 \quad \to \quad L M_2 \tilde{R}^\dagger \qquad \text{with} \qquad \tilde{R} = X^\dagger R X, \tag{2.77}$$

where the matrix X needs to commute with $\exp i\tau_3$ in order to be $U(1)_Y$ invariant. Therefore $X = \exp i\gamma\tau_3$. Under these transformations, $\mathrm{tr}[M_1 X M_2^\dagger]$

is also invariant and the potential can be written as:

$$\begin{aligned} V(M_1, M_2) &= \frac{1}{2}m_{11}^2 \mathrm{tr}[M_1^\dagger M_1] + m_{22}^2 \mathrm{tr}[M_2^\dagger M_2] + \frac{1}{8}\Lambda_1 \left(\mathrm{tr}[M_1^\dagger M_1]\right)^2 \\ &+ \frac{1}{8}\Lambda_2 \left(\mathrm{tr}[M_2^\dagger M_2]\right)^2 + \frac{1}{4}\Lambda_3 \mathrm{tr}[M_1^\dagger M_1]\mathrm{tr}[M_2^\dagger M_2] \\ &+ \frac{1}{2}\Lambda_4 \left(\mathrm{tr}[M_1 X M_2^\dagger]\right)^2 - m_{12}^2 \mathrm{tr}[M_1 X M_2^\dagger] \\ &+ \left(\Lambda_6 \mathrm{tr}[M_1^\dagger M_1] + \Lambda_7 \mathrm{tr}[M_2^\dagger M_2]\right) \mathrm{tr}[M_1 X M_2^\dagger]. \end{aligned} \tag{2.78}$$

The different values of the newly introduced γ parameter provide different realizations of a custodial invariant 2HDM. Going back to the radiative corrections in (2.65), the cancellation condition in (2.68) is achieved in the previously mentioned models with

$$m_{A^0} = m_{H^+}. \tag{2.79}$$

However, the last potential introduced allows a different degeneracy relation in the particular case where $\gamma = \pi$: [63]

$$m_{H^0} = m_{H^+}. \tag{2.80}$$

This twisted scenario, where the pseudoscalar might be light, leads to an interesting phenomenology that has been widely studied in [64].

2.2.3 CP violation in the 2HDM

One of the important features that the 2HDM possesses with respect to the SM is that it can introduce additional sources of CP violation both in the potential as well as in the Yukawa sector. We have previously mentioned that the only source of CP violation in the SM is the V_{CKM} matrix and that it alone, though succesful, is not able to account for the baryon assymmetry of the Universe. In the 2HDM, on the other hand, the CP symmetry can be violated both explicitly and spontaneously. We will now consider both cases.

Explicit CP violation

We have mentioned after (2.3) that there are, in the most general scalar potential, four complex parameters: m_{12}, Λ_5, Λ_6 and Λ_7. However, one of the

phases of those parameters can be absorved by rephasing one of the doublets through a $U(1)$ transformation. Besides, a transformation can be applied to the doublets in order to obtain diagonal quadratic terms and get rid of the m_{12} term without any loss of generality. There are therefore only two independent complex phases in the most general 2HDM potential. Imposing CP invariance, however, does not mean that the two remaining parameters need to be real. As it has been shown by [65], starting with the most general CP transformation for n Higgs doublets

$$\Phi_i \xrightarrow{CP} \sum_{j=1}^{n} U_{ij}\Phi_j^* \qquad \Phi_i^\dagger \xrightarrow{CP} \sum_{j=1}^{n} U_{ij}^*\Phi_j^T, \tag{2.81}$$

one can obtain the conditions on the parameters m_{ij} and Λ_i for the potential (2.3) to conserve CP. In [65] these conditions are found to be:

- Λ_5 is real and Λ_6 and Λ_7 have equal phases or phases differing by π
- $\mathrm{Im}[\Lambda_5(\Lambda_6^* + \Lambda_7^*)^2] = 0$.

The addition of the new coupling matrices to the second doublet in the Yukawa sector introduces more sources of CP violation as well. Therefore, if CP is not imposed on the whole Lagrangian, it is necessarly violated both in the scalar and Yukawa sectors.

Spontaneous CP violation

In order to have spontaneous CP violation, one must have a CP invariant Lagrangian such that after SSB the vacuum is not invariant under CP. In the SM, where there is only one Higgs doublet, hermicity requires that the parameters of the scalar potential be real and that the scalar potential does not violate CP. Spontaneous CP violation is also ruled out, due to the possibility of using a $U(1)$ gauge transformation to remove the phase of the vev. In the 2HDM, the vev in (2.2) could in principle induce spontaneous CP violation. However, identifying the vev as CP-violating is not so straightforward. Actually, a CP invariant Lagrangian allows a number of different transformations -that can be interpreted as CP- under each of which it remains invariant. Therefore, the following conditions need to be satisfied for the vev to be CP violating.

- The Lagrangian allows different CP transformations for all of which it remains invariant.
- There is no CP transformation which leaves both the vacuum and the Lagrangian invariant.

We can illustrate this by making use of the CP transformation defined in (2.81). If the vev is CP invariant, i.e. $CP|0\rangle = |0\rangle$, then we have

$$\langle 0|\Phi_i|0\rangle = \sum_{j=1}^{2} U_{ij} \langle 0|\Phi_i|0\rangle^*. \tag{2.82}$$

If no transformation of the form (2.81) satisfies (2.82), CP is spontaneously broken. One of the first 2HDM to be studied, Lee's model [66], is an example of a 2HDM that spontaneously violates CP. 2HDMs where additional symmetries have been imposed have less opportunities to violate CP (even if the vacuum is complex) because the number of possible U matrices verifying (2.82) is larger. Notice that, since the Lagrangian should be invariant under CP, a realistic model needs to be able to account for the CP violation in flavour physics that the CKM mechanism is able to explain, without introducing complex phases in the Yukawa couplings.

Despite the attractiveness of the possibility of building a model where CP is violated spontanleously, there have been important arguments in the litterature about how models with spontaneously broken discrete symmetries can lead to grave difficulties in the context of cosmology [67]. The reason is that spontaneously broken discrete symmetries imply the existence of several degenerate ground states. After the big bang, causally disconnected spatial regions will have no special tendency to make the same choice of degenerate ground state. Therefore, at a later stage in the evolution, when the homogeneous ground state is approached everywhere locally, the different ground state regions will be separated by stable domain walls. As previously causally disconnected regions are always newly entering the horizon, it should be expected that at least one domain wall of roughly the dimension of the horizon will exist [68]. The domain wall total mass is proportional to $\sigma R^2(t)$ where σ corresponds to the domain wall mass per unit area and $R(t)$ to the cosmic scale factor. Therefore, the energy density scales as $1/R(t)$. This decrease in energy density is much

slower than the one found for ordinary radiation ($1/R^4(t)$) or nonrelativistic matter ($1/R^2(t)$) implying that stable domain walls quickly come to dominate the mass of the universe, which is in disagreement with observation.

CP-violation and NFC models

While models with sofly broken $\mathbb{Z}_2$ symmetry can explicitly violate CP, this is not the case for spontaneous CP violation. To prove this, we simply need to find a U matrix such that (2.82) holds. In the $\mathbb{Z}_2$ invariant case, the doublets vacuum configuration is given by

$$\langle \Phi_1 \rangle = \begin{pmatrix} 0 \\ v_1 e^{i\frac{\pi}{2}} \end{pmatrix} \quad \text{and} \quad \langle \Phi_2 \rangle = \begin{pmatrix} 0 \\ v_2 \end{pmatrix}. \tag{2.83}$$

The $\mathbb{Z}_2$ matrix acting on $(\Phi_1, \Phi_2)^T$, i.e.,

$$U = \begin{pmatrix} -1 & 0 \\ 0 & 1 \end{pmatrix}, \tag{2.84}$$

satisfies (2.82)

$$\begin{pmatrix} -1 & 0 \\ 0 & 1 \end{pmatrix} \begin{pmatrix} v_1 e^{i\frac{\pi}{2}} \\ v_2 \end{pmatrix}^* = \begin{pmatrix} v_1 e^{i\frac{\pi}{2}} \\ v_2 \end{pmatrix}, \tag{2.85}$$

and there is no spontaneous CP violation. This feature is no longer present in models with three doublets [69]. Indeed, the authors in [70] found a counterexample of a CP-violating vacuum in a Three Higgs Doublet Model with NFC. With respect to CP violation in the Yukawa sector in models with $\mathbb{Z}_2$ symmetry, since the diagonalization of the mass matrices automatically diagonalizes all the Yukawa couplings, there are no additional sources of CP violation in this case. In the aligned model [50], however, the couplings ξ_I^i in (2.62) (2.63) are free parameters of the theory, and complex phases can be introduced accounting for additional CP violation.

CP-violation and custodial symmetry

Let us now analyze the possibility of a custodial invariant 2HDM violating the CP symmetry. We will consider each of the three formalisms introduced in

section 2.2.2. In the formalism introduced through the matrix (2.69) there is a requirement on the vacuum [61] such that after SSB $SU(2)_L \times SU(2)_R$ is broken down to $SU(2)_V$,

$$\langle M_i \rangle = v_i \mathbf{1} \qquad \Rightarrow \qquad \langle \phi_i^0 \rangle = \langle \phi_i^{0*} \rangle = v_i \in \mathbb{R}. \tag{2.86}$$

This result already rules out the possibility of Spontaneous CP violation. Regarding explicit CP violation, we can define a CP transformation for the M_i matrix

$$M_i(\vec{x}, t) \to \tau_2 M_i(-\vec{x}, t)\tau_2 \qquad i = 1, 2. \tag{2.87}$$

Such a transformation is contained in the custodial transformations given in (2.70). Therefore, this model is also CP invariant.
The second case was given by the representation (2.73). The condition on the vacuum is

$$\langle M_{21} \rangle \propto \mathbf{1} \qquad \Rightarrow \qquad \langle \phi_1^0 \rangle = \langle \phi_2^{0*} \rangle = v_i \in \mathbb{C}. \tag{2.88}$$

The CP transformation in this case is given by

$$M_{21}(\vec{x}, t) \to \tau_2 M_i(-\vec{x}, t)\tau_2. \tag{2.89}$$

This transformation is of the same type as (2.74). Therefore, a custodial invariant Lagrangian in this formalism will also be CP invariant. With regards to the fact that the vevs in (2.89) can be complex, we can easily prove that spontaneous CP violation cannot be generated since the vacuum is also CP invariant:

$$(CP)\langle M_{21} \rangle (CP)^\dagger = \langle M_{21} \rangle. \tag{2.90}$$

The proof of the third case introduced in 2.2.2, is very similar to the first case, but with the corresponding custodial transformations in (2.76) and (2.77).The authors in [63] also explain that since the custodial invariant potential built in their formalism conserves $\mathbb{Z}_2$ symmetries as well, the CP symmetry is automatically conserved.

The strong CP problem

As we have already explained in the previous chapter, the strong CP problem is one of the most troubling issues of the SM. To solve this issue, most solutions

propose some symmetry that ensures $\theta = 0$.

One of the most elegant solutions was proposed by Peccei and Quinn [71]. Their model introduces a global chiral symmetry $U(1)_{PQ}$ under which the quarks and the Higgses transform non-trivially. In order to do so, the model consists of a 2HDM where the pseudoscalar is massless at tree-level. When the Higgs doublets acquire a vacuum, the $U(1)_{PQ}$ symmetry is spontaneously broken and the massless pseudoscalar acts as a Goldstone boson. However, since the $U(1)_{PQ}$ symmetry is anomalous, the pseudoscalar a_0, known as the axion, becomes a pseudo-Goldstone boson and ends up acquiring a small mass through instanton effects. The Peccei-Quinn model is able to solve the strong CP problem because the parameter θ is associated to a dynamical field, rather than being a constant, and can be dynamically set to zero. For several decades, the axion has been searched for, but has been eluding detection until now. The axion in the mass range of the model described above has actually already been ruled out. Therefore, more complex models which preserve the axion as the solution to the strong CP problem, but which do not run into conflict with experiment (for example through the addition of a complex singlet Higgs field with $V \gg v$), are still being looked for in helioscopes like CAST at CERN [2].

If such a symmetry is not imposed, one might think that $\Delta\theta$ corrections could provide insight into how the θ parameter can be kept small. The physical $\bar{\theta}$ parameter is actually given by the two contributions $\bar{\theta} = \theta_{QCD} + \theta_{QFD}$ as explained in (1.99) and (1.101). $\Delta\theta$ computations in the SM framework have already been carried out in the past. The two-loop corrections computed in [72,73] rely on perturbative short distance (SD) approaches that treat corrections to θ_{QCD} and θ_{QFD} separately. In the approach [74], the authors compute $\Delta\theta$ through $\eta' \to \pi\pi$ decays, providing direct access to the physical parameter $\bar{\theta}$.

One could in principle consider a similar approach in the case of 2HDM. However, the two scalar doublet extension possesses a supplementary issue since it can already introduce divergent corrections to θ_{QFD} at the one-loop level. A possible way out would be to find a mechanism between the new sources of CP violation, both in the scalar as in the Yukawa sector, that might be able

[2] CAST: CERN Axion Solar Telescope

to cancel the one-loop corrections for special values of the parameters. This would, in addition, provide a way to furtherly constrain the 2HDM.

2.2.4 Minimal Flavour Violation in the 2HDM

The flavour symmetry present in the SM is only broken, in a very particular way, by the Yukawa couplings which generate the mixing and masses of the fermions. When adding an additional doublet to the model, new Yukawa couplings need to be introduced. These couplings are arbitrary 3×3 matrices that may violate flavour and CP in a sizable way compared to the SM. The mass hierarchy between the fermion masses and mixing parameters in the SM is not explained by any mechanism and remains an intriguing feature of the SM. In the 2HDM case, the addition of new Yukawa matrices would imply adding arbitrary parameters to the theory. One may wish to describe the new flavour structures in terms of the SM ones, in order to let the already known masses and mixing parameters be the only ones responsible for flavour breaking. A method that has been widely used lately in flavour studies starts from the so-called Minimal Flavour Vioaltion (MFV) hypothesis [75]. To formulate the hypothesis, let us first go back to the SM flavour sector. If we restrain ourselves to the quark sector, we realize that the flavour symmetry $G_f = SU(3)_{Q_L} \times SU(3)_{U_R} \times SU(3)_{D_R}$ can be restored in the Yukawa Lagrangian (1.43) by imposing suitable transformation laws under G_f to the Yukawa couplings

$$Y'_U \sim (3, \bar{3}, 1)_{SU(3)^3}, \qquad Y'_D \sim (3, 1, \bar{3})_{SU(3)^3}. \tag{2.91}$$

By doing so, the Yukawa couplings are promoted into auxiliary fields or spurions. Although this symmetry conservation is achieved artificially, we realize that, if any flavour structure is constructed from these spurions in a G_f invariant way, the physical quantities associated to them will also be flavour invariant. This type of G_f invariant flavour structures would give rise to couplings of the form:

$$Y'_U Y'^{\dagger}_U, \qquad Y'^{\dagger}_D Y'_U Y'^{\dagger}_U Y'_D. \tag{2.92}$$

Once the Y_i couplings are frozen to their real values, the flavour breaking will still be controlled by the SM masses and mixing parameters. The MFV hypothesis takes advantage of this realization in order to study flavour physics

in models beyond the SM. We will define the MFV hypothesis by two conditions as it is done in [76]:

1. The first condition concerns the minimality of the hypothesis. MFV states that all the new structures beyond the SM must be invariant under the G_f group. To implement this condition, the new flavour structures are written as series in terms of the spurions. However, only the spurions needed to account for the known fermion masses and mixings are allowed. The spurions are therefore the building blocks for the new flavour structures, without any physical content.
   In the past, spurions were introduced for a straightforward isospin decomposition of the weak $K \to \pi\pi$ decay amplitudes, or to provide Goldstone bosons with a small mass in a chiral invariant effective theory for strong interactions. Here, MFV gives rise to an effective low-energy theory which does not make any assumption on the possible underlying high-energy dynamics of the spurions.

2. The second condition can be considered a naturality condition. Since every physical flavour observable will be written as series in terms of the spurions, if the coefficients of these series were arbitrary, they could involve complex phases or unnaturally introduce new hierarchies. To avoid any additional fine-tuning, we demand that the coefficients of the MFV expansion be natural, i.e. $\mathcal{O}(1)$, so that only the already known masses and mixing parameters are responsible for suppression or enhancement effects, CP violation, etc. If in one particular process a very small value of the MFV coefficients is needed to fit the data, this would mean that MFV fails to explain the flavour structure of the process. If, on the contrary, a value greater than one is needed for the coefficients, this would point to an additional flavour structure beyond the SM one.

MFV in the Higgs basis

The MFV hypothesis has already been applied to the 2HDM in several works [77–79]. However, the way the hypothesis is implemented and the choice of

flavour structures that are taken as the spurions can lead to quite different models, at least with respect to the fermion couplings. In [79], for example, the couplings Δ'_D and Γ'_U in the generic basis (2.1) are taken as the spurions and the remaining couplings, Γ'_D and Δ'_U, are written as a series of G_f invariant spurion structures. However, one could have chosen Γ'_D and Δ'_U to be the spurions and develop Δ'_D and Γ'_U as a series.

Since in the SM the Yukawa couplings to the two doublets for a same fermion family -let us choose the d quarks for example- cannot be simultaneously diagonalized, none of the couplings Δ'_D and Γ'_D in (2.1) correspond to the SM Yukawa coupling Y'_D that once diagonalized provides the d quarks with a mass. In the MFV implementation prescription that we have previously introduced, we have stated that "*the new flavour structures are written as series in terms of the spurions. However, only the spurions which are needed to account for the known fermion masses and mixings are allowed*". Following this prescription we have chosen to work on the Higgs basis (2.37), where the couplings $Y'_{D,U}$ are the only ones responsible for the quark masses just like in the SM. Furthermore, the CKM mixing matrix is also a consequence of the impossibility of simultaneously diagonalizing the up and down quark mass matrices, i.e. Y'_D and Y'_U. The Beyond the Standard Model (BSM) flavour structures are the $Z'_{D,U}$ couplings to the second doublet, which does not acquire a vev in the Higgs basis. Therefore, a way to realize the MFV requirement consists in developing the $Z'_{D,U}$ couplings as series of $H_{D,U} = Y'_{D,U}Y'^{\dagger}_{D,U}$:

$$Z'_U = [\alpha_0 + \alpha_1 H_D + \alpha_2 H_U + \alpha_3 H_D H_U + ...]Y'_U, \tag{2.93}$$

$$Z'_D = [\epsilon_0 + \epsilon_1 H_D + \epsilon_2 H_U + \epsilon_3 H_D H_U + ...]Y'_D. \tag{2.94}$$

One can easily prove that these series are actually finite. Using the Cayley-Hamilton theorem for a generic 3×3 matrix $\mathbf{M}$:

$$\mathbf{M}^3 - \langle \mathbf{M} \rangle \mathbf{M}^2 + \frac{1}{2}(\langle \mathbf{M} \rangle^2 - \langle \mathbf{M}^2 \rangle) - \det \mathbf{M} = 0, \tag{2.95}$$

where $\langle \mathbf{M} \rangle$ is the trace of the matrix, we can reduce the number of terms to 17 [76]. Furthermore, considering that when the diagonalized spurions Y_D and Y_U are frozen to their background values we have the relations $(Y_{D,U}Y^{\dagger}_{D,U})^2 \sim Y_{D,U}Y^{\dagger}_{D,U}$, we can reduce the series to four terms. Writing

$$Z'_D = QY'_D; \quad Z'_U = QY'_U, \tag{2.96}$$

we obtain

$$Q = x_0 + x_1 H_D + x_2 H_U + x_3\{H_D, H_U\} + i x_4 [H_D, H_U], \tag{2.97}$$

where the coefficients in Q are different for the different couplings Z'_D and Z'_U. In [78], a useful notation in terms of operators has been introduced. Taking into account the fact that the $Y'_{U,D}$ couplings once diagonalized generate the quark masses, we can rewrite the $H_{D,U}$ structures in the following way:

$$H_D = Y'_D Y'^{\dagger}_D = V^d_L M^2_D V^{d\dagger}_L = \frac{2}{v^2} V^d_L \left(\sum_i m^2_{d_i} P_i \right) V^{d\dagger}_L = \frac{2}{v^2} \sum_i m^2_{d_i} P_i^{d_L}, \tag{2.98}$$

$$H_U = Y'_U Y'^{\dagger}_U = V^u_L M^2_U V^{u\dagger}_L = \frac{2}{v^2} V^u_L \left(\sum_i m^2_{u_i} P_i \right) V^{u\dagger}_L = \frac{2}{v^2} \sum_i m^2_{u_i} P_i^{u_L}, \tag{2.99}$$

where $V^{d,u}_L$ are the diagonalization unitary matrices and P_i is a projector defined by $(P_i)_{jk} = \delta_{ij}\delta_{jk}$ and $P_i^{(d,u)_L} = V_L^{(d,u)} P_i V_L^{\dagger(d,u)}$. In this formalism, the $Z'_{D,U}$ couplings, once written in the quark mass basis, become

$$\begin{aligned} Z_D &= \frac{v}{\sqrt{2}} V^{d\dagger}_L Z'_D V^d_R \\ &= [\epsilon_0 + \epsilon_1 \frac{2}{v^2} \sum_i m^2_{d_i} P_i + \epsilon_2 \frac{2}{v^2} \sum_i m^2_{u_i} V^{\dagger}_{CKM} P_i V_{CKM} + ...] M_D \end{aligned} \tag{2.100}$$

$$\begin{aligned} Z_U &= \frac{v}{\sqrt{2}} V^{u\dagger}_L Z'_U V^u_R \\ &= [\upsilon_0 + \upsilon_1 \frac{2}{v^2} \sum_i m^2_{d_i} V_{CKM} P_i V^{\dagger}_{CKM} + \upsilon_2 \frac{2}{v^2} \sum_i m^2_{u_i} P_i + ...] M_U \end{aligned} \tag{2.101}$$

Some important observations need to be made at this point. Equations (2.100) and (2.101) show that tree-level FCNC remain after diagonalization of the quark mass matrices, since the ϵ_2 term in Z_D and the υ_1 term in Z_U contain non-diagonal terms. However, these FCNC are weighed by the V_{CKM} matrix elements and the M_D and M_U quark masses, as should be the case from the MFV hypothesis. One can therefore expect FCNC in 2HDM with MFV to be highly suppressed. We will nevertheless study their consequences in some physical processes in the next chapter.

It is worth noting as well, that despite de *naturalness* condition of the MFV coefficients that requires no new CP violation sources other than the already present in the SM, (2.97) introduces a CPV term through ix_4. Besides, in [80] it is argued that when the MFV expansion is truncated, complex coefficients of the MFV expansion are in principle generated. However, in this work, we

restrain ourselves to the case where the MFV coefficients are assumed to be real, and therefore the ix_4 term is not taken into account. We believe this is a choice we make in the way the MFV hypothesis is conceived and implemented since our departing point is that the only mass hierarchies and CP violation sources are the ones present in the SM.

BGL models

Another attempt which is quite similar to MFV, in that it aims at controlling all flavour and CP violation by the quark masses and CKM structures, has been proposed in [81]. In this particular case, horizontal symmetries are introduced in such a way that only the V_{CKM} elements involving the top quark will be relevant. In order to see this, let us take the Yukawa Lagrangian in a generic basis (2.1). The horizontal symmetry imposed is given by

$$S: \quad Q'_{L3} \to e^{i\alpha} Q'_{L3}; \quad u'_{R3} \to e^{i2\alpha} u'_{R3}; \quad \phi_2 \to e^{i\alpha}\phi_2; \quad \alpha \neq 0, \pi, \tag{2.102}$$

with all the other fields transforming trivially under S. Under this symmetry, the most general Yukawa couplings with three generations of quarks take the following form:

$$\Delta'_D = \begin{pmatrix} * & * & * \\ * & * & * \\ 0 & 0 & 0 \end{pmatrix}; \quad \Gamma'_D = \begin{pmatrix} 0 & 0 & 0 \\ 0 & 0 & 0 \\ * & * & * \end{pmatrix}; \tag{2.103}$$

$$\Delta'_U = \begin{pmatrix} * & * & 0 \\ * & * & 0 \\ 0 & 0 & 0 \end{pmatrix}; \quad \Gamma_U = \begin{pmatrix} 0 & 0 & 0 \\ 0 & 0 & 0 \\ 0 & 0 & * \end{pmatrix}. \tag{2.104}$$

From these couplings, we can already make the following observations:

- Since only the third row of Γ'_D is not equal to 0, once the diagonalization matrices $V^d_{L,R}$ are be applied to Γ'_D, only $(V^{d\dagger}_L)_{3j}$ will be relevant.
- since the Γ'_U and Δ'_U matrices are block diagonal, then $(V^u_L)_{3i} = (V^u_L)_{i3} = \delta_{i3}$ and since $V_{CKM} = V^{u\dagger}_L V^d_L$, we have $(V_{CKM})_{3j} = (V^d_L)_{3j}$.

- Due to the form of both Δ'_D and Γ'_D we obtain the following relation as well:

$$\Gamma'_D = \frac{v}{v_2} P_3 Y_D; \quad P_3 = \begin{pmatrix} 0 & 0 & 0 \\ 0 & 0 & 0 \\ 0 & 0 & 1 \end{pmatrix}. \tag{2.105}$$

Taking into account the previous remarks as well as equations (2.38), we obtain[3]:

$$\begin{aligned} Z_D &= \frac{v}{\sqrt{2}} V_L^{d\dagger} Z'_D V_R^d \\ &= \left[\frac{v_2}{v_1} - \left(\frac{v_2}{v_1} + \frac{v_1}{v_2} \right) V_L^{d\dagger} P_3 V_L^d \right] M_D = \left[\frac{v_2}{v_1} - \left(\frac{v_2}{v_1} + \frac{v_1}{v_2} \right) V^\dagger P_3 V \right] M_D \end{aligned} \tag{2.106}$$

$$\begin{aligned} Z_U &= \frac{v}{\sqrt{2}} V_L^{u\dagger} Z'_U V_R^u, \\ &= \left[\frac{v_2}{v_1} - \left(\frac{v_2}{v_1} + \frac{v_1}{v_2} \right) V_L^{u\dagger} P_3 V_L^u \right] M_U = \left[\frac{v_2}{v_1} - \left(\frac{v_2}{v_1} + \frac{v_1}{v_2} \right) P_3 \right] M_U. \end{aligned} \tag{2.107}$$

A comparison of these two last equations with the MFV expansion given in (2.100) and (2.101) leads us to conclude that this BGL model corresponds to a particular case of the MFV expansion, where all the quark masses are neglected with respect to the Higss vev except for the top quark mass. In this model, the previously "unknown" ϵ coefficients acquire a particular value in terms of the ratios of the vevs of the two doublets. However, it is important to note that in the BGL case, the form of the Yukawa couplings is given by an imposed symmetry, while in the case of the MFV expansion, some terms need to be neglected to give similar expressions.

There are actually six types of BGL models corresponding to six types of S symmetries. Three of them display FCNC in the down sector (when u'_{Rj} transforms non-trivially under S) and three of them show FCNC in the up sector (when d'_{Rj} transforms non-trivially under S).

[3]To simplify the expression we take $V_{CKM} \equiv V$

The aligned 2HDM

The aligned 2HDM with CP violation developed in [50] and mentioned in 2.2.1 can also be considered as a special case of MFV. In this model, the relations between the $Y'_{D,U}$ and the $Z'_{D,U}$ couplings in the Higgs basis are given by the alignment relations

$$Z'_D = \varsigma_d Y'_D, \qquad Z'_U = \varsigma_u Y'_U, \tag{2.108}$$

where the $\varsigma_{d,u}$ are simple coefficients which are allowed to take complex values, so that when the $Y'_{D,U}$ matrices are diagonalized so are the $Z'_{D,U}$. If the alignment coefficients $\varsigma_{d,u}$ are constrained to be real and $\mathcal{O}(1)$, the aligned 2HDM would be equivalent to a 2HDM with MFV where the expansions in (2.93) and (2.94) are taken to the 0^{th} order in $H_{D,U}$.

2.2.5 CP and Flavour invariants

In our study of CP violation in the SM framework, we have underlined the importance of the flavour structure of the model in order to construct quantities which are invariant under "weak basis" transformations, that is, transformations in the flavour space. In the previous chapter we showed that the necessary and sufficient condition for CP violation in the SM is given by (1.92). The 2HDM has a much richer flavour structure than the SM, even if symmetries can be imposed on the flavour parameters in order to constrain them. It seems useful, nevertheless, to define invariants which may appear in physical quantities and which can be helpful to check the flavour structure and CP violating properties of a flavour model, by comparing them with experimental results.
In the weak basis where both quark mass matrices M_U and M_D are diagonal, the flavour structure of the SM contains 10 parameters: the three up quark masses; the three down quark masses; the three angles of the V_{CKM} matrix; and its complex phase. It has been shown [82] that from the four invariants $\text{tr}(H_U H_D)$, $\text{tr}(H_U H_D^2)$, $\text{tr}(H_U^2 H_D)$ and $\text{tr}(H_U^2 H_D^2)$, one can construct the full V_{CKM} matrix. In a general 2HDM, we have the previous amount of parameters plus nine angles and nine phases for each of the Z_D and Z_U arbitrary complex matrices. If one introduces flavour symmetries in one particular weak basis, as in MFV or BGL models, the invariants constructed from the flavour quantities

must account for these symmetries regardless of the weak basis in wich they have been computed.

It is obvious by now that, in the 2HDM framework, one can build flavour invariants which do not appear in the SM. Each one of them will give some insight into the impact of the model on various physical phenomena. For example, the invariants [83]

$$\mathrm{tr}(Y'_D Z'^{\dagger}_D) = \frac{2}{v^2}\left[m_d (Z_D)^*_{dd} + m_s (Z_D)^*_{ss} + m_b (Z_D)^*_{bb}\right], \quad (2.109)$$

$$\mathrm{tr}(Y'_U Z'^{\dagger}_U) = \frac{2}{v^2}\left[m_u (Z_U)^*_{uu} + m_c (Z_U)^*_{cc} + m_t (Z_U)^*_{tt}\right], \quad (2.110)$$

probe the phases of the diagonal terms of the Z_U and Z_D which can contribute to quark electric dipole moments. In the MFV and BGL models introduced in the previous section, the diagonal terms of the Z_D and Z_U matrices are always real, therefore, the previous invariants will not contribute to quark electric dipole moments in these particular 2HDM. In the SM, the invariant in (1.92) measures CP violation arising from the misalignment of the Y'_D and Y'_U Yukawa couplings. In the 2HDM, with the presence of two additional Yukawa matrices, one can study CP violation effects arising from the misalignment between the SM and the new matrices:

$$\mathrm{tr}\left[Y_U Y_U^{\dagger}, Z_D Z_D^{\dagger}\right]^3 \propto (m_t^2 - m_u^2)(m_t^2 - m_c^2)(m_c^2 - m_u^2)(z_b^2 - z_d^2)(z_b^2 - z_s^2)(z_s^2 - z_d^2) Im Q, \quad (2.111)$$

where z_i are the eigenvalues of Z_D, and Q is a similar structure to (1.93), but with the unitary matrix involved $V^u_{Z_D}$ reflecting the misalignment between the Y_U and Z_D diagonalization matrices (V^u_L and $V^{Z_d}_L$) by the relation $V^u_{Z_D} = V^{u\dagger}_L V^{Z_D}_L$. There are three other invariants of this class, plus four other that are sensitive to the misalignment between the right-handed diagonalization matrices. In the MFV and BGL models previously introduced, the Z_D and Z_U are both described in terms of the SM mass and CKM matrices as can be seen in (2.100), (2.101), (2.106) and (2.107). This particular feature implies that invariants of the type (2.111) will again depend on V_{CKM} rather than on new misalignment matrices. However, an interesting characteristic of MFV and BGL models is that invariants of lower order than (1.92) can already account for CP violation. For example, in BGL models, the invariant

$$\begin{aligned}&\mathrm{Im\ tr}\left[M_D Z_D^{\dagger} M_D M_D^{\dagger} M_U M_U^{\dagger} M_D M_D^{\dagger}\right] \\ &\propto (m_b^2 - m_s^2)(m_b^2 - m_d^2)(m_s^2 - m_d^2)(m_c^2 - m_u^2)\mathrm{Im}(V_{22}^* V_{32} V_{33}^* V_{23}),\end{aligned} \quad (2.112)$$

accounts for CP violation even though the order in quark masses is lower than in the SM. This is because, in these kind of models, CP violation can also appear in FCNC but still depending on V_{CKM} parameters. Besides, even if there was a mass degeneracy between the top and another same charge quark, the invariant would still not vanish.
The previous discussion could be generalized to different cases of 2HDM with MFV where new sources of CP violation are allowed, through the expansion coefficients for example, or to a 2HDM where CP violation is not a symmetry of the scalar potential. In the second case, CP violation invariants depending on physical parameters will also include Higgs potential parameters [84].

2.3 Experimental constraints on 2HDM

Since the 2HDM is one of the simplest extensions of the SM Higgs sector, a large amount of work has been carried out since the first data release on the newly discovered boson, in order to constrain the 2HDM parameter space and look for any hint of its additional predicted particles. The LHC-discovered boson seems to own every feature of the SM-predicted one, from its quantum numbers to its couplings to other particles. Therefore, any 2HDM attempting to be consistent with the data, must identify one of its scalars with the newly discovered one and study a limit where it behaves like the SM scalar. Concerning flavour, most studies have been carried out in models with NFC, due to the flavour constraints coming from the unitary triangle and B meson rare decays wich are extremely sensitive to quark flavour mixing. Besides, the presence of several free parameters in a 2HDM doesn't allow us to rule out the model as a whole and only some points of the parameter space can be constrained. There are also numeruous different realizations of the 2HDM and studies tend to only concentrate in some of them. We include a short summary of what we consider the most relevant constraints related to our work.

- Concerning the direct Higgs searches, the constraints can only be fully applied to the SM-like scalar h^0 in a 2HDM where CP is conserved. The additional scalar and pseudoscalar of the 2HDM (H^0 and A^0) couple in different ways to the SM particles. In a general 2HDM with NFC and im-

posing the h^0 couplings to be SM-like ($\cos(\beta-\alpha) \ll 1$), the H^0 trilinear coupling to vector bosons is very small while A^0, being a pseudo-scalar, does not have such a coupling. This has a lot of implications not only concerning the WW and ZZ decays, but also concerning the production mechanism, since it will be mainly gluon fusion driven. The ATLAS collaboration having provided a limit on a fully ggF generated Higgs-like boson decaying into two photons [85], provides an upper limit to the boson mass that could in principle be applied to the additional neutral (pseudo-)scalar $m_{A^0,H^0} > 200$ GeV depending on their couplings to fermions. Other limits on the pseudoscalar mass m_{A^0} come mainly from $\tau\tau$ decays as a function of $\tan\beta$ [86]. A search for a pseudoscalar A^0 decaying into a Z boson and the 125 GeV scalar h^0 has been carried out by the CMS collaboration [87]. No evidence of background deviation has been observed and upper limits have been set on the cross-section branching ratio product in the context of type-I and type-II models. Concerning the charged Higgs boson $H^\pm$, the most constraining limits are still those provided by B physics experiments. However, we will give more details on these constraints in the next chapter, once we have introduced the specificities of our model, since we will only consider the limits relevant to our study.

- A complete study which corrects the width used in the CMS and ATLAS analyses to the H^0 and A^0 widths in a CP conserving 2HDM with NFC, has been carried out in [58]. They consider both the case where the 125 GeV scalar is the lightest neutral scalar, and the case where it is the heaviest. They conclude that detection of additional Higgs particles is still possible within LHC searches. In the case where the 125 GeV scalar is the lightest one, the most favoured scenario is the 2HDM taken to the decoupling limit, where the masses of the other Higgs particles $m_{H^0} \approx m_{A^0} \approx m_{H^\pm}$ are very large and their detection at the LHC seems impossible. However, the authors highlight a particular type-II model case with a lighter scalar where the detection of the pseudoscalar A^0 could still be possible.

- Several studies on type-II 2HDM have underlined another interesting case in the parameter space still allowed by the data. Two major scenarios

of a type-II CP conserving 2HDM with an 8-parameter potential are favoured. The first scenario is an SM-like case, where h^0 is the 125 GeV boson and the other Higgs particles are very heavy and decoupled. In the second case, called the "wrong-sign scenario", the Higgs coupling to down-type quarks changes sign relative to the SM, while couplings to up-type quarks and massive gauge bosons are the same. The case with wrong-sign couplings to up-quarks has been ruled out, since it requires a small value of $\tan\beta$ already incompatible with observations [88]. The "wrong-sign scenario" was first studied in [88] and has led to several studies after the LHC data release [58–60, 89]. The main consclusion being that, as more data are released by the LHC at $\sqrt{s} = 14$ TeV, a higher precision determination of the $h\gamma\gamma$ coupling could either rule out or confirm the wrong-sign scenario. In particular, the charged Higgs contribution to this decay suppresses the diphoton branching ratio to an amount such that the LHC could be sensitive enough.

2.4 Summary

The SM of elementary particles and fundamental interactions is based on gauge symmetries. However, some sectors of the SM have shown themselves to *accidentally* conserve additional symmetries. These symmetries are responsible for numerous features which have been experimentally confirmed to a very high precision level. A simple extension of the SM such as the 2HDM, loses, in its most general case, several of these accidental symmetries.

In this chapter we introduced the formalism of a general 2HDM. We then analysed, one by one, the constraints which need to be applied to the 2HDM Lagrangian in order to preserve the SM accidental symmetries or at least break them as minimally as possible. This was done with the aim of being able to take advantage of the richer phenomenology provided by an extended scalar sector, while at the same time maintaining the outstanding features of the SM that have guaranteed its impressive success. Finally, we summarized the most relevant constraints on the 2HDM provided by the LHC data.

Chapter 3

Phenomenology of a custodial invariant 2HDM with MFV

Despite the undeniable success of the SM and its very specific characteristics, we have shown in the previous chapter that several of its accidental symmetries can still be imposed to a more involved model with two scalar doublets. In this chapter we will focus on the predictions of a particular realization of the 2HDM that minimally breaks the custodial, the flavour and the CP symmetries. First, we will specify the properties of the model which we will be studying. Then, we will focus on the predictions of the model concerning flavour physics. We will analyze Kaon and B-meson physics. We will focus our work on the ϵ_K parameter that measures the amount of CP violation in the neutral kaon system and its real part $\mathrm{Re}(\epsilon_K)$ that can also be extracted from experiments. With respect to B-meson physics, we will study the neutral strange B-mesons mass difference ΔM_{B_s} and the neutral B-meson rare decays into two muons $B_{s,d} \to \mu^+\mu^-$ recently measured for the first time at the LHC. Lastly, we will analyze some LHC phenomenology.

3.1 The Model

In the previous chapter we studied constraints are to be applied to the 2HDM scalar potential in order for it to be custodial invariant. This way, corrections to (2.65) are kept small and the source of the custodial symmetry breaking is the same as in the SM, i.e. radiative corrections due to gauge boson and fermion loops. The presence of additional scalars will modify these corrections, but the source of the breaking remains the same as in the SM. It was also shown previously that any custodial invariant scalar potential will conserve CP as well. Neglecting CP violation in the strong sector, the only CP breaking sources will therefore come from the Yukawa Lagrangian. Instead of specifying a particular custodial invariant scalar potential and deriving all the specific properties, we stay as general as possible [46] and classify the scalars in triplet and singlet irreducible representations of the unbroken $SU(2)_{L+R}$, namely

$$\Phi_1 \ni \begin{pmatrix} G^+ \\ G^0 \\ G^- \end{pmatrix} \oplus \{h^0 + \frac{v}{\sqrt{2}}\}; \qquad v = (\sqrt{2}G_F)^{-\frac{1}{2}} \approx 246 \text{ GeV} \tag{3.1}$$

and

$$\Phi_2 \ni \begin{pmatrix} H^+ \\ A^0 \\ H^- \end{pmatrix} \oplus \{H^0\} \text{ or } \begin{pmatrix} H^+ \\ H^0 \\ H^- \end{pmatrix} \oplus \{A^0\}. \tag{3.2}$$

A particularity of the specific model introduced in (3.1) and (3.2) is that only Φ_1 contains a non vanishing vev. These assignments, with h^0 behaving as the SM scalar and all the new physical states beyond the SM being in Φ_2, would correspond to a particular case of the Higgs basis introduced in the previous chapter with a further assumption on the $H^0 - h^0$ mixing angle, namely $\alpha = \beta - \frac{\pi}{2}$. The triplet in (3.1) corresponds to the massless Nambu-Goldstone bosons. The two possibilities presented in (3.2) correspond to the two cases where either the pseudoscalar A^0 forms a triplet of $SU(2)_{L+R}$ with $H^\pm$, or it is the additional scalar H^0 that forms the triplet with $H^\pm$. These two cases are equivalent to the particular realizations of a custodial invariant 2HDM potential presented in (2.79) and (2.80). In the limit where the scalar triplet in (3.2) is also degenerate in mass, the custodial $SU(2)_{L+R}$ symmetry is minimally broken as in the SM, i.e., by m_b, m_t and g'. Actually, all the additional scalar

contributions to the ρ parameter cancel. In [90] it has been shown that in a general 2HDM, the only scalar vacuum polarization diagrams contributing to ρ are those with trilinear couplings. Since in our model Φ_2 is vectophobic, meaning that it does not have trilinear couplings to vector bosons, its quantum corrections to the ρ parameter cancel.

Concerning the masses of the different particles, several constraints can be applied. In our work in [46], we considered the case where the singlet component of (3.2) is light compared to its triplet partners:

$$m_{H^0} < m_{A^0} \approx m_{H^\pm} \quad \text{or} \quad m_{A^0} < m_{H^0} \approx m_{H^\pm}, \tag{3.3}$$

while the mass of the SM-like Higgs boson h^0 was left as a free parameter of the theory. Given the latest LHC results, where the newly found particle seems to possess all the properties of the SM scalar, it appears to be no longer possible to make the hypothesis in (3.3) by identifying the light BSM (pseudo)scalar with the observed one. Therefore we will study the properties of the model assuming that h^0 is the newly discovered boson at 125 GeV. We are hence left with two main mass hierarchies. The so-called decoupling limit, where the SM-like Higgs is decoupled from the rest of the Higgs particles,

$$m_{h^0} \ll m_{H^\pm}, m_{A^0}, m_{H^0}, \tag{3.4}$$

seems less interesting from a phenomenological point of view. Since its BSM particles are too heavy to be detected in any current experiment, the phenomenological signature of this model reduces to the SM one. The other hierarchy still not ruled out would be

$$m_{h^0}, m_{A^0(H^0)} < m_{H^0(A^0)} = m_{H^\pm}. \tag{3.5}$$

It actually covers the two different cases where either the pseudoscalar, or the additional neutral scalar is the one degenerated with $H^\pm$.

The strongest constraints on the charged Higgs mass come from B-meson physics. That is why, before stating them and studying how to apply them to our particular model, we need to specify the flavour sector of our model and how the two scalar doublets couple to flavoured particles. To do so, let us take a look at the quark Yukawa Lagrangian written, in the Higgs basis, namely in terms of Φ_1 and Φ_2:

$$\mathcal{L}_Y = -\bar{Q}'_L \left(Y'_D \Phi_1 + Z'_D \Phi_2\right) d'_R - \bar{Q}'_L \left(Y'_U \tilde{\Phi}_1 + Z'_U \tilde{\Phi}_2\right) u'_R + h.c. \tag{3.6}$$

In this model, all the fermions acquire a mass through their coupling Y to Φ_1 after SSB, while tree-level FCNC are induced by their coupling Z to the new spin-0 felds in Φ_2.

As we have previously stated, we will be applying the MFV hypothesis to our specific model. Following the prescription given in the previous chapter, the MFV formalism can be applied in this case by expressing the additional flavour structures Z_i as series of the Y_i couplings in a $G_f = SU(3)_{Q_L} \times SU(3)_{U_R} \times SU(3)_{D_R}$ invariant way, as done in (2.93) and (2.94). Instead of taking the full series into account, we make a quite accurate approximation based on the fact that, once the flavour matrices $Y'_{D,U}$ are diagonalized, they give rise to the quark mass matrices. Making use of our knowledge of the quark masses hierarchy, we can neglect the down-quark mass contributions with respect to the top mass, and the MFV series are therefore given by [46]:

$$Z'_D \cong \{\delta_0 + \delta_1 Y'_U Y'^{\dagger}_U\} Y'_D, \tag{3.7}$$

$$Z'_U \cong \{\upsilon_0 + \upsilon_1 Y'_U Y'^{\dagger}_U\} Y'_U, \tag{3.8}$$

where the $\delta_i, \upsilon_i \leq 1$ are arbitrary real coefficients of order one to avoid any fine-tuning. In the quark mass eigenstate basis, where the $Y_{U,D}$ matrices are diagonalized, the misalignment between the down and up quark masses causes the Z_D couplings to be non-diagonal. Since the second doublet Φ_2 alone is concerned with these couplings, only H^0 and A^0 will be the FCNC mediators. Considering only the top mass contribution, the non-diagonal FCNC couplings are then given by

$$(Z_D)_{ij} = 4G_F \delta_1 (V^*_{ti} V_{tj}) m_t^2 \frac{m_{d_j}}{v} \qquad i \neq j. \tag{3.9}$$

From the previous equation we note that CP violation could appear in FCNC as well through the standard CKM matrix elements.

3.2 Comparison with other models

Although some models have already been mentioned in previous sections, let us stop here for a while to compare the particular realization of the MFV hypothesis in a custodial invariant 2HDM with other models present in the literature.

3.2.1 Models with NFC

The first comparison we want to make concerns models with NFC, where the flavour conservation has been achieved by imposing $\mathbb{Z}_2$ discrete symmetries. Since we are focusing on the quark sector alone, these NFC models are mainly the Type-I and Type-II models introduced in 2.2.1. These models have been built to avoid any FCNC at tree-level, which is one of the main differences between NFC and MFV. Using equations (2.60) and (2.61) and assuming that there is no relative phase δ between the two doublets' vevs, we obtain analogous relations to (3.7) and (3.8):

$$\text{Type-I} \begin{cases} Z'_D = \cot\beta Y'_D \\ Z'_U = \cot\beta Y'_U \end{cases}, \qquad \text{Type-II} \begin{cases} Z'_D = -\tan\beta Y'_D \\ Z'_U = \cot\beta Y'_U \end{cases}. \tag{3.10}$$

From these relations we notice that both Type-I and Type-II seem to be particular cases of MFV when the series expansion is stopped at the first order, and with particular values of the coefficients related to $\tan\beta$. However, in the Type-II case, the previous statement is not totally correct, since both $\tan\beta$ and $\cot\beta$ cannot be simultaneously of $\mathcal{O}(1)$ except for the very particular case where $\beta = \pi/4$. Therefore, this model does not in general verify the requirement imposed on the MFV expansion coefficients. Nevertheless, in processes where only charged currents contribute, the study of Type-I 2HDM contributions can be used to impose constraints on our MFV 2HDM with the proper translation between $\tan\beta$ and the MFV expansion coefficients.

3.2.2 Models with flavour alignment

A similar conclusion as in the NFC case can be drawn from the study of the aligned 2HDM [50]. The relations between the two doublets Yukawa couplings in this model are given by

$$Z_D = \varsigma_D Y_D \quad \text{and} \quad Z_U = \varsigma_U Y_U, \tag{3.11}$$

where the coefficients ς_i can be complex. We believe that this is in fact almost equivalent to the MFV case developed here when taken to the first order (where no FCNC are present at tree-level). In [50] the authors argue that FCNC

are driven by the same structures as in the MFV case. There are however two main differences between these two approaches. One is that, as far as we understand, no constraint is imposed on the ς_i coefficients, while in the MFV case the coefficients must be $\mathcal{O}(1)$. The second difference is that, since in the aligned model the new FCNC contributions are produced by quantum corrections, they are suppressed by loop factors. In the general MFV case, FCNCs appear at tree-level without any extra suppression. However, if the ς_i coefficients are free to take any value, the small loop factors can always be compensated by these coefficients and provide sizeable contributions, while in the first order MFV case we do not have this freedom and suppressions are only due to quark masses and V_{CKM} matrix elements.

Regarding the fermion couplings with the charged Higgs, they are given, in our model, by the following Lagrangian [77]:

$$\mathcal{L}_{H^+} = \frac{\sqrt{2}}{v}\sum_{i,j=1}^{3}\bar{u}_i\left[A_d^i m_j\frac{1+\gamma_5}{2} - A_u^i m_i\frac{1-\gamma_5}{2}\right]V_{ij}d_j H^+ + h.c., \tag{3.12}$$

with

$$A_d^i = \delta_0 + \delta_1\frac{2m_t^2}{v^2}\delta_{i3}, \qquad A_u^i = \upsilon_0 + \upsilon_1\frac{2m_t^2}{v^2}\delta_{i3}. \tag{3.13}$$

As already mentioned before, the well-known Type-I and Type-II 2HDM correspond to particular relations between the series parameters in this model and $\tan\beta$:

$$\text{Type I:} \qquad A_d^i = A_u^i = \cot\beta, \tag{3.14}$$

$$\text{Type II:} \qquad A_d^i = -1/A_u^i = -\tan\beta. \tag{3.15}$$

A similar relation can also be found with the aligned 2HDM:

$$A_u = |\varsigma_u|, \qquad A_d = |\varsigma_d|, \tag{3.16}$$

while taking into account the MFV constraint $A_{u,d} \sim \mathcal{O}(1)$ and the fact that $\varsigma_{u,d}$ are allowed to be complex. Establishing a relation between our parameters and NFC models parameters may be useful to constrain our model by using the limits on the 2HDM parameters. As a matter of fact, we have made use of some constraints from the aligned 2HDM [50] regarding the charged Higgs mass. Although in [77] the model studied shows more similarities with our model and the same observables are studied in order to constrain the charged Higgs

mass, we will also take a look at similar studies on the aligned 2HDM [91, 92] in order to have a more complete and updated view. The authors in [91] constrain the charged Higgs mass through the analysis of the $Z \to b\bar{b}$ decay. The charged Higgs contribution to this decay is related to the H^+tb coupling that is proportional to both m_t and $V_{tb} \approx 1$ and is therefore expected to provide a bigger contribution than the $Z \to s\bar{s}$ or $Z \to d\bar{d}$ decays. A simple way to get rid of the QCD and EW corrections dependence is by studying the ratio [91]

$$R_b \equiv \frac{\Gamma(Z \to \bar{b}b)}{\Gamma(Z \to \text{hadrons})} = \left[1 + \frac{S_b}{s_b} C_b^{QCD}\right]^{-1} \tag{3.17}$$

with $C_b^{QCD} \approx 1$ being a factor including QCD corrections and where

$$s_q = [(\bar{g}_b^L - \bar{g}_b^R)^2 + (\bar{g}_b^L + \bar{g}_b^R)^2] \left(1 + \frac{3\alpha}{4\pi} Q_q^2\right); \qquad S_b = \sum_{q \neq b,\ell} s_q. \tag{3.18}$$

The model-dependence enters through the $\bar{g}_b^{L,R}$ parameters. Adapting the expressions given in [91] to our own model we obtain

$$\bar{g}_b^L = \bar{g}_{b,SM}^L + \frac{\sqrt{2} G_f m_W^2}{16\pi^2} \frac{m_t^2}{m_W^2} A_u^2 \left[f_1(t_h) \frac{\alpha_s}{3\pi} f_2(t_h)\right], \tag{3.19}$$

$$\bar{g}_b^R = \bar{g}_{b,SM}^R - \frac{\sqrt{2} G_f m_W^2}{16\pi^2} \frac{m_b^2}{m_W^2} A_d^2 \left[f_1(t_h) \frac{\alpha_s}{3\pi} f_2(t_h)\right], \tag{3.20}$$

where $t_h = \frac{m_t^2}{m_{H^\pm}^2}$ and the $f_i(t_h)$ are loop functions related to NLO corrections that can be found in [77]. Because of the relative factor between the top and bottom masses, the constraints to be applied on A_d are much weaker than those on A_u. Therefore, we neglect its contribution and obtain the following bound:

$$\frac{|A_u|}{m_{H^\pm}} < 0.0024 \text{ GeV}^{-1} + \frac{0.72}{m_{H^\pm}} < 0.011 \text{ GeV}^{-1}. \tag{3.21}$$

The previous boundary ensures that the charged scalar mass should be heavier than 116 GeV if we impose the MFV to be smaller than the unity, what constitutes a quite weak constraint. In [91], and later on in [92], a very detailed study about the $\bar{B} \to X_s\gamma$ decay rate and CP asymmetry was carried out. Here, we apply their main results to our model in order to further constrain the charged Higgs mass $m_{H^\pm}$. Given that our model does not provide any additional sources of CP violation that could have some impact on the

CP asymmetry, we focus on their results on the $\bar{B} \to X_s\gamma$ branching ratio. Following [93] we can express the branching ratio as

$$\mathcal{B}(\bar{B} \to X_s\gamma)_{E_\gamma < E_0} = \mathcal{B}(\bar{B} \to X_c e\bar{\nu})_{exp} \left|\frac{V_{ts}^* V_{tb}}{V_{cb}}\right|^2 \frac{6\alpha}{\pi C_B}[P(E_0) + N(E_0)], \tag{3.22}$$

where

$$C_B = \left|\frac{V_{ub}}{V_{cb}}\right|^2 \frac{\Gamma(\bar{B} \to X_c e\bar{\nu})}{\Gamma(\bar{B} \to X_u e\bar{\nu})} = 0.580 \pm 0.016. \tag{3.23}$$

The interest of the previous normalization lies in the cancellation of non-perturbative corrections that minimizes the sources of uncertainty. In the approximation $m_s = 0$, the charged Higgs effects appear in the Wilson coefficients of the perturbative part:

$$C_i^{eff}(\mu_W) = C_{i,SM} + |A_u|^2 C_{i,uu} - (A_u A_d) C_{i,ud}. \tag{3.24}$$

The BSM contributions are virtual top-quark dominated and their exact expressions can be found in [77]. We make use of the results in [91] for the real values of their parameters. These constraints are much more stringent than the previous case, however, for a charged Higgs mass heavier than 400 GeV, values of A_u and A_d of order one are still allowed. Besides, it is worth noting that the case where A_u and A_d have opposite signs considerably loosens the constraints.

3.2.3 Alignment limit in the scalar sector

Given the impressive compatibility between the newly discovered 125.5 GeV scalar boson and the SM Higgs boson couplings, the alignment limit of the 2HDM seems one of the most interesting realisations of the 2HDM where NP phenomenology could still be observed. This particular limit consists on the assumption that one of the neutral Higgs mass eigenstates of the 2HDM is aligned with the vev. The previous assumption implies as a direct consequence that the 'aligned' mass eigenstate has SM-like couplings to all the SM particles [94]. The custodial invariant 2HDM introduced in (3.1) and (3.2) can be considered as a case of optimal alignment by construction. In [94], the conditions to achieve the alignment limit are given in terms of the mixing parameters

between the neutral scalar h^0 and H^0, allowing to further constrain the CP invariant scalar potential. The neutral scalars are given in terms of the two doublets H_1 and H_2 in the Higgs basis as follows:

$$H^0 = (\sqrt{2}\mathrm{Re}H_1^0 - v)\cos(\beta-\alpha) - \sqrt{2}\mathrm{Re}H_1^0 \sin(\beta-\alpha) \tag{3.25}$$

$$h^0 = (\sqrt{2}\mathrm{Re}H_1^0 - v)\sin(\beta-\alpha) + \sqrt{2}\mathrm{Re}H_1^0 \cos(\beta-\alpha). \tag{3.26}$$

The alignment condition can be achieved in two different cases. First of all, if the mixing angle between the two states verifies the condition $\cos(\beta-\alpha) \ll 1$, then h^0 aligns with the vev and has SM-like couplings to fermions and vector bosons. On the other hand, if $\sin(\beta-\alpha) \ll 1$, it is H^0 who has SM-like couplings. As we already mentioned in 3.1, our model requires the mixing angle relation $\alpha = \beta - \pi/2$ that verifies $\cos(\beta-\alpha) = 0$.

The well-kown decoupling limit, where all the Higgs particles but one neutral scalar are heavy with respect to v, also has one of the neutral scalars behaving like the SM Higgs boson. The case where both are verified, i.e. alignment and decoupling, is called double decoupling limit, but the alignment without decoupling could in principle provide a more interesting phenomenology since it allows lighter BSM particles with a very SM-like Higgs boson.

In [94] and [95] the phenomenological analysis of the alignment limit has been carried out for $m_{h^0} = 125.5$ GeV ($\cos(\beta-\alpha) \ll 1$) and $m_{H^0} = 125.5$ GeV ($\sin(\beta-\alpha) \ll 1$) respectively. They impose NFC and study the fermion couplings and the constraints to be applied to the 2HDM of type I and type II. Given that the LHC expected precision on the measurement of the Higgs to vector boson couplings is of about 1 %, the analysis is carried out by assuming the minimum alignment condition necessary to match this level of precision and look at fermion couplings and signal strengths in order to analyze the compatibility with experiments.

The analysis of the fermion couplings allows to estimate how much a small departure from the limit $\cos(\beta-\alpha) \ll 1$ can have an impact on the decays $h \to \gamma\gamma$ or $h \to gg$. In some cases, like the type II, the alignment limit can be compensated by large $\tan\beta$ leading to big down-type couplings to the SM-like Higgs. However, such a compensation does not take place in our model here, because the custodial arrangement in (3.1) and (3.2) is not the consequence of taking a particular limit but the result of imposing a symmetry to the scalar sector.

The direct observation of the BSM particles H^0 and A^0 is also pointed out in the articles mentioned above in the framework of the alignment limit. One of the decays that could also be relevant for our model as well is the Higgs to Higgs decay in $gg \to H^0 \to ZA^0$. We will discuss it in more depth in section 3.5.

3.3 Flavour Phenomenology

The flavour sector can be considered as the most intriguing one. Within the SM, the Higgs mechanism introduces masses for the flavour particles in a gauge invariant way but does not predict their values. Cancellations take place in a very subtle way thanks to the CKM matrix unitarity and its resulting GIM mechanism, ensuring the absence of FCNC. When studying BSM physics, these subtleties often disappear and one of the easiest ways to constrain the BSM model is by looking at its flavour physics predictions.
The particular model we are studying does not provide us with a better understanding of the flavour masses and mixing parameters hierarchies compared to the SM. However, by imposing MFV, we have ensured that the same subtleties that take place in the SM play a role in our model as well. In this section we will study the way this happens in some particular observables and how much it constraints our model.

3.3.1 CP-violation in the neutral Kaon mixing

The $\Delta S = 2$ Weak transitions given in Fig.1.1, imply a non vanishing mixing between the neutral Kaon states K^0 and $\bar{K}^0$. This mixing generates a violation of the CP symmetry in $K \to \pi\pi$ decays that has been experimentally observed. To understand how this happens, let us define the neutral Kaon CP eigenstates K_1 and K_2 as

$$K_1 \overset{CP}{\to} +K_1, \qquad K_2 \overset{CP}{\to} -K_2. \tag{3.27}$$

The observed physical states can, in turn, be written in terms of the CP eigenstates as

$$K_S = \frac{1}{\sqrt{(1+|\bar{\epsilon}|^2)}}\,(K_1 + \bar{\epsilon}\; K_2)\,, \tag{3.28}$$

$$K_L = \frac{1}{\sqrt{(1+|\bar{\epsilon}|^2)}}\,(K_2 + \bar{\epsilon}\; K_1)\,. \tag{3.29}$$

These states are built by assuming that $\bar{\epsilon}$ is small, which means that K_S is almost CP-even while K_L is almost CP-odd. This hypothesis is in agreement with the observations since $K_L \to \pi\pi$ is very suppressed with respect to $K_S \to \pi\pi$.[1] (3.29) clearly shows two different ways of violating CP in this system. If K_L decays into two pions through its CP-even component K_1, the transition is known as mixing-induced or indirect CP violating (ICPV). On the other hand, if K_L decays into two pions through its CP odd component K_2, the transition is called direct CP violating (DCPV). To further explore the neutral Kaon system, one can also work in the strong interaction eigenstate basis defined in terms of CP eigenstates as:

$$K^0 = \sqrt{2}(K_2 + K_1), \qquad \bar{K^0} = \sqrt{2}(K_2 - K_1). \tag{3.30}$$

These states $K^0 = |\bar{s}d\rangle$ and $\bar{K}^0 = |\bar{d}s\rangle$ are actual members of the $SU(3)_F$ pseudoscalar octet (π, K, η) and are CP conjugates of each other. Since the $K^0 - \bar{K}^0$ mixing can be considered a weak interaction perturbation of the strong interaction, we are allowed to use perturbation theory tools. The $K^0 - \bar{K}^0$ transitions are given by the effective Hamiltonian

$$H = \begin{pmatrix} M_{11} - \frac{i}{2}\Gamma_{11} & M_{12} - \frac{i}{2}\Gamma_{12} \\ M_{21} - \frac{i}{2}\Gamma_{21} & M_{22} - \frac{i}{2}\Gamma_{22} \end{pmatrix}, \tag{3.31}$$

with

$$M_{12} = \langle \bar{K^0}|H_W^{\Delta S=2}|K^0\rangle + \sum_n P\frac{\langle \bar{K^0}|H_W^{\Delta S=1}|n\rangle\langle n|H_W^{\Delta S=1}|K^0\rangle}{M_K - E_n}, \tag{3.32}$$

$$\Gamma_{12} = 2\pi \sum_n \langle \bar{K^0}|H_W^{\Delta S=1}|n\rangle\langle n|H_W^{\Delta S=1}|K^0\rangle\delta(M_K - E_n), \tag{3.33}$$

[1] The numerical values of the K_S and K_L two pion decay rates are [14]:

$\mathcal{B}(K_S \to \pi^0\pi^0) = (30.69 \pm 0.05)$ $\quad$ $\mathcal{B}(K_L \to \pi^0\pi^0) = (8.64 \pm 0.06) \times 10^{-4}\%$

$\mathcal{B}(K_S \to \pi^+\pi^-) = (69.20 \pm 0.05)$ $\quad$ $\mathcal{B}(K_L \to \pi^+\pi^-) = (1.967.64 \pm 0.010) \times 10^{-3}\%$

where P in (3.32) means the principal part at $E_n = M_K$. Hermiticity and CPT symmetry ensure

$$M_{11} = M_{22} \equiv M_0, \quad \Gamma_{11} = \Gamma_{22} \equiv \Gamma_0, \quad M_{21} = M_{12}^*, \quad \Gamma_{21} = \Gamma_{12}^*. \tag{3.34}$$

The eigenvalue problem is therefore given by

$$H \begin{pmatrix} K_L \\ K_S \end{pmatrix} = \lambda \begin{pmatrix} K_L \\ K_S \end{pmatrix}, \tag{3.35}$$

and we find for the eigenvalues

$$\lambda_L = m_L - \frac{i}{2}\gamma_L = M_0 - \frac{i}{2}\Gamma_0 + \sqrt{\left(M_{12} - \frac{i}{2}\Gamma_{12}\right)\left(M_{12}^* - \frac{i}{2}\Gamma_{12}^*\right)}, \tag{3.36}$$

$$\lambda_S = m_S - \frac{i}{2}\gamma_S = M_0 - \frac{i}{2}\Gamma_0 - \sqrt{\left(M_{12} - \frac{i}{2}\Gamma_{12}\right)\left(M_{12}^* - \frac{i}{2}\Gamma_{12}^*\right)}. \tag{3.37}$$

The neutral kaon mass difference and decay width difference are defined in terms of the real and imaginary parts of the eigenvalues. Their experimental measurements are given by [14]:

$$\begin{aligned}\Delta M_K \equiv m_L - m_S &= 2\ \mathrm{Re}\left[\sqrt{\left(M_{12} - \frac{i}{2}\Gamma_{12}\right)\left(M_{12}^* - \frac{i}{2}\Gamma_{12}^*\right)}\right] \\ &= (3.483 \pm 0.006) \cdot 10^{-12}\ \mathrm{MeV},\end{aligned} \tag{3.38}$$

$$\Delta\Gamma_K \equiv \gamma_L - \gamma_S = -4\ \mathrm{Im}\left[\sqrt{\left(M_{12} - \frac{i}{2}\Gamma_{12}\right)\left(M_{12}^* - \frac{i}{2}\Gamma_{12}^*\right)}\right] \approx -\gamma_S. \tag{3.39}$$

The latest approximation comes from the observation that there exists a large hierarchy between the long and short Kaon lifetimes : $\tau_{K_L} = \gamma_L^{-1} = (5.116 \pm 0.020) \cdot 10^{-8}$ s whereas $\tau_{K_S} = \gamma_S^{-1} = (0.8953 \pm 0.0005) \cdot 10^{-10}$ s [14]. This feature can easily be explained thanks to (3.29). The fact that K_L is almost CP odd implies that it will mostly decay into a CP-odd state, mainly a 3π state. Although K_L is slightly heavier than K_S, the amount of phase-space available in a 3π decay is smaller and therefore K_L lifetime is longer.
Another interesting experimental relation is given by the ratio $-2\Delta M_K/\Delta\Gamma_K$, which is almost one [14]. Following the last remark, let us define the angle

$$\phi_\epsilon = \arctan\frac{2\Delta M_K}{\Delta\Gamma_K}, \tag{3.40}$$

that will be used in the following. Finding the eigenvectors will allow us to obtain the expression of the mixing parameter $\bar{\epsilon}$ in terms of known quantities. The diagonalization will give us the coordinates of mass eigenstates (K_S, K_L) in the strong eigenstates basis $(K^0, \bar{K}^0)$. Since $(H - \lambda_L)K_L = 0$ can be written as

$$\begin{pmatrix} -\frac{1}{2}(\lambda_L - \lambda_S) & M_{12} - \frac{i}{2}\Gamma_{12} \\ M_{12}^* - \frac{i}{2}\Gamma_{12}^* & -\frac{1}{2}(\lambda_L - \lambda_S) \end{pmatrix} \begin{pmatrix} 1+\bar{\epsilon} \\ 1-\bar{\epsilon} \end{pmatrix} = \begin{pmatrix} 0 \\ 0 \end{pmatrix}, \tag{3.41}$$

we finally obtain

$$\frac{1-\bar{\epsilon}}{1+\bar{\epsilon}} = \frac{(\Delta M_K - \frac{i}{2}\Delta\Gamma_K)/2}{M_{12} - \frac{i}{2}\Gamma_{12}} = \frac{M_{12}^* - \frac{i}{2}\Gamma_{12}^*}{(\Delta M_K - \frac{i}{2}\Delta\Gamma)/2}. \tag{3.42}$$

The exact solution of (3.42) is:

$$\bar{\epsilon} = \frac{\left[\frac{1}{2}\mathrm{Im}\Gamma_{12} + \left(\mathrm{Re}M_{12} - \frac{1}{2}\Delta M_K\right)\right] + i\left[\mathrm{Im}M_{12} - \frac{1}{2}\left(\mathrm{Re}\Gamma_{12} - \frac{1}{2}\Delta\Gamma_K\right)\right]}{\left[\frac{1}{2}\mathrm{Im}\Gamma_{12} + \left(\mathrm{Re}M_{12} + \frac{1}{2}\Delta M_K\right)\right] + i\left[\mathrm{Im}M_{12} - \frac{1}{2}\left(\mathrm{Re}\Gamma_{12} + \frac{1}{2}\Delta\Gamma_K\right)\right]}. \tag{3.43}$$

These expressions can be further simplified. Given that $\mathrm{Br}(K_L \to \pi\pi) \approx 10^{-3}$, we know that $\bar{\epsilon}$ must be very small. Therefore, in the strict $\bar{\epsilon} = 0$ limit we have

$$\left(\mathrm{Re}M_{12} - \frac{1}{2}\Delta M_K\right) + \frac{1}{2}\mathrm{Im}\Gamma_{12} = 0 \quad \text{and} \quad \left(\mathrm{Re}\Gamma_{12} - \frac{1}{2}\Delta\Gamma_K\right) + \mathrm{Im}M_{12} = 0; \tag{3.44}$$

and

$$\left(\mathrm{Re}M_{12} - \frac{1}{2}\Delta M_K\right) - \frac{1}{2}\mathrm{Im}\Gamma_{12} = 0 \quad \text{and} \quad \left(\mathrm{Re}\Gamma_{12} - \frac{1}{2}\Delta\Gamma_K\right) - \mathrm{Im}M_{12} = 0. \tag{3.45}$$

The previous relations imply that mixing (or indirect) CP violation is absent as soon as both imaginary parts of M_{12} and Γ_{12} vanish, in which case, mass and width differences are completly fixed by $\mathrm{Re}M_{12}$ and $\mathrm{Re}\Gamma_{12}$ respectively, i.e.:

$$\mathrm{Re}M_{12} = \frac{1}{2}\Delta M_K, \quad \text{and} \quad \mathrm{Re}\Gamma_{12} = \frac{1}{2}\Delta\Gamma_K. \tag{3.46}$$

Therefore, at the 10^{-3} level we have:

$$\bar{\epsilon} = \frac{i\left[\mathrm{Im}M_{12} - \frac{i}{2}\mathrm{Im}\Gamma_{12}\right]}{\Delta M_K - \frac{i}{2}\Delta\Gamma_K + i\left[\mathrm{Im}M_{12} - \frac{i}{2}\mathrm{Im}\Gamma_{12}\right]} \approx \frac{i\left[\mathrm{Im}M_{12} - \frac{i}{2}\mathrm{Im}\Gamma_{12}\right]}{\mathrm{Re}M_{12} - \frac{i}{2}\mathrm{Re}\Gamma_{12}}. \tag{3.47}$$

To obtain the last approximate identity, we have used the approximations

$$\mathrm{Re}M_{12} >> \mathrm{Im}M_{12} \quad \text{and} \quad \mathrm{Re}\Gamma_{12} >> \mathrm{Im}\Gamma_{12}, \tag{3.48}$$

which follow from (3.42) that could be rewritten as

$$\frac{1-\bar{\epsilon}}{1+\bar{\epsilon}} = \sqrt{\frac{\mathrm{Re}M_{12} - \frac{i}{2}\mathrm{Re}\Gamma_{12} - i\left(\mathrm{Im}M_{12} - \frac{i}{2}\mathrm{Im}\Gamma_{12}\right)}{\mathrm{Re}M_{12} - \frac{i}{2}\mathrm{Re}\Gamma_{12} + i\left(\mathrm{Im}M_{12} - \frac{i}{2}\mathrm{Im}\Gamma_{12}\right)}} \tag{3.49}$$

$$= 1 - i\frac{\mathrm{Im}M_{12} - \frac{i}{2}\mathrm{Im}\Gamma_{12}}{\mathrm{Re}M_{12} - \frac{i}{2}\mathrm{Re}\Gamma_{12}} + \mathcal{O}(\mathrm{Im}M_{12}^2, \mathrm{Im}\Gamma_{12}^2) \tag{3.50}$$

given that $(1-\bar{\epsilon})/(1+\bar{\epsilon}) \approx 1$ is almost real. Equation (3.47) can therefore be put in the form

$$\bar{\epsilon} = \frac{\sin 2\phi_\epsilon}{2}\left[\frac{1}{2}\left(\frac{\mathrm{Im}M_{12}}{\mathrm{Re}M_{12}} - \frac{\mathrm{Im}\Gamma_{12}}{\mathrm{Re}\Gamma_{12}}\right) - i\left(\frac{\mathrm{Im}M_{12}}{\mathrm{Re}\Gamma_{12}} + \frac{1}{4}\frac{\mathrm{Im}\Gamma_{12}}{\mathrm{Re}M_{12}}\right)\right]. \tag{3.51}$$

The real and complex parts of the $\bar{\epsilon}$ parameter are finally given by

$$\mathrm{Re}(\bar{\epsilon}) = \cos\phi_\epsilon \sin\phi_\epsilon \left(\frac{\mathrm{Im}M_{12}}{\Delta M_K} + \xi_\Gamma\right), \tag{3.52}$$

$$\mathrm{Im}(\bar{\epsilon}) = \sin\phi_\epsilon \sin\phi_\epsilon \left(\frac{\mathrm{Im}M_{12}}{\Delta M_K} + \xi_\Gamma\right) - \xi_\Gamma, \tag{3.53}$$

where

$$\xi_\Gamma \equiv -\frac{1}{2}\frac{\mathrm{Im}\Gamma_{12}}{\mathrm{Re}\Gamma_{12}}. \tag{3.54}$$

It is worth noting that $\bar{\epsilon}$ is not a physical parameter since any wave function rephasing $s \to e^{i\varphi}s$ will modify M_{12} and Γ_{12} and therefore $\bar{\epsilon}$ as well. It is therefore necessary to find observables related to it that can give us a measure of the amount of CP violation in the neutral Kaon system. The easiest way to measure CP violation in neutral kaon decays to two pions are the following ratios:

$$\eta_{+-} = \frac{A(K_L \to \pi^+\pi^-)}{A(K_S \to \pi^+\pi^-)}, \qquad \eta_{00} = \frac{A(K_L \to \pi^0\pi^0)}{A(K_S \to \pi^0\pi^0)}. \tag{3.55}$$

Let us consider the isospin decompositions of the decay amplitudes

$$A(K^0 \to \pi^+\pi^-) = A_0 e^{i\delta_0} + \frac{1}{\sqrt{2}}A_2 e^{\delta_2}, \tag{3.56}$$

$$A(K^0 \to \pi^0\pi^0) = A_0 e^{i\delta_0} - \sqrt{2}A_2 e^{i\delta_2}, \tag{3.57}$$

where δ_0 and δ_2 are the strong phases developed by $\pi\pi$ final state interactions and defined as

$$A(K^0 \to (\pi\pi)_{I=0}) = A_0 e^{i\delta_0}, \qquad A(K^0 \to (\pi\pi)_{I=2}) = A_2 e^{i\delta_2}. \tag{3.58}$$

Introducing the new parameters

$$\epsilon_K = \frac{A(K_L \to (\pi\pi)_{I=0})}{A(K_S \to (\pi\pi)_{I=0})}; \;\; \epsilon_2 = \frac{A(K_L \to (\pi\pi)_{I=2})}{A(K_S \to (\pi\pi)_{I=0})}; \;\; \omega = \frac{A(K_S \to (\pi\pi)_{I=2})}{A(K_S \to (\pi\pi)_{I=0})}, \tag{3.59}$$

and using the assumption $\bar{\epsilon} \ll 1$ lead us to the following expressions:

$$\eta_{+-} = \frac{\epsilon_K + \frac{1}{\sqrt{2}}\epsilon_2 e^{-i\delta_{02}}}{1 + \frac{\omega}{\sqrt{2}}e^{-i\delta_{02}}} \qquad \eta_{00} = \frac{\epsilon_K - \sqrt{2}\epsilon_2 e^{-i\delta_{02}}}{1 - \sqrt{2}\omega e^{-i\delta_{02}}}, \tag{3.60}$$

where $\delta_{02} \equiv \delta_0 - \delta_2$. Looking at these expressions we can clearly see the two different sources of CP violation. The ϵ_K parameter in both η_{+-} and η_{00} is dominantly the ICPV contribution. The remaining piece is the DCPV component and can be expressed in terms of yet another parameter:

$$\epsilon' = \frac{e^{-i\delta_{02}}}{\sqrt{2}}\omega\left(\frac{\epsilon_2}{\omega} - \epsilon_K\right), \tag{3.61}$$

if we define

$$\eta_{+-} = \epsilon_K + \frac{\epsilon'}{1 + \frac{\omega}{\sqrt{2}}e^{-i\delta_{02}}}, \qquad \eta_{00} = \epsilon_K - \frac{2\epsilon'}{1 - \sqrt{2}\omega e^{-i\delta_{02}}}. \tag{3.62}$$

Another common expression for the ϵ' parameter is in terms of the isospin amplitudes in (3.58):

$$\epsilon' = \frac{1}{\sqrt{2}}\mathrm{Im}\left(\frac{A_2}{A_0}\right)e^{-i\delta_{02}} \tag{3.63}$$

The ω parameter can be determined experimentally and is known to be very small ($\Delta I = 1/2$ rule). Therefore, we can make the following approximations:

$$\eta_{+-} \simeq \epsilon_K + \epsilon', \qquad \eta_{00} \simeq \epsilon_K - 2\epsilon'. \tag{3.64}$$

In order to obtain a theoretical prediction of the ϵ_K parameter we can use the definition in (3.59) and relate it to $\bar{\epsilon}$. Departing from

$$K_{S,L} = \frac{1 + \bar{\epsilon}}{\sqrt{2(1 + \bar{\epsilon}^2)}}K^0 \mp \frac{1 - \bar{\epsilon}}{\sqrt{2(1 + \bar{\epsilon}^2)}}\bar{K}^0, \tag{3.65}$$

we obtain

$$\epsilon_K = \frac{(1+\bar{\epsilon})A_0 + (1-\bar{\epsilon})A_0^*}{(1+\bar{\epsilon})A_0 - (1-\bar{\epsilon})A_0^*} = \frac{\bar{\epsilon}\mathrm{Re}(A_0) + i\mathrm{Im}(A_0)}{\mathrm{Re}(A_0) + i\bar{\epsilon}\mathrm{Im}(A_0)} = \frac{\bar{\epsilon} + i\xi_0}{1 + i\xi_0} \simeq \bar{\epsilon} + i\xi_0, \tag{3.66}$$

with

$$\xi_0 \equiv \frac{\mathrm{Im}(A_0)}{\mathrm{Re}(A_0)}. \tag{3.67}$$

Using (3.52) and (3.53), we obtain a theoretical expression of both the real and the imaginary part of the ICPV parameter ϵ_K:

$$\mathrm{Re}(\epsilon_K) = \mathrm{Re}(\bar{\epsilon}) = \cos\phi_\epsilon \sin\phi_\epsilon \left(\frac{\mathrm{Im}M_{12}}{\Delta M_K} + \xi_\Gamma\right), \tag{3.68}$$

$$\mathrm{Im}(\epsilon_K) = \mathrm{Im}(\bar{\epsilon}) + \xi_0 = \sin\phi_\epsilon \sin\phi_\epsilon \left(\frac{\mathrm{Im}M_{12}}{\Delta M_K} + \xi_\Gamma\right) + (\xi_0 - \xi_\Gamma). \tag{3.69}$$

Measurement of ϵ_K and SM prediction

Based on the already mentioned $\Delta I = 1/2$ rule, the approximation $\xi_0 = \xi_\Gamma$ has often been made. The $\Delta I = 1/2$ rule reflects the fact that $|(\pi\pi)_{I=0}\rangle$ largely saturates the neutral kaon decay widths. Hence, one can make the following approximation for the absorptive part of the $K^0 - \bar{K}^0$ mixing:

$$\Gamma_{21} = \Gamma_{12}^* = \sum_f A(K^0 \to f) A(\bar{K}^0 \to f)^* \simeq (A_0)^2, \tag{3.70}$$

leading to the result:

$$\xi_\Gamma = -\frac{1}{2}\frac{\mathrm{Im}(\Gamma_{12})}{\mathrm{Re}(\Gamma_{12})} = \frac{1}{2}\frac{\mathrm{Im}(A_0)^2}{\mathrm{Re}(A_0)^2} \simeq \frac{\mathrm{Im}A_0}{\mathrm{Re}A_0} = \xi_0. \tag{3.71}$$

This approximation gives rise to the common formula of ϵ_K:

$$\epsilon_K = e^{i\phi_\epsilon} \sin\phi_\epsilon \left(\frac{\mathrm{Im}M_{12}}{\Delta M_K} + \xi_0\right). \tag{3.72}$$

In their estimation of ϵ_K within the SM, several authors have tried to compute $\mathrm{Im}M_{12}$ in the most accurate way possible. We have already mentioned the fact that M_{12} is generated by the box diagrams in Fig.1.1. However, long distance effects coming from box diagrams with u quarks in the loops as well as double-penguin diagrams should be taken into account leading to $\mathrm{Im}M_{12} = \mathrm{Im}M_{12}^{SD} + \mathrm{Im}M_{12}^{LD}$. In [96], a new parametrization that includes these effects together with $\phi_\epsilon \neq \pi/4$ was introduced as well as an estimation of ξ providing the following formula for ϵ_K:

$$\epsilon_K = \frac{\kappa_\epsilon}{\sqrt{2}} \frac{\mathrm{Im}M_{12}^{SD}}{\Delta M_K}. \tag{3.73}$$

The latest estimation of κ_ϵ [97] gives

$$\kappa_\epsilon = 0.940 \pm 0.013 \pm 0.023. \tag{3.74}$$

In the SM, due to the GIM mechanism, the computation of M_{12}^{SD} only takes into account the c and t box diagrams, and is related to the following effective Hamiltonian:

$$2m_K(M_{12}^{SD})^* = \langle \bar{K}^0 | \mathcal{H}_{eff}(\Delta S = 2) | K^0 \rangle, \tag{3.75}$$

$$\mathcal{H}_{eff}(\Delta S = 2) = \frac{G_F^2 m_W^2}{16\pi^2}(\eta_{cc}\lambda_c^2 S_0(x_c) + \eta_{tt}\lambda_t^2 S_0(x_t) + \eta_{ct} 2\lambda_c\lambda_t S_0(x_c, x_t))\mathcal{O}_{\Delta S=2}, \tag{3.76}$$

where the $S_0(x_i)$ are Inami-Lim loop functions in Appendix B, the η_i are the QCD correction factors and $\mathcal{O}_{\Delta S=2}$ is the current-current operator

$$\mathcal{O}_{\Delta S=2} = (\bar{s}d)_{V-A}(\bar{s}d)_{V-A} + h.c. \tag{3.77}$$

The $\lambda_i = V_{is}^* V_{id}$ can be estimated in terms of measured quantities using the Wolfenstein parametrization discussed in (1.85). Indeed, proceeding that way, one can use quantities measured in B physics to predict observables in K physics, testing their compatibility within the framework of the unitary CKM matrix as can be seen in Fig.1.4. Finally, in order to estimate the matrix element of the dimension six operator in (3.76), one introduces the so-called B_K parameter that measures the deviation from the vacuum insertion approximation as follows:

$$\langle \bar{K}^0 | (\bar{s}d)_{V-A}(\bar{s}d)_{V-A} | K^0 \rangle = \frac{2}{3} B_K m_K^2 f_K^2. \tag{3.78}$$

This parameter has been estimated by the lattice as well as through several theoretical computations. To this day, it constitutes, together with V_{cb}, one of the main sources of uncertainty of the ϵ_K parameter theoretical prediction.
The uncertainty on V_{cb} comes from the fact that its determinations from both inclusive and exclusive semileptonic B meson decays are only marginally consistent. The limitations arise mainly from our inability to precisely account for form factors and higher-order perturbative and non-perturbative effects. The values obtained from inclusive and exclusive measurements are [14]

$$|V_{cb}| = (42.2 \pm 0.8) \times 10^{-3} \qquad \text{inclusive} \tag{3.79}$$

$$|V_{cb}| = (39.2 \pm 0.7) \times 10^{-3} \qquad \text{exclusive.} \tag{3.80}$$

Instead of using an average value, in this work we use the best fit value provided by [4]. With all this information available, the estimation of the short distance contribution to the ϵ_K parameter in the framework of the SM is given by the formula

$$|\epsilon_K|_{SM} = \frac{\kappa_\epsilon G_F^2 m_W f_K^2 m_K}{6\sqrt{2}\pi^2 \Delta M_K} B_K V_{cb}^2 V_{us}^2 \times \left(\frac{1}{2} V_{cb}^2 R_t^2 \sin 2\beta \eta_{tt} S_0(x_t) + R_t \sin\beta(\eta_{ct} S_0(x_c, x_t) - \eta_{cc} x_c)\right), \quad (3.81)$$

where β and R_t are respectively one of the angles and one of the sides of the unitary triangle in Fig.1.4. The angle $\sin 2\beta$ is extracted experimentally from $B_d \to J_{/\Psi} K_S$ while R_t can be extracted from B-physics quantities like:

$$R_t = \frac{\xi_s}{|V_{us}|}\sqrt{\frac{m_{B_s}}{m_{B_d}}}\sqrt{\frac{\Delta M_d}{\Delta M_{B_s}}}, \qquad \xi_s = \frac{f_{B_s}\sqrt{B_{B_s}}}{f_{B_d}\sqrt{B_{B_d}}}. \quad (3.82)$$

Our theoretical prediction of $|\epsilon_K|$ within the framework of the SM is given by the value[2]

$$|\epsilon_K|_{SM} = (1.97 \pm 0.23) \times 10^{-3}. \quad (3.83)$$

The CKMfitter collaboration that uses all the latest experimental and lattice results to give the best fit of CKM related parameters provides the following result for $|\epsilon_K|$ [4]:

$$|\epsilon_K|_{SM} = (2.20^{+0.47}_{-0.49}) \times 10^{-3}. \quad (3.84)$$

Experimentally, one can access the modules of ϵ_K through the $K_L \to \pi\pi$ asymmetries thanks to the highly accurate approximation

$$|\epsilon_K| = \frac{2|\eta_{+-}| + |\eta_{00}|}{3}, \quad (3.85)$$

providing the experimental value [14]

$$|\epsilon_K|_{exp} = (2.228 \pm 0.011) \times 10^{-3}. \quad (3.86)$$

Although much progress has been made towards the improvement of the theoretical prediction by trying to reduce all theoretical and lattice calculation

[2] All the theoretical and experimental inputs used as well as the Inami-Lim functions can be found in Appendix A and B. An alternative theoretical prediction given in [98] is:

$$|\epsilon_K|_{SM} = (1.81 \pm 0.28) \times 10^{-3}.$$

The difference with (3.83) is explained by the different values of the theoretical and experimental inputs.

uncertainties, the current experimental error is one order of magnitude smaller than the theoretical one.

Measurement of $Re(\epsilon_K)$ and SM prediction

It is important to note that the approximation made in (3.71) only affects the imaginary part of the ϵ_K parameter. Besides, the real part of ϵ_K can be extracted from experiments on its own; thereby providing an additional way of testing the accuracy of its theoretical prediction. Considering the semi-leptonic decays $K_L \to \pi\ell\nu_\ell$, we can define the asymmetry

$$\delta_\ell \equiv \frac{\Gamma(K_L \to \pi^-\ell^+\nu_\ell) - \Gamma(K_L \to \pi^+\ell^-\bar{\nu}_\ell)}{\Gamma(K_L \to \pi^-\ell^+\nu_\ell) + \Gamma(K_L \to \pi^+\ell^-\bar{\nu}_\ell)}. \tag{3.87}$$

Using symmetry arguments (the $\Delta S = \Delta Q$ rule [99]) one can eliminate the semi-leptonic matrix elements associated to the amplitudes, and the expression of δ_ℓ is given in terms of the $K^0 - \bar{K}^0$ dependence of K_L, that is, as a function of $\bar{\epsilon}$:

$$\delta_\ell = \frac{|1+\bar{\epsilon}|^2 - |1-\bar{\epsilon}|^2}{|1+\bar{\epsilon}|^2 + |1-\bar{\epsilon}|^2} = \frac{2\mathrm{Re}(\bar{\epsilon})}{1+|\bar{\epsilon}|^2} \approx 2\mathrm{Re}(\bar{\epsilon}). \tag{3.88}$$

Experimentally, the leptonic universality is quite well verified since one has [14]:

$$\left.\begin{array}{l} \delta_e = 0.334 \pm 0.007\% \\ \delta_\mu = 0.304 \pm 0.025\% \end{array}\right\} \delta_\ell = 0.332 \pm 0.006. \tag{3.89}$$

Folowing (3.68), we can therefore conclude that the current experimental value of $\mathrm{Re}(\bar{\epsilon})$ is given by

$$2\mathrm{Re}(\epsilon_K)_{exp} = (3.32 \pm 0.06) \times 10^{-3}. \tag{3.90}$$

Theoretically, one can make use of the large number of colours hypothesis [100] where LD effects as well as deviations from $\phi_\epsilon = \pi/4$ can be neglected at $\mathcal{O}(\frac{1}{N_c})$. In the large N_c framework, B_K can also be estimated [101,102] giving the result $B_K = 3/4$. This value is quite close to the lattice result in Appendix

B. Therefore, in the SM, the large N_c limit for $\mathrm{Re}(\epsilon_K)$ gives[3]

$$2\mathrm{Re}(\epsilon_K)(N_c \to \infty) = (2.91 \pm 0.33) \times 10^{-3}. \tag{3.91}$$

While both experimental measurements of $|\epsilon_K|$ and $2\mathrm{Re}(\epsilon_K)$ have a similar level of precision, it is interesting to study their theoretical accuracy. The $|\epsilon_K|$ theoretical uncertainty is due, to some extent, to the hadronic parameters and V_{cb}, and therefore relies on the lattice calculations' accuracy, while $2\mathrm{Re}(\epsilon_K)$ determination in this work relies mostly on the large N_c hypothesis. With respect to the consequences of the model we are studying on these two particular observables, the results are expected to be very similar in both cases without one providing any additional information with respect to the other. That is why, moving forward, we will limit ourselves to the study of the contributions of our 2HDM to $|\epsilon_K|$ only.

Measurement of $\frac{\epsilon'}{\epsilon}$ and SM prediction

Before ending this section about CP-violation in the neutral Kaon mixing we would like to adress the current status, within the SM, of the $\frac{\epsilon'}{\epsilon}$ ratio where ϵ' is the parameter introduced in (3.61). Given what has been explained in the previous paragraphs, this ratio measures the size of direct CP violation in $K_L \to \pi\pi$ decays with respect to the indirect CP violation given by ϵ_K.
The results by the NA68 [103] and KTeV [104, 105] experiments provide the average value

$$(\epsilon'/\epsilon)_{exp} = (16.6 \pm 2.3) \times 10^{-4}. \tag{3.92}$$

From the theory point of view, several factors have contributed to the difficulty of making a precise prediction of this ratio. Although the topic has been studied for years, with the improvement of lattice numerical simulations as well as the development of some analytical methods in order to reduce the hadronic uncertainties, it has been recently pointed out that the SM seems unable to

[3] All the theoretical and experimental inputs used as well as the Inami-Lim functions can be found in Appendix A and B. A previous result using slightly different values of the parameters gave [100]:

$$2\mathrm{Re}(\epsilon_K)(N_c \to \infty) = (2.96 \pm 0.38) \times 10^{-3}.$$

account for the experimental value of the ratio [106–108] hinting to a possible NP contribution. We will not provide here a full explanation of the calculations but rather try to explain what are the main issues regarding the compatibility of the SM predictions with the experimental result.

Within the SM, the ϵ' parameter is dominated by positive contributions from QCD penguins, while the electroweak penguins contribute mainly negatively. This interplay demands a more accurate knowledge of the different contributions in order to provide a useful prediction of the ratio. While short distance contributions, that are given by the Wilson coefficients of both QCD and electroweak penguins, are known at the NLO level [107], the problem lies in the accurate computation of the hadronic matrix elements of the different operators involved.

The authors in [107] propose a method in order to avoid the direct computation of the hadronic matrix elements, better identify the main sources of uncertitude and provide a more accurate prediction. This method is an improvement based on a previous work [109] where the main hypothesis is that $Re(A_0)$ and $Re(A_2)$, which are the main characters of the $\Delta I = 1/2$ rule, are fully described by SM dynamics. This way, the matrix elements associated to the $(V-A)\times(V-A)$ operators can be extracted from experiments. Actually the main operator of this type involved in the ϵ'/ϵ ratio is the QCD penguin operator

$$Q_4 = (\bar{s}_\alpha d_\beta)_{V-A} \sum_{u,d,s,c,b} (\bar{q}_\alpha q_\beta)_{V-A}. \tag{3.93}$$

Its contribution is not as big as the $(V-A)\times(V+A)$ operators

$$Q_6 = (\bar{s}_\alpha d_\beta)_{V-A} \sum_{u,d,s,c,b} (\bar{q}_\alpha q_\beta)_{V+A}, \qquad Q_8 = \frac{3}{2}(\bar{s}_\alpha d_\beta)_{V-A} \sum_{u,d,s,c,b} e_q (\bar{q}_\alpha q_\beta)_{V+A}, \tag{3.94}$$

coming from QCD and electroweak penguins respectively. However, due to their opposite sign contributions, a better knowledge of the Q_4 associated matrix element is a very important improvement. Following the previous assumptions, the authors are able to provide a formula of the ϵ'/ϵ ratio whose main uncertitudes are the Q_6 and Q_8 matrix element parameters $B_6^{(1/2)}$ and $B_8^{(3/2)}$. The values of these parameters have been provided by lattice calculations and the most recent results by (RBC-UKQCD) [107] are

$$B_6^{(1/2)}(m_c) = 0.57 \pm 0.19, \qquad B_8^{(3/2)}(m_c) = 0.76 \pm 0.05 \tag{3.95}$$

which lead to the following SM prediction of the ratio

$$(\epsilon'/\epsilon)_{SM} = (1.9 \pm 4.5) \times 10^{-4} \qquad \text{(Lattice)}. \tag{3.96}$$

This prediction happens to differ with the experimental value in (3.92) to a 3σ significance. On the other hand, in [106], a computation of the same hadronic parameters in the large N limit, with N being the number of colors, is provided. In this framework the following bound is derived

$$B_6^{(1/2)} \leq B_8^{(3/2)} < 1 \tag{3.97}$$

A saturation of the bound (3.97), confirms the discrepancy between the SM prediction and the experimental result in (3.92)

$$(\epsilon'/\epsilon)_{SM} = (8.6 \pm 3.2) \times 10^{-4} \qquad \text{(Large N)}. \tag{3.98}$$

Even in the hypothetical case of improved lattice calculations, where the parameters in (3.95) would have bigger values, the large N bound in (3.97) suggests that there is still something missing in the determination of the ϵ'/ϵ hinting to a new possible road to look for new physics. Despite it being one of the current main issues regarding the neutral kaon system, we will not provide a possible solution within the framework of the model presented in this work given that it only introduces scalar operators that would not contribute to relax the tension.

3.3.2 ΔM_{B_s}

The case of the neutral B-meson system is slightly different from the K meson one. The quantity that better estimates the strength of the $B_q^0 - \bar{B}_q^0$ mixing is the mass difference ΔM_{B_q}, where q can be d or s whether it is the B_d or the B_s system. We will only focus on ΔM_{B_s} moving forward, since it is the quantity that is expected to be the most sensitive to our BSM extension. Because the B mesons are much heavier than the Kaons, they have many possible decay channels and there is no sizeable difference between the lifetimes. That is why the neutral states are called heavy and light, in contrast to long and short which were used in the Kaon system, and the mass difference is defined by

$$\Delta M_s = m_H^s - m_L^s. \tag{3.99}$$

The mass difference can be expressed in terms of the off-diagonal element in the neutral B-meson mass matrix by using the formula developed previously for the K-meson system:

$$\Delta M_s = 2|M_{12}^s|. \tag{3.100}$$

However, there are several differences with respect to the Kaon mixing explained above. The first difference concerns the approximation $\Delta M_K \simeq 2\mathrm{Re}M_{12}$ that cannot be made in this case since $\Gamma_{12}^s \ll M_{12}^s$ in the B system. Besides, there are no LD effects to be expected in this case and the estimation of M_{12}^s reduces to the computation of the box diagrams. A final feature of this system is that, due to the particular values of the CKM matrix elements involved and $m_t \gg m_{c,u}$, only the top quark contribution to the box diagram needs to be computed. Taking all of this into account, the off-diagonal term M_{12}^s in the neutral strange B-meson mass matrix is given by:

$$2m_{B_s}|M_{12}^s| = |\langle B_s^0|\mathcal{H}_{eff}(\Delta B = 2)|\bar{B}_s^0\rangle|, \tag{3.101}$$

where

$$\mathcal{H}_{eff}(\Delta B = 2) = \frac{G_F^2}{16\pi^2} m_w (V_{tb}^* V_{td})^2 \eta_B S_0(x_t)(\bar{b}s)_{V-A}(\bar{b}s)_{V-A} + h.c. \tag{3.102}$$

Similar to the neutral Kaon system, the main uncertainties in the estimation of this mass difference within the SM framework, come from the hadronic parameters associated with the matrix element of the dimension six operator in (3.102). However, the precision in the lattice computation of those parameters has considerably improved these last years reducing the uncertainty of the SM prediction. The final formula of ΔM_{B_s} within the SM is

$$\Delta M_{B_s} = \frac{G_F^2}{6\pi^2} \eta_B m_{B_s} (B_{B_s} f_{B_s}^2) m_W^2 S_0(x_t) |V_{ts}|^2. \tag{3.103}$$

Using all the parameters listed in Appendix A and the loop functions in B, our prediction of ΔM_s is given by

$$(\Delta M_{B_s})_{SM} = (1.178 \pm 0.061) \times 10^{-11} \text{ GeV}. \tag{3.104}$$

The uncertainty in this theoretical prediction is smaller than in the Kaon case. However, it remains larger than the experimental one [14]:

$$(\Delta M_{B_s})_{exp} = (1.1688 \pm 0.0014) \times 10^{-11} \text{ Gev}. \tag{3.105}$$

Therefore, efforts still need to be made in order to reduce it as much as possible.

3.3.3 $\Delta F = 2$ results in the custodial invariant 2HDM with MFV

In this section we will analyze the implications of our custodial 2HDM with MFV in $\Delta F = 2$ transitions. We will focus on the observables introduced before, that is $|\epsilon_K|$ and ΔM_{B_s}. The reasons for limiting ourselves to these quantities are as follows:

- ϵ_K parametrizes ICPV in the Kaon sector. Its experimental determination is quite accurate and its main short distance contribution is due to box diagrams with top quarks. The other quantity that can give us insight into the $K^0 - \bar{K}^0$ mixing is ΔM_K. However, due to the MFV nature of our model, BSM contributions to ΔM_K are expected to be small since it is dominated by lighter quarks box diagrams.

- ΔM_{B_s} measures the mixing between neutral states in the strange B sector. The study of CPV in this sector is not expected to provide us with a lot of information because the CKM elements involved are almost real. However, MFV can have an impact since the loop particles concerned in this system are heavier quarks. This also accounts for why we will concentrate ourselves on ΔM_{B_s} since it involves heavier quarks than ΔM_{B_d}.

We will also divide this section in two sub-parts. The first part consists of the study of the contribution of our model tree-level FCNC to these quantities. In the second part we will analyze the contributions due to box diagrams with charged Higgs in the loops updating the results given in [46].

FCNC effects on $\Delta F = 2$ transitions

The coupling between different flavour down quarks is given by (3.9). Based on that, we can build an effective Hamiltonian describing the tree-level contri-

bution of both scalar H^0 and pseudoscalar A^0 to the $M^0 - \bar{M}^0$ mixing:

$$\mathcal{H}^{\Delta F=2}_{2HDM}(H^0, A^0) = \left(-\frac{1}{m_{H^0}} \frac{[(Z_D)_{ij} - (Z_D^\dagger)_{ij}]^2}{2} + \frac{1}{m_{A^0}} \frac{[(Z_D)_{ij} + (Z_D^\dagger)_{ij}]^2}{2} \right) (\bar{d}^i_R d^j_L)(\bar{d}^i_R d^j_L). \tag{3.106}$$

We aim at expressing the new contribution in terms of the SM one. So, we try to relate the density-density operator in (3.106) to the SM current-current operator:

$$\mathcal{O}_{SM} = (\bar{d}^i_L \gamma_\mu d^j_L)(\bar{d}^i_L \gamma^\mu d^j_L). \tag{3.107}$$

We can decompose the operator in (3.106) into a scalar and a pseudoscalar part. Since we know that at the hadronic level the scalar part will not contribute, we keep only the pseudoscalar part in the factorization limit:

$$-\frac{1}{4}(\bar{d}^i i\gamma_5 d^j)(\bar{d}^i i\gamma_5 d^j). \tag{3.108}$$

Making use of the Dirac equation, we obtain

$$\partial^\mu(\bar{d}^i \gamma_\mu \gamma_5 d^j) = (m_i + m_j)(\bar{d}^i i\gamma_5 d^j). \tag{3.109}$$

And applying twice, we finally have

$$m^2_M(\bar{d}^i \gamma_\mu \gamma_5 d^j)^2 = (m_i + m_j)^2(\bar{d}^i i\gamma_5 d^j)(\bar{d}^i i\gamma_5 d^j). \tag{3.110}$$

Therefore, at the hadronic level, we obtain the following relation between the two different operator matrix elements:

$$\frac{\langle \bar{M}^0 | (\bar{d}^i_R d^j_L)(\bar{d}^i_R d^j_L) | M^0 \rangle}{\langle \bar{M}^0 | (\bar{d}^i_L \gamma_\mu d^j_L)(\bar{d}^i_L \gamma^\mu d^j_L) | M^0 \rangle} = -\frac{m^2_M}{(m_i + m_j)^2}. \tag{3.111}$$

The latest result allows us to write the FCNC effective Hamiltonian matrix element in terms of the SM one. In [46], we gave an expression of this relation when neglecting the charm box contribution:

$$\langle \bar{M}^0 | \mathcal{H}^{\Delta F=2}_{2HDM}(H^0, A^0) | M^0 \rangle \simeq \langle \bar{M}^0 | \mathcal{H}^{\Delta F=2}_{SM} | M^0 \rangle \left[1 + 16\pi^2 x \delta_1^2 m^2_M \left(\frac{1}{m^2_{H^0}} - \frac{1}{m^2_{A^0}} \right) \right], \tag{3.112}$$

with

$$x = \frac{2m_t^4}{m_W v^2 S_0(x_t)} \simeq 1.61. \tag{3.113}$$

It is worth mentioning that the pseudoscalar contribution in (3.112) induces a negative interference with respect to the SM one. This allows us to get a glimpse into the behaviour of the 2HDM contribution for a light pseudoscalar that will tend to reduce the $\Delta F = 2$ transition amplitude with respect to the SM prediction.

Charged Higgs effects on $\Delta F = 2$ transitions

In the SM only the $W^+ - W^-$ gauge bosons generate flavour changing neutral currents through box diagrams. In the 2HDM, however, the charged Higgs boson is also responsible for flavour changing up-down currents. When studying the SD contributions to K and B meson mixings, one needs to compute the pure $H^+ - H^-$ and mixed $H^\pm - W^\pm$ box diagrams as well.

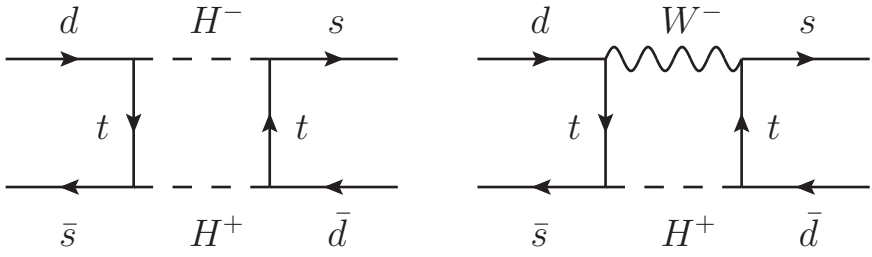

Figure 3.1: *Box diagrams with the charged Higgs contributing to the $M^0 - \bar{M}^0$ mixing*

Given our implementation of the MFV hypothesis, the charged current Higgs Feynman rules in Fig.3.2 are given by the Lagrangian in (3.12).

The A_u^i and A_d^i coefficients in (3.13) are the same as those given in [77].

$i\frac{\sqrt{2}}{v}V_{ij}^\dagger\left(m_{u_j}A_u^j\frac{1+\gamma_5}{2} - m_{d_j}A_d^j\frac{1-\gamma_5}{2}\right)$ $\quad i\frac{\sqrt{2}}{v}\left(m_{u_i}A_u^i\frac{1-\gamma_5}{2} - m_{d_i}A_d^i\frac{1+\gamma_5}{2}\right)V_{ij}$

Figure 3.2: *$H^\pm$-quark coupling Feynman rules*

Given the rules above and considering that the charged Higgs contribution with charm quarks in the loop will be highly suppressed since the Higgs couplings

are proportional to the quark masses, we can neglect both the A_d terms and the box diagrams with two c quarks. The dominant effective Hamiltonian describing the charged Higgs contribution to the $M^0 - \bar{M}^0$ mixing is therefore given by

$$\mathcal{H}^{\Delta F=2}_{2HDM}(H^\pm) = \frac{G_f^2 m_W^2}{16\pi^2}\left[\lambda_t^2 C^{tt} + 2\lambda_c\lambda_t C^{ct}\right](\bar{d}^i_R d^j_L)(\bar{d}^i_R d^j_L) + h.c. \qquad (3.114)$$

where

$$C^{tt} = 2(A_u)^2 x_t^2\left[m_W^2 D_2(m_t^2, m_W^2, m_{H^\pm}^2)\right.$$
$$\left. -4m_W^4 D_0(m_t^2, m_W^2, m_{H^\pm}^2)\right] + (A_u)^4 x_t^2 m_W^2 D_2(m_t^2, m_{H^\pm}^2), \qquad (3.115)$$
$$C^{ct} = 2(A_u)^2 x_c x_t\left[m_W^2 D_2(m_c^2, m_t^2, m_W^2, m_{H^\pm}^2)\right.$$
$$\left. -4m_W^4 D_0(m_c^2, m_t^2, m_W^2, m_{H^\pm}^2)\right] + (A_u)^4 x_c x_t m_W^2 D_2(m_c^2, m_t^2, m_{H^\pm}^2). \qquad (3.116)$$

The D_i functions are listed in appendix B.

Numerical results on 2HDM effects on $\Delta F = 2$ transitions

In this section we analyze the 2HDM contributions to both ϵ_K and ΔM_{B_s} for different values of the model parameters.

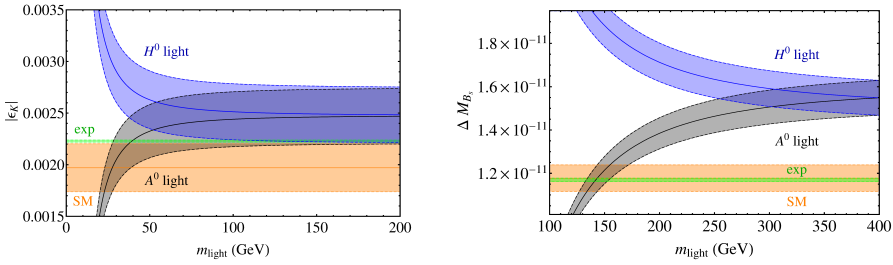

Figure 3.3: *$|\epsilon_K|$ and ΔM_{B_s} as a function of the H^0 and A^0 masses with MFV coefficients $\delta_1 = 1$ and $A_u = 1$. The thin horizontal (green) lines indicate the experimental values; the broad horizontal (orange) areas indicate the 1σ SM prediction; the upper (blue) areas show the 1σ prediction for $m_{H^0} \ll m_{A^0} = m_{H^\pm} = 400$ GeV; and the lower (grey) areas correspond to the analog prediction for $m_{A^0} \ll m_{H^0} = m_{H^\pm} = 400$ GeV.*

In Fig.3.3 one can see similar plots to the ones in [46] where we carried out a study without considering the charged Higgs loop effects that now lead us to much stronger constraints. First of all, in both ϵ_K and ΔM_{B_s}, the addition of the charged scalar loops implies a considerable shift (30%) with respect to the SM, even when the FCNC effect is almost negligible, i.e. when the mass of the lightest BSM scalar is big enough (400 GeV). Although the plots in Fig.3.3 are made for the maximal values of the MFV coefficients, we can draw some definitive conclusions from them. Firstly, we can see that the case where the scalar H^0 is light is highly disfavoured since the tree-level induced FCNC together with the charged Higgs loop effects sum up to deviate (severely in the ΔM_{B_s} case) from the SM prediction and from the measured experimental value as well. Besides, we already mentioned in section 2.3 that a limit on a fully ggF-generated scalar decaying into two photons has been made by the ATLAS collaboration, providing the following constraint on the additional neutral scalar: $m_{H^0} > 200$ GeV [85]. The case where the pseudoscalar A^0 is light, on the other hand, is more interesting since, looking at ΔM_{B_s}, both effects compensate for values around $m_{A^0} = 140$ GeV. The $|\epsilon_K|$ parameter constraint is less stringent. Although there is a shift with respect to the SM predictions due to the charged Higgs loops, it remains compatible with the experimental measurement for masses of the lightest BSM particle being higher than 50 GeV. Given that ΔM_{B_s} imposes much stronger constraints, with a light H^0 more unlikely than the SM prediction, we will, moving forward, only consider the twisted case where the pseudoscalar A^0 can be light.

Let us now analyze some variations of the model parameters. In the following figures we have always considered the case of exact custodial symmetry with the degeneracy relations $m_{H^\pm} = m_{A^0(H^0)}$. Nevertheless, we have verified that a small departure from the degeneracy relation (around 10%) does not modify the results and will therefore consider the case case of exact degeneracy from now on.

First of all, in Fig.3.4, we study the m_{A^0} dependence of the parameters for two different values of the custodial triplet masses: $m_{H^0,H^\pm} = 200$ and 400 GeV. Similar to the previous case, ΔM_{B_s} imposes a larger constraint on the model parameters than $|\epsilon_K|$ does. This is easily explained by the MFV nature of the Yukawa couplings that makes the effects depend on the masses and CKM ma-

trix elements of the quarks involved. However, it is interesting to note that, in the case where $m_{H^0,H^\pm} = 400$ GeV, there is a wide mass spectrum for A^0 that accomodates the experimental value of ϵ_K better than in the SM. This way, from $m_{A^0} = 50$ GeV, where the model prediction and the experimental value are compatible, up to the decoupling limit $m_{h^0} \ll m_{A^0,H^0,H^\pm}$, the 2HDM with MFV gives a quite satisfying theoretical prediction for ϵ_K. Given that $|\epsilon_K|$ does not favour the case where $m_{H^0,H^\pm} = 200$ GeV, we analyze ΔM_{B_s} for $m_{H^0,H^\pm} = 400$ GeV. The observable only agrees with its experimental value in the case where $m_{A^0} \simeq 150$ GeV.

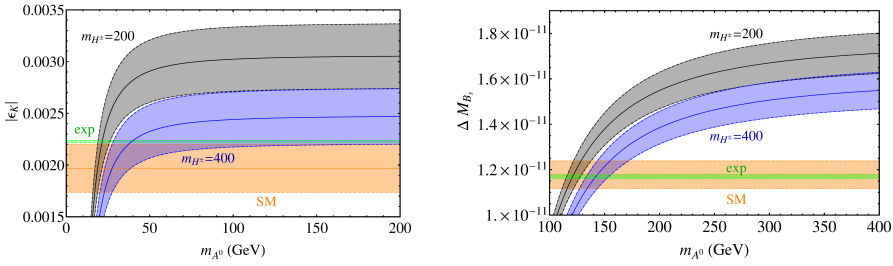

Figure 3.4: $|\epsilon_K|$ *and* ΔM_{B_s} *as a function of* m_{A^0} *with MFV coefficients* $\delta_1 = 1$ *and* $A_u = 1$. *The thin horizontal (green) lines indicate the experimental values; the broad horizontal (orange) areas indicate the 1σ SM predictions; the upper (grey) areas show the 1σ prediction for* $m_{H^0} = m_{H^\pm} = 200$ *GeV; and the lower (blue) areas correspond to the analog prediction for* $m_{H^0} = m_{H^\pm} = 400$ *GeV.*

This result is of course dependent on the values for the MFV coefficients which we have fixed to unity. The latest remark leads us to our next parameter study, where we analyze the impact of variation of the MFV coefficients. In Fig.3.5 and 3.6, we allow the variation of the MFV coefficients A_u and δ_1 respectively. We make the following observations:

- The case where $A_u = 0.5$ seems to easier accomodate the experimental result than both the $A_u = 1$ case and the SM for some values of m_{A^0}. Looking at $|\epsilon_K|$ in Fig.3.5, from $m_{A^0} = 50$ GeV, the concordance between the experimental results and the theoretical prediction is slightly better in the 2HDM than in the SM. ΔM_{B_s} seems to best fit the results around $m_{A^0} = 250$ GeV. However, for even bigger masses of the pseudoscalar,

the theoretical prediction is still less than 2σ away from the experimental prediction.

- The variation of δ_1 does not have a big impact on $|\epsilon_K|$. Looking at Fig.3.6 we observe that the m_{A^0} values for which $|\epsilon_K|$ better accomodates the experimental result are totally ruled out by ΔM_{B_s}. However, excepting the case where the pseudoscalar is very light ($m_{A^0} < 40$ GeV), the theoretical prediction of ϵ_K in the context of our model is as compatible as in the SM. The strange neutral B mesons mass difference on the other hand exhibits a rather different behaviour when $\delta_1 = 0.5$. A smaller value of δ_1 shifts the best fitting value of m_{A^0} to the left, allowing a lighter pseudoscalar but in a very narrow mass spectrum.

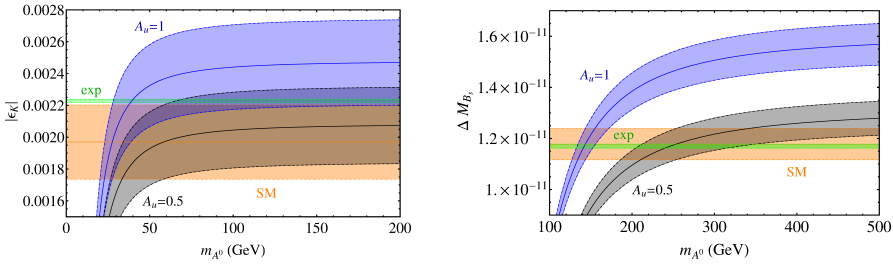

Figure 3.5: $|\epsilon_K|$ *and* ΔM_{B_s} *as a function of* m_{A^0} *with* $\delta_1 = 1$ *and* $m_{H^0} = m_{H^\pm} = 400$ *GeV. The thin horizontal (green) lines indicate the experimental values; the broad horizontal (orange) areas indicate the* 1σ *SM predictions; the upper (blue) areas show the* 1σ *prediction for* $A_u = 1$*; while the lower (grey) areas correspond to the analog prediction for* $A_u = 0.5$.

From the joint study of these two quantities, we can try to identify some benchmark points. Having taken a look at the previous plots, we conclude that ΔM_{B_s} can be used as the quantity to constrain our model parameters, and $|\epsilon_K|$ can be used to verify that the consequences of the allowed BSM physics in the B-sector are not dramatic on the Kaon sector. Considering the fact that the charged Higgs loop effects are too big when the charged scalar mass is light, we will take all our benchmark points in the case where we have $m_{H^0,H^\pm} = 400$ GeV. In table 3.1 we have listed the regions in the m_{A^0} space allowed at 1σ for different values of the MFV parameters.

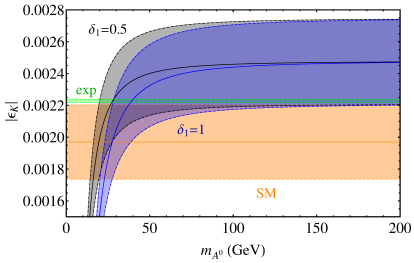

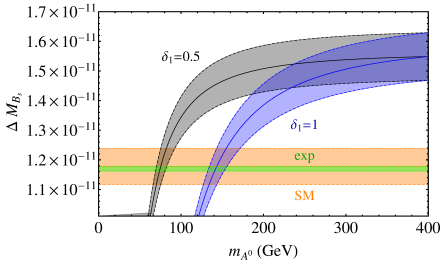

Figure 3.6: $|\epsilon_K|$ *and* ΔM_{B_s} *as a function of* m_{A^0} *with* $A_u = 1$ *and* $m_{H^0} = m_{H^\pm} =$ 400 *GeV. The thin horizontal (green) lines indicate the experimental values; the broad horizontal (orange) areas indicate the* 1σ *SM predictions; the blue areas show the* 1σ *prediction for* $\delta_1 = 1$*; while the grey areas correspond to the analog prediction for* $\delta_1 = 0.5$.

Parameters	$\lvert\epsilon_K\rvert$	ΔM_{B_s}
$\delta_1 = 1,\ A_u = 1$	$m_{A^0} > 20$ GeV	130 GeV$< m_{A^0} <$ 150 GeV
$\delta_1 = 1,\ A_u = 0.5$	$m_{A^0} > 50$ GeV	$m_{A^0} > 180$ GeV
$\delta_1 = 0.5,\ A_u = 1$	$m_{A^0} > 15$ GeV	60 GeV$< m_{A^0} <$ 80 GeV

Table 3.1: *Regions of* m_{A^0} *allowed by* ΔM_{B_s} *and* $|\epsilon_K|$ *for different values of the MFV parameters.*

3.3.4 $B_s \to \mu^+\mu^-$

As mentioned in previous sections, neutral B meson decays to two charged leptons constitute one of the cleanest decays on a theoretical level in the field of B-physics. Within the SM, the main diagrams contributing to these decays are Z-penguins and box diagrams involving top-quark exchanges. The effective Hamiltonian of these processes in the SM framework is [110]

$$\mathcal{H}_{eff}(\Delta F = 1) = -\frac{G_F}{\sqrt{2}}\frac{\alpha}{2\pi\sin^2\theta_W}\lambda_t 4\eta_Y Y_0(x_t)(\bar{b}q)_{V-A}(\bar{\ell}\ell)_{V-A} + h.c. \quad (3.117)$$

where η_Y takes QCD corrections into account and $Y_0(x_t)$ is a loop function whose exact expression can be found in Appendix B.This Hamiltonian leads to the following formula for the branching ratio:

$$\mathcal{B}(B_q \to \mu^+\mu^-) = \tau_{B_q}\frac{G_F^2}{\pi}\left(\frac{\alpha}{4\pi\sin^2\theta_W}\right) f_{B_q}^2 m_\mu^2 m_{B_q}\sqrt{1-4\frac{m_\mu^2}{m_{B_q}^2}}|V_{tb}^* V_{tq}|^2\eta_Y^2 Y_0^2(x_t). \quad (3.118)$$

In this study, we only focus on the $B_s \to \mu^+\mu^-$ decay for two main reasons. First of all, the strange neutral B meson decay has been observed by the CMS and LHCb collaborations (1.110) providing an already quite satisfying experimental result. The second reason is due to the MFV nature of our model. Because MFV is proportional to the masses of the quarks involved, the effects in the B_d case are weaker and are not expected to lead to relevant results.
The uncertainty caused by the lack of precision in the determination of the hadronic parameters has led some authors [111] to propose the use of the experimental value of ΔM_{B_s} in the SM prediction of $\mathcal{B}(B_s \to \mu^+\mu^-)$. This way, the f_{B_s} together with the uncertainty of the CKM elements were removed. However, another uncertainty appeared through the hadronic parameter B_s:

$$\mathcal{B}(B_s \to \mu^+\mu^-) = \tau_{B_s} \frac{3G_F^2}{4\pi} \frac{m_W^2 \eta_Y^2 Y_0^2(x_t)}{B_s \eta_B S_0(x_t)} m_\mu^2 \sqrt{1 - 4\frac{m_\mu^2}{m_{B_s}^2}} \Delta M_{B_s}. \tag{3.119}$$

Currently, the uncertainty due to f_{B_s} is around the same order of magnitude as the one on B_s [112] and the difference in precision between the two determinations of the branching ratio is not really significant. Our results in the SM framework are given below[4] and are to be compared with the experimental result in (1.110).

$$\mathcal{B}(B_s \to \mu^+\mu^-)_{SM} \overset{f_{B_s}}{=} (3.69 \pm 0.19) \times 10^{-9} \tag{3.120}$$

$$\mathcal{B}(B_s \to \mu^+\mu^-)_{SM} \overset{\Delta M_{B_s}}{=} (3.68 \pm 0.14) \times 10^{-9}. \tag{3.121}$$

FCNC effects on $B_s \to \mu^+\mu^-$

The presence of FCNC in our 2HDM leads to A^0 and H^0 mediated tree-level contributions to the $B_s \to \mu^+\mu^-$ decay amplitude. Once the FCNC present in our model are taken into account, the effective Hamiltonian in (3.117) is modified with the addition of two new operators:

$$\mathcal{H}_{eff}(\Delta F = 1)(A^0, H^0) = -\frac{G_F}{\sqrt{2}} \frac{\alpha}{2\pi \sin^2\theta_W} \lambda_t (-C_S Q_S - C_P Q_P + C_A Q_A) + h.c. \tag{3.122}$$

[4] All the theoretical and experimental inputs used as well as the Inami-Lim function can be found in Appendix A and B. Other theoretical predictions within the SM were given in (1.108).

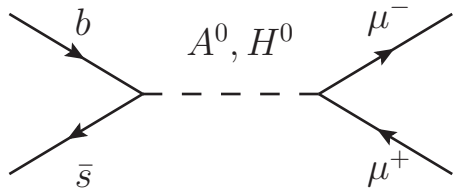

Figure 3.7: *Tree-level FCNC neutral Higgs contribution to the* $B_s \to \mu^+\mu^-$ *decay amplitude.*

where

$$Q_S = m_b(\bar{b}_R s_L)(\bar{\mu}\mu); \qquad Q_P = m_b(\bar{b}_R s_L)(\bar{\mu}\gamma_5\mu); \qquad Q_A = (\bar{b}q)_{V-A}(\bar{\mu}\mu)_{V-A}. \tag{3.123}$$

The SM coefficient is $C_A = 2\eta_Y Y_0(x_t)$. In order to determine the coefficient of the scalar and pseudoscalar operators, we need to implement the MFV hypothesis in the lepton sector as well. This can easily be carried out by analogy with the quark sector. However, given the very well known lepton mass spectrum, we are able to truncate the MFV series for Z_ℓ at first order:

$$Z_\ell = \lambda_0 Y_\ell. \tag{3.124}$$

Therefore, the C_S and C_P coefficients in our model are given by

$$C_{S(P)} = \frac{\Delta}{m^2_{H^0(A^0)}}, \qquad \text{with} \qquad \Delta = \frac{4\pi^2\delta_1\lambda_0 m_t^2}{m_W^2}; \tag{3.125}$$

and the decay branching ratio becomes

$$\mathcal{B}(B_s \to \mu^+\mu^-) = \mathcal{B}(B_s \to \mu^+\mu^-)_{SM}\left[\left(1 + m^2_{B_s}\frac{C_P}{C_A}\right)^2 + \left(1 - \frac{4m_\mu^2}{m^2_{B_s}}\right) m^4_{B_s}\frac{C_S^2}{C_A^2}\right]. \tag{3.126}$$

With respect to the contribution due to the charged Higgs boson, we can neglect it based on the fact that the charged Higgs contribution to this decay only takes place, as in the $\Delta F = 2$ transitions, through box diagrams with inner $W^\pm$, $H^\pm$, up quarks and neutrinos. Since the $H^\pm$-fermions coupling is always proportional to the fermion masses, we can expect these effects to be negligible

given the very small values of the neutrino masses.

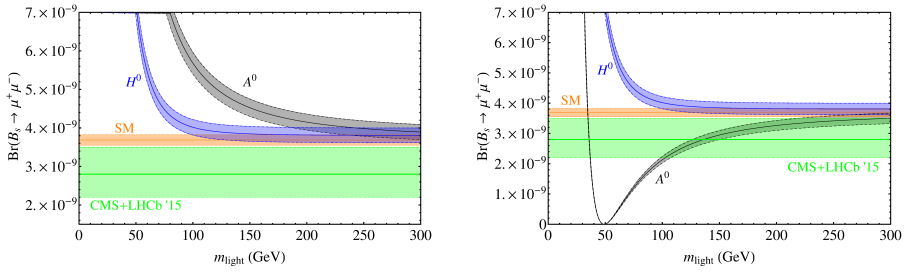

Figure 3.8: $\mathcal{B}(B_s \to \mu^+\mu^-)$ *as a function of the* H^0 *and* A^0 *masses with MFV coefficients* $\delta_1 = \lambda_0 = 1$ *(left) and* $\delta_1 = -\lambda_0 = 1$ *(right). The thin horizontal (green) lines indicate the LHCb and CMS combined result of the experimental measurement; the broad horizontal (orange) areas indicate the* 1σ *SM prediction; the blue areas show the* 1σ *prediction for* $m_{H^0} \ll m_{A^0} = m_{H^\pm} = 400$ *GeV; while the lower grey areas correspond to the analog prediction for* $m_{A^0} \ll m_{H^0} = m_{H^\pm} = 400$ *GeV.*

In Fig.3.8 we show our results for both $m_{H^0} < m_{A^0,H^\pm}$ and $m_{A^0} < m_{H^0,H^\pm}$ cases. An interesting feature of (3.126) is the interference term between the SM and the pseudoscalar operator. This characteristic leads, for the first time in our analysis, to a sensitivity of the branching ratio to the sign of the MFV coefficients. A difference in sign between the two coefficients implied, λ_0 and δ_1, cause the interference term to suppress the branching ratio in the light pseudoscalar case, providing a better compatibility with the experimental result than the SM for $m_{A^0} > 100$ GeV. When the scalar H^0 is light, the MFV theoretical prediction departs from the SM one in the wrong direction giving us an additional argument to favour the $m_{A^0} < m_{H^0,H^\pm}$ mass hierarchy. We therefore conclude that the $\mathcal{B}(B_s \to \mu^+\mu^-)$ study favours a pseudoscalar in the mass range $100 < m_{A^0} < 200$ GeV when $\delta_1 = -\lambda_0 = 1$. As previously done in the $\Delta F = 2$ case, we have studied the case where the values of the coefficients are taken to be smaller than one. As an example, in the case of $\delta_1 = -\lambda_0 = 0.5$, the presence of a lighter pseudo-scalar, $m_{A^0} \approx 60$ GeV, would already be able to provide a more satisfying compatibility with the observations.

The $B \to K^* \mu^+ \mu^-$ decay

After the first release of the LHCb results on the $B \to K^* \mu^+ \mu^-$ decay angular observables [9], this rare decay has revealed itself as one of the privileged places to look for new physics. Indeed, decays involving $b \to s\mu^+\mu^-$ transitions are very rare in the SM, since they are both CKM and loop suppressed, but are sensitive probes of NP given that many extensions of the SM are able to produce measurable effects. The kinematics and the angular distribution of the four body final state of the $B \to K^* \mu^+ \mu^-$ decay, where K^* indicates the $K^*(892) \to K^+\pi^-$ decay, give access to numerous observables sensitive to possible BSM contributions.
The differential angular distribution of the final state is given by [8]

$$\begin{aligned}\frac{1}{d\Gamma/dq^2}\frac{d^4\Gamma}{d\cos\theta_l d\cos\theta_k d\phi dq^2} =& \frac{9}{32\pi}\left[\frac{3}{4}(1-F_L)\sin^2\theta_k + F_L\cos^2\theta_k\right. \\ &+ \frac{1}{4}(1-F_L)\sin^2\theta_k\cos 2\theta_l - F_L\cos^2\theta_k\cos 2\theta_l \\ &+ S_3\sin^2\theta_k\sin^2\theta_l\cos 2\phi + S_4\sin 2\theta_k\sin 2\theta_l\cos\phi \\ &+ S_5\sin^2\theta_k\sin\theta_l\cos\phi + S_6\sin^2\theta_k\cos\theta_l \\ &+ S_7\sin 2\theta_k\sin\theta_l\sin\phi + S_8\sin 2\theta_k\sin 2\theta_l\sin\phi \\ &\left.+ S_9\sin^2\theta_k\sin^2\theta_l\sin 2\phi\right], \end{aligned} \tag{3.127}$$

where F_L and S_i are q^2 dependent bilinear combinations of the K^* decay amplitude. They are functions of the Wilson coefficients, containing information about the short distance effects, and form factors, encoding long distance effects. Therefore, it has been suggested to introduce observables that are combinations of these F_L and S_i functions in order to reduce the uncertainties, in particular in the low q^2 limit. They are defined as

$$P'_{i=4,5,6,8} = \frac{S_{j=4,5,7,8}}{F_L(1-F_L)}. \tag{3.128}$$

In [8], the LHCb collaboration determined a set of angular observables in the $B_0 \to K_0^* \mu^+ \mu^-$ decay using data collected during 2011 and found a local deviation with respect to the SM prediction in one of the observables, P'_5, with a significance corresponding to 3.7 standard deviations. More recently, the LHCb collaboration has released and updated analysis using the LHCb Run 1 full data sample [9], confirming the P'_5 inconsistency with the SM at the level of 3.4 standard deviations.

This inconsistency as well as the possibility of NP contributions being able to solve it have been widely discussed in the litterature [113–118]. Here, we would like to adress the argument provided in [11] about the possibility of the $Q_{S,P}$ operators introduced in (3.123) being able to give an appropriate contribution to P_5' in order to solve the tension with its experimental result. In the SM, the $b \to s$ transitions are gouverned by the the effective hamiltonian

$$\mathcal{H}_{eff}^{SM} = \frac{4G_F}{\sqrt{2}}(V_{ts}^* V_{tb}) \sum_{i=1}^{10} C_i \mathcal{O}_i. \tag{3.129}$$

The $B \to K^* \mu^+ \mu^-$ decay is dominated by the following tensor, axial and axial vector operators

$$\mathcal{O}_7 = \frac{e}{16\pi^2} m_b (\bar{s}\sigma_{\alpha\beta} P_L b) F^{\alpha\beta}, \tag{3.130}$$

$$\mathcal{O}_9 = \frac{\alpha_{em}}{4\pi} (\bar{s}\gamma_\alpha P_R b)(\mu\gamma^\alpha \mu), \tag{3.131}$$

$$\mathcal{O}_{10} = \frac{\alpha_{em}}{4\pi} (\bar{s}\gamma_\alpha P_R b)(\mu\gamma^\alpha \gamma_5 \mu). \tag{3.132}$$

Beyond the SM, new chirally flipped ($P_{L(R)} \to P_{R(L)}$) $\mathcal{O}_7'$, $\mathcal{O}_9'$ and $\mathcal{O}_{10}'$ as well as the $Q_{S,P}$ operators introduced in (3.123) may also be generated. However, the study carried out in [119] shows that the observable P_5' is especially sensitive to the contribution of the BSM operators $\mathcal{O}_9'$ and $\mathcal{O}_{10}'$. As pointed out in [11], the contribution of the $Q_{S,P}$ operators needed to release the tension of the P_5' measurement would affect other radiative and rare $b \to s$ modes, like $B_s \to \mu^+\mu^-$, providing a prediction of their branching ratios that would be incompatible with the already available experimental values. Therefore, we conclude that the deviations observed in the LHCb experiment can not be explained within our 2HDM once the results on $B_s \to \mu^+\mu^-$are taken into account.

3.4 Two-photon Higgs decay at the LHC

In our work in [46] we analyzed the possibility of observing one of the BSM neutral bosons A^0 and H^0 in the two-photon invariant mass spectrum at the LHC. More precisely, we studied the possibility of the observed excess around 125 GeV to be one of the non SM-like scalars. Currently, with the release of

much more precise data, the possibility that the observed boson is not a scalar or does not have the SM couplings has become very unlikely. In this section we will assess the situation of our 2HDM concerning the two-photon decay with the available data.

In the SM, the dominant contributions to the diphoton decay of the Higgs boson are the top and W loops. With respect to the SM scalar, a main differences of both the scalar H^0 and the pseudoscalar A^0 in the particular realization of the 2HDM that we have introduced, is that they are both vectophobic (i.e. $g_{HVV} = g_{AVV} = 0$ with $V = W^{\pm}, Z^0$) and therefore only top loop contributions have to be considered.

The number of events in the diphoton invariant mass spectrum is proportional to the production cross-section multiplied by the decay branching ratio. It is convenient to normalise it to the SM rate in order to study the possible enhancement ($R > 1$) or suppression ($R < 1$) by a BSM particle:

$$R \equiv \frac{\sigma \times \mathcal{B}(H^0, A^0 \to \gamma\gamma)}{\sigma_{SM} \times \mathcal{B}(h^0 \to \gamma\gamma)_{SM}}. \tag{3.133}$$

At the time of our study in [46] we made the assumption, both in the SM as in the 2HDM case, that the production cross-section was gluon-gluon fusion (ggF)-dominated. We also considered the limit where the total decay widths are dominated by the $b\bar{b}$ final state and computed the ratio R in the $m_{H^0,A^0} \ll 2m_t, 2m_W$ regime[5].

However, both the CMS [32] and the ATLAS [85] experiments have proved their ability to disentangle different diphoton events by their production mechanisms and provide a combination of the differently produced number of events. These analyses show evidence of Vector Boson Fusion (VBF) and Vector Higgs (VH) enriched diphoton selected events. The ATLAS collaboration [85] has furthermore studied the possibility of a fully ggF-produced scalar being compatible with the observed data and has set a lower limit of 200 GeV. These results, together with the observation of the diboson final states decays [32, 36], lead to the conclusion that the observed 125 GeV particle is neither the scalar H^0 nor the pseudoscalar A^0 in our custodial invariant 2HDM with MFV.

[5] A detailed explanation of the computations is given in Appendix C.

3.5 Experimental constraints on the custodial invariant 2HDM with MFV

In the previous chapter we have already summarized the state of the art regarding experimental contraints and direct searches of 2HDM particles. However, in this section, we will carry out a more complete and systematic analysis regarding the particular 2HDM considered in this work.

Constraints from the h_{SM} coupling measurements. In [120] a combination of the measurements of the Higgs boson production and decay rates from CMS and ATLAS is given for the full data collected in 2011 and 2012. The SM Higgs boson couplings can therefore be constrained from five production mechanisms; gluon-gluon fusion, vector-boson fusion and associated production with a gauge boson W or Z or a top pair. Six decay modes are combined as well; decays to two bosons: $H \to WW$, $H \to ZZ$ and $H \to \gamma\gamma$ and to two fermions: $H \to \tau\tau$, $H \to bb$ and $H \to \mu\mu$. The analysis provides the coupling measurements of the significant observations related to gluon-gluon fusion and ZZ, WW and $\gamma\gamma$ decays, the signal strengths and the constraints on the rest of the couplings. The results in this paper are significant enough to conclude that the newly observed boson at the LHC has SM-like couplings. Since the h^0 particle of the 2HDM introduced in this work has SM-like couplings to all the SM particles, we underline the compatibility between our model and those results.
In section 3.2.3, we have already mentioned the constraints on the alignment limit of the 2HDM coming from the h_{SM} coupling measurements. We will therefore sumarize the discussion by saying that the model considered in this work corresponds to a case of perfect alignment by construction and therefore, in regards of the SM-like boson couplings, the associated h^0 scalar is compatible with the observed scalar boson.

Direct searches of scalars and pseudoscalars. In the phenomenological analysis of the previous sections, we have already set some limits on the NP particles A^0, H^0 and $H^\pm$ that come from experimental results. We summarize

these constraints and explain how to apply them to the custodial invariant 2HDM with MFV.

As mentioned in 2.3, a limit on a fully ggF generated Higgs-like boson decaying into two photons is provided in [85]. Both A^0 and H^0 are fully ggF generated in this particular model and do not have a trilinear coupling to vector bosons. Consequently, this analysis can be applied to the BSM particles too. From the previous section, as well as from the appendix C, it can be seen that the ratio R defined in (C.1) is close to one around 200 GeV in the A^0 case, while significantly smaller in the H^0 case. Therefore, the upper limit $m_H > 200$ GeV obtained from this particular analysis only applies to the pseudoscalar A^0. However, as we have seen, more stringent constraints coming from the flavour analysis previously carried out are applied to the scalar H^0 favouring at the same time the custodial degeneracy $m_{H^0} \approx m_{H^\pm}$ and implying that the charged Higgs constraints should be applied to the additional scalar boson.

Direct searches on pseudoscalars have also been mentioned in 2.3. Regarding the pseudoscalar introduced in this work, the particular limits obtained in [86] cannot be fully applied since the analysis takes place in the framework of the MSSM 2HDM relying on the contribution of SUSY particles that are absent in our model. Another analysis that has been previously mentioned is carried out in [87] by CMS and [121] by ATLAS where limits on 2HDM are set from the search of the $A^0 \to h^0 Z$ decay. Yet, the custodial invariant 2HDM has no tree-level Zh^0A^0 coupling.

Concerning the limits on the charged Higgs $H^\pm$, the comparison in 3.2.2 provides the most stringent constrains with $m_{H^\pm} \gtrsim 400$ GeV.

Constraints on $H^0 \to A^0 Z$ from searches for a new resonance decaying into a lighter resonance and a Z boson. The $H^0(A^0) \to A^0(H^0)Z$ decay has been previously pointed out in the litterature [64] as a priviledged decay for 2HDM particles to be phenomenologically tested. The CMS collaboration has released the results on the search for neutral resonances decaying into a Z boson and a pair of b jets or τ leptons [122]. In the mentioned analysis, the two main assumptions are the degeneracy of the heaviest resonance with the charged Higgs, which is the case in the $H^0 \to A^0 Z$ interpretation within the custodial invariant 2HDM, and a $\mathbb{Z}_2$ symmetry leading to type-I or type-

II fermion couplings. There is no significant deviation observed with respect to the SM, and limits are set on the 2HDM parameter space. But, it is worth mentioning that two moderate excesses are observed for the $\tau\tau bb$ channel in the regions around $(m_{bb}, m_{\ell\ell bb}) = (95, 285)$ GeV and $(575, 660)$ GeV. Their local significance is 2.6σ and 2.85σ, respectively. In the $\ell\ell\tau\tau$ channel, no significant excess is observed.
In [122] the excess around $(m_{bb}, m_{\ell\ell bb}) = (95, 285)$ GeV is found compatible with the benchmark signal hypothesis of a type-II 2HDM at $m_{H^0} = 270$ GeV and $m_{A^0} = 104$ GeV and with the 2HDM parameters $\tan\beta = 1.5$ and $\cos(\beta - \alpha) = 0.01$. We adress the compatibility of this potentially significant excess with the 2HDM proposed in this work. Only the $H^0 \to A^0 Z$ scenario is considered since $m_{H^0} < m_{A^0} = m_{H^\pm}$ has already been ruled out in the previous section. After comparing the hypothesis made in [122], we underline the following differences with our framework:

- The analysis carried out by CMS assumes a 2HDM in the alignment limit $\cos(\beta-\alpha) = 0.01$. Therefore, the difference with our model, regarding the cross section of the production mechanism of the H^0 scalar, only relies on its coupling to fermions. Instead of being $\cot\beta$ dependent, like in type-II models, the production cross-section would introduce a $R^t_{H^0}$ factor (see (C.6)).

- The HAZ coupling coming from the Higgs kinetic terms, is not different from the one of a 2HDM in the alignment limit.

- The A^0 decay to fermions is also modified. While in the type-II 2HDM the coupling of the pseudo-scalar to both a bb pair and a τ-lepton pair is proportional to $\tan\beta$, in the custodial invariant with MFV the coupling to a bb pair is given by $R^b_{A^0}$ in (C.12) and the one to a τ-lepton pair is given by the λ_0 coefficient in (3.124).

The first remark leads to the conclusion that a $R^t_{H^0}$ factor is expected to slightly enhance the production cross section with respect to a type-II model with $\tan\beta = 1.5$, although keeping it at the same order of magnitude. The third remark indicates that the $R^b_{A^0}$ factor would provide a similar result for the $A^0 \to bb$ decay rate as the one in the framework of the type-II 2HDM in

the alignment limit. In the case of the decay to two leptons, since $\lambda_0 < \tan\beta$, the type-II observed number of events are expected to be higher than those in the 2HDM with MFV. This is coherent with the fact that no excess is observed in the analysis of this channel by CMS. Taking all this remarks into account, we conclude that the excess of events reported in [87], while non significant as it stands, could still be compatible with a $H^0 \to A^0 Z$ decay in the framework of the model presented in this work with $m_{H^0} > 270$ GeV. A heavier H^0 would compensate the $R^t_{H^0}$ factor enhancement while favouring the custodial condition $m_{H^0} \approx m_{H^\pm}$. As we have commented in 3.3.3, a slight departure from the custodial degeneracy does not affect our flavour results. Having $m_{H^\pm} > m_{H^0} > 270$ GeV is thus a fairly acceptable hypothesis.

3.6 Summary

In this chapter we have introduced a particular realization of the 2HDM that minimally violates both custodial and flavour symmetries. We have also analyzed the consequences of this particular model especially on some flavour observables and on the LHC results. In our analysis of the $\Delta F = 2$ transition observables ϵ_K and ΔM_{B_s}, we have studied both the A^0 and H^0 mediated FCNC contributions as well as the $H^\pm$ loop contributions. To get a glimpse of the order of magnitude of the two different contributions, we make use of the following parametrization for ϵ_K:

$$\begin{aligned} |\epsilon_K| =& |\epsilon_K^{SM} + \epsilon_K^{FCNC} + \epsilon_K^{H^\pm}| \\ =& |\epsilon_K^{SM}|(1 + \delta_{\epsilon_K}^{FCNC}(\delta_1, m_{A^0}, m_{H^0}) + \delta_{\epsilon_K}^{H^\pm}(v_0 + y_t v 1, m_{H^\pm})) \end{aligned} \tag{3.134}$$

with

$$\delta_{\epsilon_K}^{FCNC}(1, 200, 400) = -0.2\%; \quad \delta_{\epsilon_K}^{H^\pm}(1, 400) = 25\%. \tag{3.135}$$

In the ΔM_{B_s} case, a similar parametrization gives

$$\delta_{B_s}^{FCNC}(1, 200, 400) = -13\% \quad ; \quad \delta_{B_s}^{H^\pm}(1, 400) = 30\%. \tag{3.136}$$

We conclude that the most stringent constraints come from ΔM_{B_s}. The ϵ_K parameter can be used to confirm that the parameter space where ΔM_{B_s} concords better with the experiments is also allowed or even favoured by the neutral Kaon constraints. From these two flavour observables we conclude that the

mass hierarchy $m_{h^0} \approx m_{A^0} < m_{H^0,H^\pm}$ is still very much compatible with the current data. The $\mathcal{B}(B_s \to \mu^+\mu^-)$ rare decay gives us an additional argument favouring this particular hierarchy when the down quark and lepton MFV coefficients verify the relation $\delta_1 = -\lambda_0 = 1$.

As a general remark, let us underline the role of the top mass in the importance of MFV contributions. Although the mass hierarchy is not better understood in this model, the top quark is essential for the MFV contributions to be relevant. The dependence of the different contributions on the MFV parameters and on the choice of $m_{H^\pm}$ is also high. However, instead of trying to fit the best value for the MFV parameters, we have considered the case where the contributions are maximal and showed that the model is still compatible with the experiments for a wide range of parameter values.

Conclusion

This work took off with the aim of studying a 2HDM that was able to provide a richer phenomenology while preserving the main features of the SM that had made it so succesful over the last few decades. Compared to the SM, a general 2HDM has many additional parameters that need to be somehow constrained to fit the available experimental data. Many studies have analysed the possibility of the 2HDM solving the issues the SM is still unable to account for. However, the approach we have taken does not aim to solve these issues, but rather to preserve what made the SM so succesful up to now. This has shown itself to be very convenient given the historical results achieved over the past few years. With the latest LHC results, the idea that the SM is the strongest contender for the explanation of nature at the EW scale has been reinforced. Moreover, the impact of the latest experimental results on BSM models has mainly been to constrain their parameter space without any NP observation.
While introducing the SM in the first chapter of this work, we have sought to underline the *accidental* features of this theory and how important they are its actual success in explaining observed data. The absence of FCNC at tree-level is one of the major succesful features of the SM. The custodial symmetry that accidentally arises in the scalar sector of the theory and ensures that corrections to the ρ parameter remain small in another one. The flavour group G_f encoded in the fermion kinetic terms, although broken in other sectors of the theory, represents an additional particular property of the SM. Finally, the way in which CP violaton appears in the flavour sector through one single phase in

the 3×3 quark mixing matrix is striking as it accounts for CP violation both in Kaon and in B meson physics with an astonishing accuracy.

We have shown how all these properties, which arise subsequently to the particle content and the gauge symmetries associated to the fundamental interactions, are usually lost in BSM physics. In particular, the 2HDM does not preserve them in general. The constraints to be imposed on the 2HDM in order to keep the main SM properties, while at the same time allowing for some ne phenomenology, have been analyzed. We have studied the very particular case of a 2HDM where the custodial symmetry is imposed on the scalar potential in such a way that one of the additional neutral Higgs particles is degenerated in mass with the charged Higgs and therefore ensures the smallness of the ρ parameter corrections. A very interesting consequence of requiring the custodial invariance is the fact that it also ensures the absence of CP violation sources in the scalar potential. This non-trivial feature is unexpected but suitable to the prospect of finding a NP model that preserves the properties that have made the SM so succesful. On the other hand, through the introduction of the MFV hypothesis in the flavour sector we have been able to avoid additional sources of flavour mixing and CP violation. This way, only the CKM matrix and the quark masses and mixing parameters are responsible for the mentioned phenomena just like in the SM. A particularity of this model compared to other MFV models is that Higgs mediated FCNC are introduced at tree-level. However, the mechanism of MFV also ensures that these FCNC are kept small enough to remain compatible with the data for some interesting values of the BSM scalar masses. While conserving so many properties of the SM, the model still manages to provide possible values of the parameter space where NP could still be observed.

After studying the predictions of the model concerning some Kaon and B-meson quantities, we have been able to constrain the parameter space still available for the BSM particles of this 2HDM. The quantities we have studied in more detail are the neutral Kaon system CPV parameter ϵ_K; the B meson mass difference ΔM_{B_s}; and the rare decay $B_s \to \mu^+\mu^-$ branching ratio. We conclude that the scalar mass hierarchy of the 2HDM introduced in this work which is still favoured by the data is

$$m_{h^0} \sim m_{A^0} < m_{H^0} \simeq m_{H^\pm}, \tag{3.137}$$

where h^0 is a scalar having the same fermion and gauge boson couplings as the SM Higgs boson; $H^\pm$ corresponds to the charged Higgs; and A^0 and H^0 are a pseudo-scalar and an additional neutral scalar respectively.

The phenomenological analysis of this model has not been exhausted with the study carried out here. At the theoretical level, we have previously underlined how the SM is unable to account for the strong experimental constraint to be imposed on the θ_{QCD} parameter by the neutron dipole moment. An interesting follow-up of this work would be to analyze the possibility of a BSM contribution that would *naturally* cancel the θ_{QCD} parameter SM contribution. This could give an explanation for the very strong neutron dipole moment upper limit which would not have to resort to any fine-tuning.
Given the more precise experimental data available on the different Higgs decays channels with precisions on the different production mechanisms, it would be interesting to see if the diphoton channel in particular would be able to shed light on this model through some potential enhancements or suppressions granted by the vectophobic nature of two of its three neutral Higgs particles.
The study of models with an enlarged scalar sector remains a very relevant way of looking for new physics signals. The currently available experimental data allow us to strongly constrain the originally free parameters of these kinds of models. However, there is still room for NP observations and their study is still highly motivated.

Appendix A

Input parameters

In this appendix we list all the input parameters used in our work together with the references from which they have been extracted. We use most of those used by the CKMfitter group [4].

Parameter	Value ±Error(s)	Reference
m_W	80.385 ± 0.015 GeV	[14]
$\bar{m}_c$	$1.286 \pm 0.013 \pm 0.040$ GeV	[4]
$\bar{m}_t$	$165.95 \pm 0.035 \pm 0.064$ GeV	[4]
m_K	497.625 ± 0.024 MeV	[14]
ΔM_K	$(4.484 \pm 0.006) \times 10^{-12}$ MeV	[14]
f_K	$155.2 \pm 0.2 \pm 0.6$ MeV	[4]
B_K	$0.7615 \pm 0.0027 \pm 0.0137$	[4]
V_{cb}	$41.00 \pm 0.33 \pm 0.74$	[4]
V_{us}	0.2163 ± 0.0005	[4]
η_{tt}	$0.5765 \pm 0 \pm 0.0065$	[4]
η_{cc}	$1.87 \pm 0 \pm 0.76$	[98]
η_{ct}	$0.497 \pm 0 \pm 0.047$	[123]
κ_ϵ	$0.94 \pm 0.013 \pm 0.023$	[97]
ϕ_ϵ	$43.51^o(5)$	[14]

Parameter	Value ±Error(s)	Reference
f_{B_s}/f_{B_d}	$1.205 \pm 0.03 \pm 0.006$	[4]
B_{B_s}/B_{B_d}	$1.023 \pm 0.013 \pm 0.014$	[4]
$\sin 2\beta$	0.691 ± 0.017	[4]
m_{B_d}	5279.58 ± 0.17 MeV	[14]
m_{B_s}	5366.77 ± 0.24 MeV	[14]
ΔM_{B_d}	0.510 ± 0.003 ps^{-1}	[14]
ΔM_{B_s}	17.757 ± 0.021 ps^{-1}	[14]
η_B	$0.5510 \pm 0 \pm 0.0022$	[4]
f_{B_s}	$225.6 \pm 1.1 \pm 5.4$ MeV	[4]
τ_{B_s}	$(1.512 \pm 0.007) \times 10^{-12}$ s	[14]
B_s	1.320 ± 0.034	[4]
η_Y	1.026 ± 0.006	[110]
$\sin^2 \theta_W$	0.23116 ± 0.00003	[112]
m_μ	$(105.6583715 \pm 0.0000035) \times 10^{-3}$ GeV	[14]

Appendix B

Loop functions

The S loop-functions are given by

$$S(x_i,x_j) = x_i x_j \left[\left(\frac{1}{4}+\frac{3}{2(1-x_i)}-\frac{3}{4(1-x_i)^2}\right)-\frac{3}{2}\left(\frac{x_i}{1-x_i}\right)\frac{1}{x_i-x_j}\mathrm{Ln}(x_i) \right.$$
$$\left. +(x_i \leftrightarrow x_j) - \frac{3}{4}\frac{1}{(1-x_i)(1-x_j)}\right]. \tag{B.1}$$

$$S(x_i) \equiv S(x_i,x_j)|_{x_j\to x_i}$$
$$= x_i\left(\frac{1}{4}+\frac{9}{4(1-x_i)}-\frac{3}{2(1-x_i)^2}\right)-\frac{3}{2}\left(\frac{x_i}{1-x_i}\right)^3\mathrm{Ln}(x_i). \tag{B.2}$$

The D loop-functions are given by

$$D_0(m_1,m_2,M_1,M_2) = \frac{m_2^2\log\frac{m_2^2}{m_1^2}}{(m_2^2-m_1^2)(m_2^2-M_1^2)(m_2^2-M_2^2)}$$
$$+\frac{M_1^2\log\frac{M_1^2}{m_1^2}}{(M_1^2-m_1^2)(M_1^2-m_2^2)(M_1^2-M_2^2)}$$
$$+\frac{M_2^2\log\frac{M_2^2}{m_1^2}}{(M_2^2-m_1^2)(M_2^2-M_1^2)(M_2^2-m_2^2)}, \tag{B.3}$$

$$
\begin{aligned}
D_0(m,M_1,M_2) \equiv & \lim_{m_2\to m} D_0(m,m_2,M_1,M_2) \\
=& \frac{M_1 \log\frac{M_1}{m}}{(m-M_1)^2(M_1-M_2)} + \frac{1}{(m-M_1)(m-M_2)} \\
& + \frac{M_2 \log\frac{M_2}{m}}{(M_2-M_1)(m-M_2)^2},
\end{aligned} \tag{B.4}
$$

$$
\begin{aligned}
D_0(m,M) \equiv & \lim_{M_2\to M} D_0(m,M,M_2) \\
=& \frac{2(m-M)+(m+M)\log\frac{M}{m}}{(m-M)^3},
\end{aligned} \tag{B.5}
$$

$$
\begin{aligned}
D_2(m_1,m_2,M_1,M_2) =& \frac{m_2^4 \log\frac{m_2^2}{m_1^2}}{(m_2^2-m_1^2)(m_2^2-M_1^2)(m_2^2-M_2^2)} \\
& + \frac{M_1^4 \log\frac{M_1^2}{m_1^2}}{(M_1^2-m_1^2)(M_1^2-m_2^2)(M_1^2-M_2^2)} \\
& + \frac{M_2^4 \log\frac{M_2^2}{m_1^2}}{(M_2^2-m_1^2)(M_2^2-M_1^2)(M_2^2-m_2^2)},
\end{aligned} \tag{B.6}
$$

$$
\begin{aligned}
D_2(m,M_1,M_2) \equiv & \lim_{m_2\to m} D_2(m,m_2,M_1,M_2) \\
=& \frac{M_1^2 \log\frac{M_1}{m}}{(m-M_1)^2(M_1-M_2)} + \frac{M_2^2 \log\frac{M_2}{m}}{(m-M_2)^2(M_2-M_1)} \\
& + \frac{m(m-M_2)}{(m-M_1)(m-M_2)^2},
\end{aligned} \tag{B.7}
$$

$$
\begin{aligned}
D_2(m,M) \equiv & \lim_{M_2\to M} D_2(m,M,M_2) \\
=& \frac{m^2+2mM\log\frac{M}{m}-M^2}{(m-M)^3}.
\end{aligned} \tag{B.8}
$$

The Y loop-function is given by

$$
Y_0(x) = \frac{x}{8}\left(\frac{4-x}{1-x} + \frac{3x}{(1-x)^2}\right)\log x. \tag{B.9}
$$

Appendix C

Computation of the diphoton decay number of events ratio R

In 3.4 we have defined the ratio R of the number of diphoton events as

$$R \equiv \frac{\sigma \times \mathcal{B}(H^0, A^0 \to \gamma\gamma)}{\sigma_{SM} \times \mathcal{B}(h^0 \to \gamma\gamma)_{SM}}. \tag{C.1}$$

If we assume that the production is ggF-dominated via top quark loops and that the total decay widths are mainly due to $b\bar{b}$ decays, we can summarize the main steps in the computation of this ratio as the following. These are: the computation of the diphoton decay rate for the different (pseudo)scalars; the ggF production cross-sections computations and finally the $b\bar{b}$ decay widths.

- First, let us compute the diphoton decay rates. The SM scalar diphoton decay receives contributions from both fermions (mainly top quarks) and W bosons. The effective Lagrangian associated to the decay is [124]

$$\mathcal{L}^{h^0}_{\gamma\gamma} = -\frac{1}{4} F^{\mu\nu} F_{\mu\nu} \left[1 + \Pi^t_{\gamma\gamma}(0) + \Pi^W_{\gamma\gamma}(0)\right], \tag{C.2}$$

  where

$$\Pi^t_{\gamma\gamma}(0) = \frac{N_c q_t^2 \alpha}{3\pi} \left(\frac{4\pi\mu^2}{m_t^2}\right)^{\epsilon} \Gamma(1+\epsilon)\frac{1}{\epsilon}, \tag{C.3}$$

$$\Pi^W_{\gamma\gamma}(0) = -\frac{\alpha}{4\pi} \left(\frac{4\pi\mu^2}{m_W^2}\right)^{\epsilon} \Gamma(1+\epsilon) \left[\frac{7}{\epsilon} + \frac{2}{3} + \mathcal{O}(\epsilon)\right], \tag{C.4}$$

are, respectively, the lowest order expressions of the top quark and W boson contributions to the (dimensionless) photon vacuum polarization function at zero momentum transfer. In the $m_{h^0} \ll 2m_t, 2m_W$ regime, the effective Lagrangian of the $h^0\gamma\gamma$ coupling reduces to

$$\mathcal{L}_{h^0\gamma\gamma} = \frac{\alpha}{2\pi} F^{\mu\nu} F_{\mu\nu} \frac{h^0}{v} \left(N_c \frac{q_t^2}{3} - \frac{7}{4} \right). \tag{C.5}$$

The $H^0\gamma\gamma$ effective Lagrangian is very similar to the SM Lagrangian, except that it lacks the W boson contribution, since H^0 is vectophobic, and it has a different factor due to its different Yukawa couplings to fermions (mainly top quarks):

$$\mathcal{L}_{H^0\gamma\gamma} = \frac{\alpha}{2\pi} F^{\mu\nu} F_{\mu\nu} \frac{H^0}{v} R^t_{H^0} N_c \frac{q_t^2}{3} \quad \text{with} \quad R^t_{H^0} = \upsilon_0 + \upsilon_1 \frac{2m_t^2}{v^2}. \tag{C.6}$$

The pseudoscalar nature of the A^0 boson gives a slightly different expression for the $A\gamma\gamma$ effective Lagrangian [124]:

$$\mathcal{L}_{A^0\gamma\gamma} = N_c q_t^2 \frac{\alpha}{8\pi} F^{\mu\nu} \tilde{F}_{\mu\nu} R^t_{A^0} \frac{A^0}{v} \quad \text{with} \quad R^t_{A^0} = \upsilon_0 + \upsilon_1 \frac{2m_t^2}{v^2}. \tag{C.7}$$

- In order to compute the h^0 gluon-gluon fusion production cross section, we proceed in a way similar to the $h^0\gamma\gamma$ case. The derivation of the effective h^0gg Lagrangian starts from

$$\mathcal{L}^{h^0}_{gg} = -\frac{1}{4} G^{a\mu\nu} G^a_{\mu\nu} \left[1 + \Pi^t_{gg}(0) \right], \tag{C.8}$$

where

$$\Pi^t_{gg}(0) = \frac{\alpha}{6\pi} \left(\frac{4\pi\mu^2}{m_t^2} \right)^{\epsilon} \Gamma(1+\epsilon) \frac{1}{\epsilon}, \tag{C.9}$$

and yields to the h^0gg coupling Lagrangian

$$\mathcal{L}_{h^0gg} = \frac{\alpha}{12\pi} G^{a\mu\nu} G^a_{\mu\nu} \frac{h^0}{v}, \tag{C.10}$$

in the $m_{h^0} \ll 2m_t, 2m_W$ regime. The H^0 case is very similar since only one additional factor, $(R^t_{H^0})$, due to its different Yukawa couplings to top quarks, should be taken into account. In the pseudoscalar case, however, the effective Lagrangian is

$$\mathcal{L}_{A^0gg} = \frac{\alpha}{8\pi} G^{a\mu\nu} \tilde{G}^a_{\mu\nu} R^t_{A^0} \frac{A^0}{v} \quad \text{with} \quad R^t_{A^0} = \upsilon_0 + \upsilon_1 \frac{2m_t^2}{v^2}. \tag{C.11}$$

- Concerning the total decay widths, since we consider they are all dominated by $b\bar{b}$ decays, we have the following relations:

$$\Gamma_{A^0} = \Gamma_{H^0} = (R^b_{A^0,H^0})^2 \Gamma_{h^0} \quad \text{with} \quad R^b_{A^0,H^0} = \delta_0 + \delta_1 \frac{2m_t^2}{v^2}. \quad \text{(C.12)}$$

After computation of the decay widths and cross-sections associated to the different effective Lagrangians, we are now able to compute the ratio R for both A^0 and H^0:

$$R_{A^0} = \frac{\sigma_{A^0} \times \mathcal{B}(A^0 \to \gamma\gamma)}{\sigma_{SM} \times \mathcal{B}(h^0 \to \gamma\gamma)_{SM}} = 9 \frac{R^t_{A^0} |I_A(\tau_t)|^2}{R^b_{A^0} |I_S(\tau_t)|^2} \frac{|N_c q_t^2 R^t_{A^0} I_A(\tau_t)|^2}{|N_c q_t^2 \frac{4}{3} I_S(\tau_t)|^2 + I_W(\tau_W)}, \quad \text{(C.13)}$$

$$R_{H^0} = \frac{\sigma_{H^0} \times \mathcal{B}(H^0 \to \gamma\gamma)}{\sigma_{SM} \times \mathcal{B}(h^0 \to \gamma\gamma)_{SM}} = \frac{R^t_{A^0}}{R^b_{A^0}} \frac{|N_c q_t^2 R^t_{H^0} \frac{4}{3} I_S(\tau_t)|^2}{|N_c q_t^2 \frac{4}{3} I_S(\tau_t)|^2 + I_W(\tau_W)}, \quad \text{(C.14)}$$

where the $I_i(\tau)$ functions have the form

$$I_S(\tau) = \frac{3}{2}\tau[1 + (1-\tau) f(\tau)], \quad \text{(C.15)}$$

$$I_A(\tau) = \tau f(\tau), \quad \text{(C.16)}$$

$$I_W(\tau) = 2 + 3\tau + 3\tau(2-\tau) f(\tau), \quad \text{(C.17)}$$

with

$$\tau_i = \left(\frac{2m_i}{m_H}\right)^2 \quad \text{and} \quad f(\tau) \begin{cases} \left(\arcsin \sqrt{\frac{1}{\tau}}\right)^2 & \text{if } \tau \geqslant 1 \\ -\frac{1}{4}\left(\log\left[\frac{1+\sqrt{1-\tau}}{1-\sqrt{1-\tau}}\right] - i\pi\right)^2 & \text{if } \tau \leqslant 1 \end{cases}. \quad \text{(C.18)}$$

In Fig.C.1 we plot the ratios R_{A^0} and R_{H^0} as functions of m_{A^0} and m_{H^0} for values of the masses below 200 GeV. The MFV are equal to one. The ratio becomes important for light values of the pseudoscalar mass m_{A^0}. However, we have already seen in the ΔM_{B_s} analysis (see Tab.3.1), that for the highest values of the MFV coefficients the pseudoscalar is not expected to be that light. As we have mentioned previously, the light H^0 case is already very much unfavoured by all the data and this is confirmed by the missing events necessary to reproduce the data.

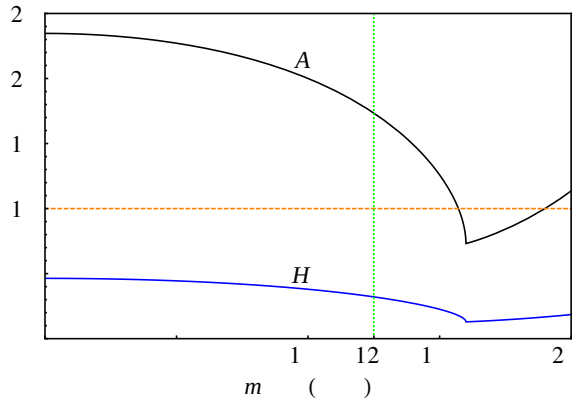

Figure C.1: *The ratio R defined in eq.* (C.1) *as a function of the* H^0 *and* A^0 *masses if the MFV coefficients are equal to one. The upper (black) curve corresponds to the case where* A^0 *is the lightest non-SM Higgs boson while the lower (blue) curve corresponds to the case where* H^0 *is the lightest non-SM Higgs boson.*

Bibliography

[1] **CMS** Collaboration, S. Chatrchyan *et al.*, "Observation of a new boson at a mass of 125 GeV with the CMS experiment at the LHC," *Phys. Lett.* **B716** (2012) 30–61, arXiv:1207.7235.

[2] **ATLAS** Collaboration, G. Aad *et al.*, "Observation of a new particle in the search for the Standard Model Higgs boson with the ATLAS detector at the LHC," *Phys. Lett.* **B716** (2012) 1–29, arXiv:1207.7214.

[3] **LHCb, CMS** Collaboration, V. Khachatryan *et al.*, "Observation of the rare $B_s^0 \to \mu^+\mu^-$ decay from the combined analysis of CMS and LHCb data," *Nature* **522** (2015) 68–72, arXiv:1411.4413.

[4] **CKMfitter Group** Collaboration, J. Charles, A. Hocker, H. Lacker, S. Laplace, F. R. Le Diberder, J. Malcles, J. Ocariz, M. Pivk, and L. Roos, "CP violation and the CKM matrix: Assessing the impact of the asymmetric B factories," *Eur. Phys. J.* **C41** no. 1, (2005) 1–131, arXiv:hep-ph/0406184.

[5] **ATLAS** Collaboration, M. Aaboud *et al.*, "Search for resonances in diphoton events at $\sqrt{s}$=13 TeV with the ATLAS detector," *JHEP* **09** (2016) 001, arXiv:1606.03833.

[6] **CMS** Collaboration, V. Khachatryan *et al.*, "Search for Resonant Production of High-Mass Photon Pairs in Proton-Proton Collisions at $\sqrt{s}$ =8 and 13 TeV," *Phys. Rev. Lett.* **117** no. 5, (2016) 051802, arXiv:1606.04093.

[7] **CMS** Collaboration, V. Khachatryan *et al.*, "Search for high-mass diphoton resonances in proton-proton collisions at 13 TeV and combination with 8 TeV search," *Phys. Lett.* **B767** (2017) 147–170, arXiv:1609.02507.

[8] **LHCb** Collaboration, R. Aaij *et al.*, "Measurement of Form-Factor-Independent Observables in the Decay $B^0 \to K^{*0}\mu^+\mu^-$," *Phys. Rev. Lett.* **111** (2013) 191801, arXiv:1308.1707.

[9] **LHCb** Collaboration, R. Aaij *et al.*, "Angular analysis of the $B^0 \to K^{*0}\mu^+\mu^-$ decay using 3 fb^{-1} of integrated luminosity," *JHEP* **02** (2016) 104, arXiv:1512.04442.

[10] W. Altmannshofer and D. M. Straub, "New Physics in $B \to K^*\mu\mu$?," *Eur. Phys. J.* **C73** (2013) 2646, arXiv:1308.1501.

[11] A. Datta, M. Duraisamy, and D. Ghosh, "Explaining the $B \to K^*\mu^+\mu^-$ data with scalar interactions," *Phys. Rev.* **D89** no. 7, (2014) 071501, arXiv:1310.1937.

[12] B. Capdevila, A. Crivellin, S. Descotes-Genon, J. Matias, and J. Virto, "Patterns of New Physics in $b \to s\ell^+\ell^-$ transitions in the light of recent data," arXiv:1704.05340.

[13] R. G, "An introduction to the Standard Model of electroweak interactions,". https://www.ge.infn.it/~ridolfi/.

[14] **Particle Data Group** Collaboration, K. A. Olive *et al.*, "Review of Particle Physics," *Chin. Phys.* **C38** (2014) 090001.

[15] S. L. Glashow, "Partial Symmetries of Weak Interactions," *Nucl. Phys.* **22** (1961) 579–588.

[16] S. Weinberg, "A Model of Leptons," *Phys. Rev. Lett.* **19** (1967) 1264–1266.

[17] A. Salam, "Weak and Electromagnetic Interactions," *Conf. Proc.* **C680519** (1968) 367–377.

[18] F. Englert and R. Brout, "Broken Symmetry and the Mass of Gauge Vector Mesons," *Phys. Rev. Lett.* **13** (1964) 321–323.

[19] P. W. Higgs, "Broken Symmetries and the Masses of Gauge Bosons," *Phys. Rev. Lett.* **13** (1964) 508–509.

[20] G. S. Guralnik, C. R. Hagen, and T. W. B. Kibble, "Global Conservation Laws and Massless Particles," *Phys. Rev. Lett.* **13** (1964) 585–587.

[21] R. N. Mohapatra and G. Senjanovic, "Neutrino Mass and Spontaneous Parity Violation," *Phys. Rev. Lett.* **44** (1980) 912.

[22] **E949** Collaboration, A. V. Artamonov *et al.*, "New measurement of the $K^+ \to \pi^+\nu\bar{\nu}$ branching ratio," *Phys. Rev. Lett.* **101** (2008) 191802, arXiv:0808.2459.

[23] M. E. Peskin and T. Takeuchi, "A New constraint on a strongly interacting Higgs sector," *Phys. Rev. Lett.* **65** (1990) 964–967.

[24] M. J. G. Veltman, "Limit on Mass Differences in the Weinberg Model," *Nucl. Phys.* **B123** (1977) 89–99.

[25] G. Passarino and M. J. G. Veltman, "One Loop Corrections for e+ e- Annihilation Into mu+ mu- in the Weinberg Model," *Nucl. Phys.* **B160** (1979) 151–207.

[26] M. B. Einhorn, D. R. T. Jones, and M. J. G. Veltman, "Heavy Particles and the rho Parameter in the Standard Model," *Nucl. Phys.* **B191** (1981) 146–172.

[27] **Gfitter Group** Collaboration, M. Baak, J. Cth, J. Haller, A. Hoecker, R. Kogler, K. Mnig, M. Schott, and J. Stelzer, "The global electroweak fit at NNLO and prospects for the LHC and ILC," *Eur. Phys. J.* **C74** (2014) 3046, arXiv:1407.3792.

[28] M. Kobayashi and T. Maskawa, "CP Violation in the Renormalizable Theory of Weak Interaction," *Prog. Theor. Phys.* **49** (1973) 652–657.

[29] N. Cabibbo, "Unitary Symmetry and Leptonic Decays," *Phys. Rev. Lett.* **10** (1963) 531–533.

[30] C. Jarlskog, "Commutator of the Quark Mass Matrices in the Standard Electroweak Model and a Measure of Maximal CP Violation," *Phys. Rev. Lett.* **55** (1985) 1039.

[31] G. 't Hooft, "Symmetry Breaking Through Bell-Jackiw Anomalies," *Phys. Rev. Lett.* **37** (1976) 8–11.

[32] **CMS** Collaboration, V. Khachatryan *et al.*, "Precise determination of the mass of the Higgs boson and tests of compatibility of its couplings with the standard model predictions using proton collisions at 7 and 8 TeV," *Eur. Phys. J.* **C75** no. 5, (2015) 212, arXiv:1412.8662.

[33] **ATLAS** Collaboration, G. Aad *et al.*, "Measurement of the Higgs boson mass from the $H \to \gamma\gamma$ and $H \to ZZ^* \to 4\ell$ channels with the ATLAS detector using 25 fb^{-1} of pp collision data," *Phys. Rev.* **D90** no. 5, (2014) 052004, arXiv:1406.3827.

[34] **ATLAS, CMS** Collaboration, G. Aad *et al.*, "Combined Measurement of the Higgs Boson Mass in pp Collisions at $\sqrt{s} = 7$ and 8 TeV with the ATLAS and CMS Experiments," *Phys. Rev. Lett.* **114** (2015) 191803, arXiv:1503.07589.

[35] **CMS** Collaboration, "Measurements of properties of the Higgs boson decaying into four leptons in pp collisions at $\sqrt{s} = 13$ TeV,".

[36] **ATLAS** Collaboration, G. Aad *et al.*, "Measurements of Higgs boson production and couplings in diboson final states with the ATLAS detector at the LHC," *Phys. Lett.* **B726** (2013) 88–119, arXiv:1307.1427.

[37] **ATLAS** Collaboration, G. Aad *et al.*, "Evidence for the spin-0 nature of the Higgs boson using ATLAS data," *Phys. Lett.* **B726** (2013) 120–144, arXiv:1307.1432.

[38] **CMS** Collaboration, V. Khachatryan *et al.*, "Constraints on the spin-parity and anomalous HVV couplings of the Higgs boson in proton collisions at 7 and 8 TeV," *Phys. Rev.* **D92** no. 1, (2015) 012004, arXiv:1411.3441.

[39] C. Bobeth, M. Gorbahn, T. Hermann, M. Misiak, E. Stamou, and M. Steinhauser, "$B_{s,d} \to l^+ l^-$ in the Standard Model with Reduced Theoretical Uncertainty," *Phys. Rev. Lett.* **112** (2014) 101801, arXiv:1311.0903.

[40] **LHCb** Collaboration, R. Aaij *et al.*, "Measurement of the $B_s^0 \to \mu^+\mu^-$ branching fraction and effective lifetime and search for $B^0 \to \mu^+\mu^-$ decays," arXiv:1703.05747.

[41] A. Pich, "Status after the first LHC run: Looking for new directions in the physics landscape," *Nucl. Instrum. Meth.* **A824** (2016) 43–46, arXiv:1507.01250.

[42] A. Pich, "ICHEP 2014 Summary: Theory Status after the First LHC Run," *Nucl. Part. Phys. Proc.* **273-275** (2016) 1–10, arXiv:1505.01813.

[43] E. Ma, "Verifiable radiative seesaw mechanism of neutrino mass and dark matter," *Phys. Rev.* **D73** (2006) 077301, arXiv:hep-ph/0601225.

[44] R. Barbieri, L. J. Hall, and V. S. Rychkov, "Improved naturalness with a heavy Higgs: An Alternative road to LHC physics," *Phys. Rev.* **D74** (2006) 015007, hep-ph/0603188.

[45] L. Lopez Honorez, E. Nezri, J. F. Oliver, and M. H. G. Tytgat, "The Inert Doublet Model: An Archetype for Dark Matter," *JCAP* **0702** (2007) 028, arXiv:hep-ph/0612275.

[46] E. Cerveró and J.-M. Gérard, "Minimal violation of flavour and custodial symmetries in a vectophobic Two-Higgs-Doublet-Model," *Phys. Lett.* **B712** (2012) 255–260, arXiv:1202.1973.

[47] S. Davidson and H. E. Haber, "Basis-independent methods for the two-Higgs-doublet model," *Phys. Rev.* **D72** (2005) 035004, arXiv:hep-ph/0504050.

[48] S. L. Glashow and S. Weinberg, "Natural Conservation Laws for Neutral Currents," *Phys. Rev.* **D15** (1977) 1958.

[49] E. A. Paschos, "Diagonal Neutral Currents," *Phys. Rev.* **D15** (1977) 1966.

[50] A. Pich and P. Tuzon, "Yukawa Alignment in the Two-Higgs-Doublet Model," *Phys. Rev.* **D80** (2009) 091702, arXiv:0908.1554.

[51] G. C. Branco, P. M. Ferreira, L. Lavoura, M. N. Rebelo, M. Sher, and J. P. Silva, "Theory and phenomenology of two-Higgs-doublet models," *Phys. Rept.* **516** (2012) 1–102, arXiv:1106.0034.

[52] A. Barroso, P. M. Ferreira, R. Santos, M. Sher, and J. P. Silva, "2HDM at the LHC - the story so far," in *Proceedings, 1st Toyama International Workshop on Higgs as a Probe of New Physics 2013 (HPNP2013): Toyama, Japan, February 13-16, 2013*. 2013. arXiv:1304.5225.

[53] C.-Y. Chen, S. Dawson, and M. Sher, "Heavy Higgs Searches and Constraints on Two Higgs Doublet Models," *Phys. Rev.* **D88** (2013) 015018, arXiv:1305.1624.

[54] B. Grinstein and P. Uttayarat, "Carving Out Parameter Space in Type-II Two Higgs Doublets Model," *JHEP* **06** (2013) 094, arXiv:1304.0028.

[55] O. Eberhardt, U. Nierste, and M. Wiebusch, "Status of the two-Higgs-doublet model of type II," *JHEP* **07** (2013) 118, arXiv:1305.1649.

[56] S. Chang, S. K. Kang, J.-P. Lee, K. Y. Lee, S. C. Park, and J. Song, "Two Higgs doublet models for the LHC Higgs boson data at $\sqrt{s} = 7$ and 8 TeV," *JHEP* **09** (2014) 101, arXiv:1310.3374.

[57] A. Celis, V. Ilisie, and A. Pich, "Towards a general analysis of LHC data within two-Higgs-doublet models," *JHEP* **12** (2013) 095, arXiv:1310.7941.

[58] B. Dumont, J. F. Gunion, Y. Jiang, and S. Kraml, "Constraints on and future prospects for Two-Higgs-Doublet Models in light of the LHC Higgs signal," *Phys. Rev.* **D90** (2014) 035021, arXiv:1405.3584.

[59] D. Fontes, J. C. Romo, and J. P. Silva, "A reappraisal of the wrong-sign $hb\overline{b}$ coupling and the study of $h \to Z\gamma$," *Phys. Rev.* **D90** no. 1, (2014) 015021, arXiv:1406.6080.

[60] P. M. Ferreira, R. Guedes, J. F. Gunion, H. E. Haber, M. O. P. Sampaio, and R. Santos, "The CP-conserving 2HDM after the 8 TeV run," in *Proceedings,*

22nd International Workshop on Deep-Inelastic Scattering and Related Subjects (DIS 2014): Warsaw, Poland, April 28-May 2, 2014. 2014. arXiv:1407.4396.

[61] A. Pomarol and R. Vega, "Constraints on CP violation in the Higgs sector from the rho parameter," *Nucl. Phys.* **B413** (1994) 3–15, arXiv:hep-ph/9305272.

[62] C. C. Nishi, "Custodial SO(4) symmetry and CP violation in N-Higgs-doublet potentials," *Phys. Rev.* **D83** (2011) 095005, arXiv:1103.0252.

[63] J. M. Gérard and M. Herquet, "A Twisted custodial symmetry in the two-Higgs-doublet model," *Phys. Rev. Lett.* **98** (2007) 251802, arXiv:hep-ph/0703051.

[64] S. de Visscher, J.-M. Gérard, M. Herquet, V. Lemaitre, and F. Maltoni, "Unconventional phenomenology of a minimal two-Higgs-doublet model," *JHEP* **08** (2009) 042, arXiv:0904.0705.

[65] G. C. Branco, M. N. Rebelo, and J. I. Silva-Marcos, "CP-odd invariants in models with several Higgs doublets," *Phys. Lett.* **B614** (2005) 187–194, arXiv:hep-ph/0502118.

[66] T. D. Lee, "A Theory of Spontaneous T Violation," *Phys. Rev.* **D8** (1973) 1226–1239.

[67] I. Yu. Kobsarev, L. B. Okun, and Ya. B. Zeldovich, "Spontaneous cp-violation and cosmology," *Phys. Lett.* **B50** (1974) 340–342.

[68] J. Preskill, S. P. Trivedi, F. Wilczek, and M. B. Wise, "Cosmology and broken discrete symmetry," *Nucl. Phys.* **B363** (1991) 207–220.

[69] S. Weinberg, "Gauge Theory of CP Violation," *Phys. Rev. Lett.* **37** (1976) 657.

[70] G. C. Branco, J. M. Gérard, and W. Grimus, "Geometrical T violation," *Phys. Lett.* **B136** (1984) 383–386.

[71] R. D. Peccei and H. R. Quinn, "CP Conservation in the Presence of Instantons," *Phys. Rev. Lett.* **38** (1977) 1440–1443.

[72] J. R. Ellis and M. K. Gaillard, "Strong and Weak CP Violation," *Nucl. Phys.* **B150** (1979) 141–162.

[73] I. B. Khriplovich, "Quark Electric Dipole Moment and Induced θ Term in the Kobayashi-Maskawa Model," *Phys. Lett.* **B173** (1986) 193–196.

[74] J.-M. Gérard and P. Mertens, "Weakly-induced strong CP-violation," *Phys. Lett.* **B716** (2012) 316–321, arXiv:1206.0914.

[75] G. D'Ambrosio, G. F. Giudice, G. Isidori, and A. Strumia, "Minimal flavor violation: An Effective field theory approach," *Nucl. Phys.* **B645** (2002) 155–187, arXiv:hep-ph/0207036.

[76] C. Smith, "Minimal flavor violation in supersymmetric theories," *Acta Phys. Polon. Supp.* **3** (2010) 53–64, arXiv:0909.4444.

[77] G. Degrassi and P. Slavich, "QCD Corrections in two-Higgs-doublet extensions of the Standard Model with Minimal Flavor Violation," *Phys. Rev.* **D81** (2010) 075001, arXiv:1002.1071.

[78] F. J. Botella, G. C. Branco, and M. N. Rebelo, "Minimal Flavour Violation and Multi-Higgs Models," *Phys. Lett.* **B687** (2010) 194–200, arXiv:0911.1753.

[79] A. J. Buras, M. V. Carlucci, S. Gori, and G. Isidori, "Higgs-mediated FCNCs: Natural Flavour Conservation vs. Minimal Flavour Violation," *JHEP* **10** (2010) 009, arXiv:1005.5310.

[80] L. Mercolli and C. Smith, "EDM constraints on flavored CP-violating phases," *Nucl. Phys.* **B817** (2009) 1–24, arXiv:0902.1949 [hep-ph].

[81] G. C. Branco, W. Grimus, and L. Lavoura, "Relating the scalar flavor changing neutral couplings to the CKM matrix," *Phys. Lett.* **B380** (1996) 119–126, arXiv:hep-ph/9601383.

[82] G. C. Branco and L. Lavoura, "Rephasing Invariant Parametrization of the Quark Mixing Matrix," *Phys. Lett.* **B208** (1988) 123–130.

[83] F. J. Botella, G. C. Branco, and M. N. Rebelo, "Invariants and Flavour in the General Two-Higgs Doublet Model," *Phys. Lett.* **B722** (2013) 76–82, arXiv:1210.8163.

[84] F. J. Botella and J. P. Silva, "Jarlskog - like invariants for theories with scalars and fermions," *Phys. Rev.* **D51** (1995) 3870–3875, arXiv:hep-ph/9411288.

[85] **ATLAS Collaboration** Collaboration, "Measurements of the properties of the Higgs-like boson in the two photon decay channel with the ATLAS detector using 25 fb^{-1} of proton-proton collision data," Tech. Rep. ATLAS-CONF-2013-012, CERN, Geneva, Mar, 2013. http://cds.cern.ch/record/1523698.

[86] **CMS** Collaboration, V. Khachatryan *et al.*, "Search for neutral MSSM Higgs bosons decaying to a pair of tau leptons in pp collisions," *JHEP* **10** (2014) 160, arXiv:1408.3316.

[87] **CMS** Collaboration, V. Khachatryan *et al.*, "Search for a pseudoscalar boson decaying into a Z boson and the 125 GeV Higgs boson in $\ell^+\ell^- b\overline{b}$ final states," *Phys. Lett.* **B748** (2015) 221–243, arXiv:1504.04710.

[88] I. F. Ginzburg, M. Krawczyk, and P. Osland, "Resolving SM like scenarios via Higgs boson production at a photon collider. 1. 2HDM versus SM," arXiv:hep-ph/0101208.

[89] P. M. Ferreira, J. F. Gunion, H. E. Haber, and R. Santos, "Probing wrong-sign Yukawa couplings at the LHC and a future linear collider," *Phys. Rev.* **D89** no. 11, (2014) 115003, arXiv:1403.4736.

[90] W. Grimus, L. Lavoura, O. M. Ogreid, and P. Osland, "A Precision constraint on multi-Higgs-doublet models," *J. Phys.* **G35** (2008) 075001, arXiv:0711.4022.

[91] M. Jung, A. Pich, and P. Tuzon, "Charged-Higgs phenomenology in the Aligned two-Higgs-doublet model," *JHEP* **11** (2010) 003, arXiv:1006.0470.

[92] M. Jung, A. Pich, and P. Tuzon, "The $\bar{B} \to X_s\gamma$ Rate and CP Asymmetry within the Aligned Two-Higgs-Doublet Model," *Phys. Rev.* **D83** (2011) 074011, arXiv:1011.5154.

[93] M. Misiak and M. Steinhauser, "NNLO QCD corrections to the $\bar{B} \to X_s\gamma$ matrix elements using interpolation in m_c," *Nucl. Phys.* **B764** (2007) 62–82, arXiv:hep-ph/0609241.

[94] J. Bernon, J. F. Gunion, H. E. Haber, Y. Jiang, and S. Kraml, "Scrutinizing the alignment limit in two-Higgs-doublet models. I. m_h=125 GeV," *Phys. Rev.* **D92** no. 7, (2015) 075004, arXiv:1507.00933.

[95] J. Bernon, J. F. Gunion, H. E. Haber, Y. Jiang, and S. Kraml, "Scrutinizing the alignment limit in two-Higgs-doublet models. II. m_H=125 GeV," *Phys. Rev.* **D93** no. 3, (2016) 035027, arXiv:1511.03682.

[96] A. J. Buras and D. Guadagnoli, "Correlations among new CP violating effects in $\Delta F = 2$ observables," *Phys. Rev.* **D78** (2008) 033005, arXiv:0805.3887.

[97] A. Lenz, U. Nierste, J. Charles, S. Descotes-Genon, A. Jantsch, C. Kaufhold, H. Lacker, S. Monteil, V. Niess, and S. T'Jampens, "Anatomy of New Physics in $B - \bar{B}$ mixing," *Phys. Rev.* **D83** (2011) 036004, arXiv:1008.1593.

[98] J. Brod and M. Gorbahn, "Next-to-Next-to-Leading-Order Charm-Quark Contribution to the CP Violation Parameter ϵ_K and ΔM_K," *Phys. Rev. Lett.* **108** (2012) 121801, arXiv:1108.2036.

[99] B. Winstein and L. Wolfenstein, "The Search for direct CP violation," *Rev. Mod. Phys.* **65** (1993) 1113–1148.

[100] J.-M. Gérard, "An upper bound on the Kaon B-parameter and $Re(\epsilon_K)$," *JHEP* **02** (2011) 075, arXiv:1012.2026.

[101] B. D. Gaiser, T. Tsao, and M. B. Wise, "Parameters of the Six Quark Model," *Annals Phys.* **132** (1981) 66.

[102] A. J. Buras and J. M. Gérard, "1/n Expansion for Kaons," *Nucl. Phys.* **B264** (1986) 371–392.

[103] **NA48** Collaboration, J. R. Batley *et al.*, "A Precision measurement of direct CP violation in the decay of neutral kaons into two pions," *Phys. Lett.* **B544** (2002) 97–112, arXiv:hep-ex/0208009.

[104] **KTeV** Collaboration, A. Alavi-Harati *et al.*, "Measurements of direct CP violation, CPT symmetry, and other parameters in the neutral kaon system," *Phys. Rev.* **D67** (2003) 012005, arXiv:hep-ex/0208007.

[105] **KTeV** Collaboration, E. T. Worcester, "The Final Measurement of $\epsilon'/epsilon$ from KTeV," in *Heavy Quarks and Leptons 2008 (HQ&L08) Melbourne, Australia, June 5-9, 2008*. 2009. arXiv:0909.2555.

[106] A. J. Buras and J.-M. Gérard, "Upper bounds on ϵ'/ϵ parameters $B_6^{(1/2)}$ and $B_8^{(3/2)}$ from large N QCD and other news," *JHEP* **12** (2015) 008, arXiv:1507.06326.

[107] A. J. Buras, M. Gorbahn, S. Jager, and M. Jamin, "Improved anatomy of ϵ'/ϵ in the Standard Model," *JHEP* **11** (2015) 202, arXiv:1507.06345.

[108] A. J. Buras and J.-M. Gérard, "Final state interactions in $K \to \pi\pi$ decays: $\Delta I = 1/2$ rule vs. ϵ'/ϵ," *Eur. Phys. J.* **C77** no. 1, (2017) 10, arXiv:1603.05686.

[109] A. J. Buras, M. Jamin, and M. E. Lautenbacher, "The Anatomy of ϵ'/ϵ beyond leading logarithms with improved hadronic matrix elements," *Nucl. Phys.* **B408** (1993) 209–285, arXiv:hep-ph/9303284.

[110] A. J. Buras, R. Fleischer, J. Girrbach, and R. Knegjens, "Probing New Physics with the $B_s \to \mu^+\mu^-$ Time-Dependent Rate," *JHEP* **07** (2013) 77, arXiv:1303.3820.

[111] A. J. Buras, "Relations between $\Delta M_{s,d}$ and $B_{s,d} \to \mu\bar{\mu}$ in models with minimal flavor violation," *Phys. Lett.* **B566** (2003) 115–119, arXiv:hep-ph/0303060.

[112] A. J. Buras, J. Girrbach, D. Guadagnoli, and G. Isidori, "On the Standard Model prediction for $\mathcal{B}(B_{s,d} \to \mu^+\mu^-)$," *Eur. Phys. J.* **C72** (2012) 2172, arXiv:hep-ph/1208.0934.

[113] A. J. Buras, F. De Fazio, and J. Girrbach, "331 models facing new $b \to s\mu^+\mu^-$ data," *JHEP* **02** (2014) 112, arXiv:1311.6729.

[114] R. Gauld, F. Goertz, and U. Haisch, "On minimal Z' explanations of the $B \to K^*\mu^+\mu^-$ anomaly," *Phys. Rev.* **D89** (2014) 015005, arXiv:1308.1959.

[115] G. Hiller and M. Schmaltz, "Diagnosing lepton-nonuniversality in $b \to s\ell\ell$," *JHEP* **02** (2015) 055, arXiv:1411.4773.

[116] B. Gripaios, M. Nardecchia, and S. A. Renner, "Composite leptoquarks and anomalies in B-meson decays," *JHEP* **05** (2015) 006, arXiv:1412.1791.

[117] B. Gripaios, M. Nardecchia, and S. A. Renner, "Linear flavour violation and anomalies in B physics," *JHEP* **06** (2016) 083, arXiv:1509.05020.

[118] A. Crivellin, G. D'Ambrosio, and J. Heeck, "Explaining $h \to \mu^\pm\tau^\mp$, $B \to K^*\mu^+\mu^-$ and $B \to K\mu^+\mu^-/B \to Ke^+e^-$ in a two-Higgs-doublet model with gauged $L_\mu - L_\tau$," *Phys. Rev. Lett.* **114** (2015) 151801, arXiv:1501.00993.

[119] A. K. Alok, A. Datta, A. Dighe, M. Duraisamy, D. Ghosh, and D. London, "New Physics in $b- > s\mu^+\mu^-$: CP-Conserving Observables," *JHEP* **11** (2011) 121, arXiv:1008.2367.

[120] **ATLAS, CMS** Collaboration, G. Aad *et al.*, "Measurements of the Higgs boson production and decay rates and constraints on its couplings from a combined ATLAS and CMS analysis of the LHC pp collision data at $\sqrt{s} = 7$ and 8 TeV," *JHEP* **08** (2016) 045, arXiv:1606.02266.

[121] **ATLAS** Collaboration, G. Aad *et al.*, "Search for a CP-odd Higgs boson decaying to Zh in pp collisions at $\sqrt{s} = 8$ TeV with the ATLAS detector," *Phys. Lett.* **B744** (2015) 163–183, arXiv:1502.04478.

[122] **CMS** Collaboration, V. Khachatryan *et al.*, "Search for neutral resonances decaying into a Z boson and a pair of b jets or τ leptons," *Phys. Lett.* **B759** (2016) 369–394, arXiv:1603.02991.

[123] J. Brod and M. Gorbahn, "ϵ_K at Next-to-Next-to-Leading Order: The Charm-Top-Quark Contribution," *Phys. Rev.* **D82** (2010) 094026, arXiv:hep-ph/1007.0684.

[124] B. A. Kniehl and M. Spira, "Low-energy theorems in Higgs physics," *Z. Phys.* **C69** (1995) 77–88, arXiv:hep-ph/9505225.